12-2016

Early bearing fault analysis using high frequency enveloping techniques

Ilya Shulkin
Purdue University

PURDUE UNIVERSITY
GRADUATE SCHOOL
Thesis/Dissertation Acceptance

This is to certify that the thesis/dissertation prepared

By Ilya Shulkin

Entitled
Early Bearing Fault Analysis Using High Frequency Acceleration Enveloping Techniques

For the degree of Master of Science

Is approved by the final examining committee:

Nancy Denton
Chair

Mark French

Haiyan Zhang

To the best of my knowledge and as understood by the student in the Thesis/Dissertation Agreement, Publication Delay, and Certification Disclaimer (Graduate School Form 32), this thesis/dissertation adheres to the provisions of Purdue University's "Policy of Integrity in Research" and the use of copyright material.

Approved by Major Professor(s): Nancy Denton

Approved by: Dr. Duane Dunlap 10/10/2016
Head of the Departmental Graduate Program Date

EARLY BEARING FAULT ANALYSIS USING HIGH FREQUENCY ACCELERATION ENVELOPING TECHNIQUES

A Thesis

Submitted to the Faculty

of

Purdue University

by

Ilya Shulkin

In Partial Fulfillment of the

Requirements for the Degree

of

Master of Science

December 2016

Purdue University

West Lafayette, Indiana

ACKNOWLEDGMENTS

The author would like to thank the following family, faculty, and sponsoring organizations who were instrumental in their support of this work:

Parents: Simon & Yelena Shulkin Fiancé: Gabrielle Broughton

Committee members: Professors Nancy Denton, Mark French, & Haiyan Zhang

Sponsoring organizations: Mechanical Engineering Technology Department at Purdue University, Vibration Institute

TABLE OF CONTENTS

Page

Page

LIST OF FIGURES

Figure Page

Figure Page

LIST OF TABLES

LIST OF ABBREVIATIONS

FFT - Fast Fourier transform

VFD - Variable frequency drive

ICP® - PCB's registered trademark that stands for "Integrated Circuit – Piezoelectric

HFE – High frequency enveloping

AM – Amplitude demodulation

GLOSSARY

acceleration enveloping (or amplitude demodulation) - a multiple-step signal processing operation that extracts signals of interest from a raw waveform (Weller, 2004).

forcing frequency – the frequency of an oscillating force applied to a system (Dictionary.com, 2016).

high frequency - refers to frequencies from 1 kHz to 40+ kHz used for acceleration enveloping (Weller, 2004).

condition monitoring -techniques collectively referred to as Condition Monitoring (CM) have a common objective of indicating the early signs of deterioration or malfunction and wear trending in structure, plant and machinery through surveillance, testing and analysis (BINDT, 2012). It is also defined as the use of advanced technologies in order to determine equipment condition, and potentially predict failure. It includes, but is not limited to, technologies such as Vibration Analysis, Infrared Thermography, Oil Analysis, Ultrasonics, and Motor Current Analysis (Dunn, 2009).

Hilbert transform - The Hilbert transform H[g(t)] of a signal g(t) is defined as

$$\mathcal{H}[g(t)] = g(t) * \frac{1}{\pi t} = \frac{1}{\pi}\int_{-\infty}^{\infty}\frac{g(\tau)}{t-\tau}\,d\tau = \frac{1}{\pi}\int_{-\infty}^{\infty}\frac{g(t-\tau)}{\tau}\,d\tau$$

.

The Hilbert transform of g(t) is the convolution of g(t) with the signal 1/πt. It is the response to g(t) of a linear time-invariant filter (called a Hilbert transformer) having impulse response 1/πt (Kschischang, 2006).

fast Fourier transform – The fast Fourier transform (FFT) converts a time domain representation of a signal into a frequency domain representation faster than traditional Discrete Fourier transform (DFT) by optimizing redundant calculations (National Instruments, 2013).

full wave rectification – process where the entire signal is inverted to keep polarity constant (Truax, 1999).

variable frequency drive – a motor speed controller that varies the input frequency and voltage supplied to the motor (Anaheim Automation, 2016).

tri-axial accelerometer – accelerometers intended for simultaneous measurement of vibration in 3 perpendicular axis (Manfred Weber, 2016)

ICP® - PCB's registered trademark that stands for "Integrated Circuit - Piezoelectric" and identifies PCB sensors that incorporate built-in, signal-conditioning electronics. The built-in electronics convert the high-impedance charge signal that is generated by the piezoelectric sensing element into a usable low-impedance voltage signal that can be readily transmitted, over ordinary two-wire or coaxial cables, to any voltage readout or recording device (PCB, 2016).

ABSTRACT

Shulkin, Ilya, M.S, Purdue University, December 2016. Early Bearing Fault Analysis Using High Frequency Enveloping Techniques. Major Professor: Nancy L. Denton.

High frequency acceleration enveloping is one of many tools that vibration analysts have at their disposal for the diagnosis of bearing faults in rotating machinery. This technique is believed to facilitate very early detection of potential failures by detecting low amplitude repetitive impacts in frequency ranges above conventional condition monitoring. One traditional enveloping method uses a mathematical operation known as the Hilbert transform along with other signal processing procedures such as band-pass filtering and full-wave rectification. For comparison, another method uses a proprietary algorithm included in National Instruments' LabVIEW™ add-on package: Sound and Measurement Suite. Enveloping's inherent problem with noise introduction is also addressed herein. A controlled, three-stage fault was induced and diagnosed utilizing both acceleration enveloping methods and traditional fast Fourier transformation (FFT) described herein. A performance assessment of the enveloping process with respect to FFT as well as the performance between individual enveloping methods is presented. In summary, several high frequency acceleration enveloping methods exist that can be effective tools in detection of bearing faults earlier than FFT alone.

CHAPTER 1. INTRODUCTION

1.1. Introduction

Condition monitoring involves regular monitoring of machinery vibration (usually tested at the bearing housing) undertaken as part of a robust predictive maintenance program. Values are trended to detect significant changes as an indicator of possible developing machinery faults. The objective is to provide valuable lead-time for maintenance program planning (SKF Group, 2012). This developing field typically uses mathematical techniques such as Fast Fourier Transformation (FFT) signal analysis to closely monitor the performance of critical rotating machinery such as turbines, fans, gearboxes, and other large manufacturing equipment in power-plants, factories, and other industrial environments. There is still research to be done in order to further develop the techniques and technologies involved in condition monitoring. High frequency acceleration enveloping is one of those techniques, and will be discussed in detail throughout this thesis.

1.2. Problem Statements

1) Can high frequency acceleration enveloping help detect impending faults in rolling element bearings earlier than traditional FFT analysis?
2) How does the performance of traditional high frequency enveloping methodology compare to a proprietary envelope processing technique from National Instruments?

1.3. Scope

This research focused on the methods used for enveloping and processing vibration signals directly from accelerometers installed on bearings and gearboxes typically used in industrial rotating machinery (e.g. turbines, shafts, and electric motors). This technique can be used to detect faults in rolling element as well as journal bearings however, rolling element bearings was the primary concern of this study. These monitoring and predictive maintenance techniques could potentially provide a significant advantage in reducing maintenance costs especially in high-dollar operations such as wind farms and power plants (Costinas, Diaconescu, & Fagarasanu, 2009).

An introduction to high frequency acceleration enveloping (HFE) theory and procedure was presented. Two LabVIEW^{TM} based methods for implementing HFE were offered and compared by performance in addition to an analysis of how enveloping performs versus fast Fourier transformation (FFT). The first enveloping method used the Hilbert transformation which constituted the traditional method. The second was a proprietary method titled, Order Analysis Toolkit (OAT) Envelope Detection function,

and was accessed through National Instrument's Sound and Vibration Measurement Suite (a supplementary package to LabVIEW™ 2012). It is however, important to note that there were several other condition monitoring software packages offering algorithms for signal enveloping such as Ascent™ (General Electric, 2016) or DEWESoft® (DEWESoft® , 2016) For the analysis presented herein, the vibration signals originated from an experimental approach to fault detection. Data was collected from a rolling element bearing using a controlled three-phase introduction of a physical defect to certain bearing components discussed in the methodology section (see chapter 3).

1.4. Significance

This study aimed to evaluate the effectiveness of the high frequency enveloping (HFE) technique when used to diagnose faults in rolling element bearings earlier than traditional vibration analysis methods. There are many industrial scale processes that require rotating machinery with shafts supported by rolling element bearings, including gearboxes and motors. Earlier detection of potential machinery problems can yield much benefit via time, labor and maintenance savings. With knowledge of an impending failure or a slower progressing fault, appropriate personnel can order replacement parts and schedule maintenance accordingly, allowing the process to continue with minimal downtime. Since many facilities operate continuously, this is a definitely a goal of any robust condition monitoring and predictive maintenance program.

HFE techniques need to be applied carefully and should never be used independently; they should be combined with standard FFT analysis to determine overall machine condition and verify suspected concerns. High frequency acceleration enveloping

involves a mathematical signal extraction of low amplitude, high frequency vibration signals. There is opportunity for certain factors to present potential problems with HFE frequencies such as high frequency damping and operational noise, variable frequency drive (VFD) interference, transducer mounting quality and location, electromagnetic interference, et cetera. For valid applications of the technique, the vibration analyst will utilize a transducer with the ability to record signals reliably up to 40 kHz or higher, and a repeatable mounting method. It was not necessary for the accelerometer to have a flat response to 40 kHz because amplitudes recorded were compared with other amplitudes at a given frequency. With regard to this work, there were no frequencies of interest above 500 Hz. In fact, most of the focus was in the lower 0-50 Hz range due to the rotational speed of the equipment. The transducer was installed as close to the bearing on the housing as possible. Amplitude in the envelope spectrum can only be compared when mounting conditions are consistent. Since acceleration enveloping is not a direct measurement, even slight changes in mounting or use of multiple transducers can yield significantly varied results that are usually apparent as an amplitude difference, not necessarily a frequency difference. As another caution, note that bearing defect vibrations tended to decrease in amplitude over time due to a smoothing effect of the damaged area and subsequent reduction in the repetitive impact resonance response as the fault progresses in severity. Although these pitfalls are important to note, appropriate application of the enveloping technique has still been shown to be an effective tool in bearing condition monitoring (Berry, 1996) (Mignano, 1996) (SKF Reliability Systems, 2012).

1.5. Statement of Purpose

High frequency acceleration enveloping (HFE) is a multi-step process with regard to signal processing. The enveloping procedure starts with a raw accelerometer waveform in the time domain. Rolling element bearing (REB) faults tend to produce periodic impacts that excite structural natural frequencies. These natural frequencies act as relatively high-frequency carrier signals where the amplitude of the carrier is modulated by bearing fault impacts. For this reason, HFE is sometimes referred to as amplitude demodulation. The impacts typically repeat at the period of a bearing fault frequency, typically ball pass frequency of the outer race (BPFO), ball pass frequency of the inner race (BPFI), or ball spin frequency (BSF and 2x BSF). Each impact excited free vibration at the structural natural frequency, which then decayed due to structural/system damping. The repetition of impacts formed a series of impulse/response pulses in the waveform. Enveloping demodulated these pulses in a way that is similar to AM radio. The signal was first band-pass (or high-pass) filtered to remove low frequency, high amplitude signal components. The filter band-pass region was set to include the range of structural natural frequencies. The filtering also removed synchronous rotor and gear mesh related vibration that could obscure the bearing fault signatures. The filtered signal was rectified, and an envelope was constructed that followed the amplitude maxima and minima of the rectified signal. The envelope typically had an approximately saw-tooth wave shape, where a fast amplitude rise at the impulse was followed by a relatively slow decay. The enveloped waveform was then passed through a fast Fourier transform (FFT) function, producing a spectrum that can be inspected for bearing fault frequencies (Hatch, Weiss, & Kalb, 2010) (Weller, 2004).

Based on the work of Berry (Berry, 1996) and other researchers such as Nathan Weller (Weller, 2004), it was clear that acceleration enveloping is a viable technique that could be explored further as a means to improve the reliability of machinery in applications where traditional vibration monitoring falls short. This thesis project continued this exploration.

1.6. Assumptions

This research study assumed the following:

1. The Hilbert transform is a mathematical function that is a valid operation based upon formal proofs accepted by the mathematics community.
2. Signal processing techniques, such as band-pass filtering and rectification, are based upon accepted industry practices.
3. The required instrumentation, such as accelerometers, signal conditioners, and data acquisition software, has appropriate documented precision and sensitivity range.

1.7. Limitations

Limitations of this study included the following:

1. Signal noise may be amplified as part of the transformation process. The noise floor can make it difficult to distinguish fault frequencies from operational noise.
2. The Hilbert transform is only one of several accepted algorithms for extracting the envelope of a signal. Other methods may be more accurate, and this is one aspect that

this study hopes to address by analyzing and comparing the results of the two enveloping methods discussed herein.

3. HFE is not adequate as a stand-alone tool to predict overall machine condition or diagnose machinery faults.
4. Any variation due to transducer selection and mounting location can make accurate trending difficult.
5. Frequency variation – machine speed must be consistent throughout the experiment to allow direct spectral comparisons.
6. Excessive damping in the system can potentially inhibit vibration signal transfer to the accelerometer.
7. After HFE processing, signal amplitudes cannot be used to directly determine fault severity due to the effect of the signal extraction and transformation process.

1.8. Delimitations

Some data analysis techniques such as FFT analysis and machine condition evaluation were referred to but not covered extensively in this study. More information on these topics can be found in the referenced literature.

1. The criterion for determining the presence and severity of faults will be based upon the accepted practices in the machinery condition monitoring industry.
2. The Fast Fourier Transform (FFT) is a universally accepted signal processing method for vibration analysis.

CHAPTER 2. REVIEW OF LITERATURE

2.1. Introduction

In order to determine how acceleration enveloping can detect early faults in rolling element bearings located inside rotating machinery, a literature review was conducted to first organize and assess existing knowledge. Literature on high frequency acceleration enveloping techniques comes from sources such as the work of Jim Berry, Nathan Weller, and Hans Konstantin-Hansen. This and other supporting work on the topics of acceleration enveloping, spectral analysis, vibration analysis, and condition monitoring was reviewed as it relates to this research, and establishes the basis for the formal research regarding HFE and early rolling element bearing fault detection.

2.2. Enveloping & Severity

According to Berry (1996), high frequency enveloping (HFE) is a tool for detection of faults in bearings which are part of rotating machinery. Any bearing imperfection may be undetectable using traditional methods until the fault progresses further, making envelope detection a useful tool for the vibration analyst. However, due to limitations of HFE, its use should be in conjunction with FFT analysis when determining fault severity. The application is most effective for early bearing fault

detection since enveloped amplitudes can actually decrease as bearing failure becomes more imminent. As a bearing continues to wear, its small, vibration-inducing flaws begin to smooth out, and the characteristic "ringing" caused by the flaws (and detected by HFE) decreases. Trending is another tool that can be utilized to properly determine fault progression over time. When enveloping data is combined with other measurements such as full spectrum machine vibration analysis, acoustical noise levels, temperature, and ultrasonic testing, the overall machinery condition can be more accurately determined (Weller, 2004).

2.3. Lubrication Issues

HFE can detect the early signs of bearing failure where other types of vibration analysis fail, allowing the engineer to anticipate the failure, and plan for a replacement. This reduces downtime, maintenance costs, and can eliminate catastrophic failures, but before enveloping can be applied effectively, it must be determined if the problem is being caused by a true bearing defect or simply poor lubrication. Under inadequate lubrication conditions, it is possible that bearing defect frequencies can misleadingly appear in the HFE spectra. A physical inspection should first be performed and the bearing lubricated if necessary. This will help to reduce the signal noise floor, facilitating the identification of vibration frequencies related to bearing components (Berry, 1996).

2.4. Spectral Analysis

The results of signal processing using enveloping are a spectrum of frequencies and their corresponding amplitudes. This spectrum can be compared against a baseline spectrum measurement taken when the machine was new, where certain bearing frequencies established through calculation can help indicate the location of a fault. These bearing frequencies include:

1. Fundamental train frequency (FTF) - cage defects or mechanical looseness

$$\text{FTF} = \frac{S}{2} * (1 - \frac{Bd}{Pd} * \cos(\emptyset))$$

2. Ball pass frequency inner race (BPFI) – fault on the inner race

$$\text{BPFI} = \frac{Nb}{2} * S * (1 + \frac{Bd}{Pd} * \cos(\emptyset))$$

3. Ball pass frequency outer race (BPFO) – fault on outer race

$$\text{BPFO} = \frac{Nb}{2} * S * (1 - \frac{Bd}{Pd} * \cos(\emptyset))$$

4. Ball spin frequency (BSF) – fault on rolling element

$$\text{BSF} = \frac{Pd}{2Bd} * S * (1 - \left(\frac{Bd}{Pd}\right)^2 * \cos(\emptyset)^2)$$

Where: Pd – pitch diameter, Bd - ball diameter, Nb – number of rollers, S – revolutions per second, $\emptyset$ - contact angle (Konstantin-Hansen, 2003).

These fault frequencies can be directly linked to certain root cause machinery conditions that should be corrected. For example, the most common cause of inner race faults (BPFI) is mass unbalance in the system. Outer race faults are generally attributed

to misalignment of the bearing to the shaft. Rolling elements themselves can be damaged by electric current, elevated temperature, or lack of lubrication (Eshleman, 2010).

2.5. Enveloping Implementation

HFE is an amplitude demodulation process that extracts low-amplitude high frequency signals typically caused by repetitive impact events that may be hidden by harmonics of the much higher amplitude low frequency vibration sources typically seen in traditional FFT spectra. To filter out these low frequencies, a high pass filter is utilized which typically reduces the amplitude by 3dB. It removes normal operating speed vibration signals while allowing the impact-generated vibration signals to remain. The second step uses full-wave rectification to detect peak-to-peak values, which doubles the carrier frequency and further separates the impact and carrier frequencies. Both carrier frequency and sidebands are artifacts of full-wave rectification (Weller, 2004). The next step in the process is to apply the enveloping algorithm. Amplitude demodulation of the filtered, rectified waveform eliminates the carrier frequency signal and leaves the signal at the repetition rate of the defect impact. A number of methods are available to accomplish demodulation, including peak detection and Hilbert transformation. The last step in the process uses a low pass filter to eliminate frequencies outside the range of fault frequencies. The resulting data are presented in the form of a standard FFT amplitude versus frequency spectrum (Berry, 1996).

Amplitude modulation can generate new frequencies, often called sidebands. Sidebands are pairs of frequencies equally spaced above and below the carrier frequency

and contain all the Fourier components of the modulated signal (except the carrier components). These impact-generated transient signals create bearing fault frequencies with low amplitude harmonics or sidebands in the FFT spectrum. If these harmonics happen to be at the fault frequency and encounter a structural resonance, then the amplitude could be multiplied by 50-100 times (Sheen, 2008).

Harmonics of fault frequencies tend to be artifacts of the enveloping process and not useful for trending purposes. Increased presence of harmonics and significant remaining frequencies, however may indicate the progression of a fault and correlated to actual problems within a machine. As defects become more severe, sidebands related to running speed may appear around defect frequencies in the spectrum (Weller, 2004).

HFE is a method that can demodulate the signal by removing the carrier frequency and leaving the modulating frequency. Amplitude modulation should not be confused with frequency modulation, which is a time-varying frequency, but with constant amplitude. Many combinations of problems can have both amplitude modulation and frequency modulation simultaneously such as a damaged gear installed on an unbalanced shaft. (Berry, 1996). Since frequency modulation is beyond the scope of this project, only amplitude demodulation methods are presented.

2.6. Instrumentation

High frequency enveloping typically makes use of a tri-axial accelerometer capable of flat response through 40+ kHz in all three axes (vertical, horizontal, and axial). It is ideally rigidly mounted on a threaded stud (after the paint is removed from the surface), with mounting paste, or by a strong magnet. A handheld probe “stinger” should

never be used for enveloping because this greatly reduces the high frequency limit of the flat frequency response range. The accelerometer mounting location and quality is critical for taking HFE spectral measurements. Consistent location, orientation, and mounting method when recording vibration data is essential for useful and repeatable results. The same transducer should also be used, as changing the measurement device mid-study can result in apparently dramatic amplitude differences in the enveloped spectrum. With HFE, close attention should be paid not so much to absolute amplitudes, but to trending how much they change from one survey to the next and the frequencies at which the amplitudes occur (Berry, 1996). For trending purposes, the accelerometer mounting should be consistent, and the band-pass filter range should be set to display frequencies without structural resonances of the machine or accelerometer and envelope the region of flat frequency response (Konstantin-Hansen, 2003).

Weller (2004) states that even though the enveloping technique can be used to detect faults in machine components, it is not a "direct" measurement. Several factors exist that can add to or diminish the enveloped signal or prevent successful enveloping implementation entirely. Joints, interfaces, gaskets, and fluid-film or squeeze-film dampers can prevent high-frequency signal transmission. These damping devices impede vibratory responses at the repetitively triggered structural resonances critical for obtaining successful enveloping results. In some cases, high-frequency operational noise may overshadow signals of interest in reciprocating machines, variable frequency drive motors, and others. Electromagnetic interference may occur in the cabling between the transducer and the signal processing device and compromise signal integrity. Since the

forcing frequency of enveloping signals is directly dependent on shaft rotational speed, the machine speed must be known and relatively constant. Otherwise, the frequency components may be affected by frequency-dependent machinery and instrumentation responses rather than changes in defect severity, and can lead to misdiagnosed machinery problems. There are two fundamental concerns that causes the amplitude in the resulting frequency spectrum to be an indirect measurement when determining fault severity; first, the physical transmission path from the fault to the transducer, and second, the various signal processing steps used to extract the low amplitude repetitive vibration. Trending the signal frequencies and corresponding amplitudes over time can help reveal any developing conditions when compared to an established baseline (Weller, 2004).

2.7. Enveloping of Signals from Large Equipment

The next section of the literature review pertains to condition monitoring as it relates to large rolling element bearings, such as those found in wind turbines. A major issue with wind power plants is the relatively high cost of operation and maintenance (OM). Wind turbines are difficult-to-access structures, and they are often located in remote areas. These factors increase the OM cost for wind power systems, and poor reliability directly reduces availability of wind power due to the turbine downtime. According to GE Energy, “a $5,000 bearing replacement can easily turn into a $250,000 project involving cranes, service crew, gearbox replacements, and generator rewinds, not to mention the downtime loss of power generation. For a turbine with over 20 years of operating life, the OM and part costs are estimated to be 10-15% of the total income for a

wind farm" (Lu, X., & Yang, 2009). Because of such costs, a comprehensive condition monitoring program is a cost effective solution.

Furthermore, a condition-based monitoring system must be designed to provide maximum benefit for its operation by targeting the failures that are most costly to repair. Much of the literature about condition monitoring of wind turbines focuses on gearboxes and other drivetrain components. This is consistent with the most common failure modes, where the gearbox failures contribute to the most expensive repairs. (Kim, Parthasarathy, Uluyol, Shuangwen, & Fleming, 2011).

A few examples of common problems the wind turbine industry is facing today include:

1) Inclusions in gear material resulting from poor quality control on the raw material manufacturing. The inclusion acts as a stress concentrator.

2) Gear surface tempering, where the surface temperature of the case hardened gear has not been controlled properly during grinding. This can even lead to re-hardening of the metal. Temper grinding burn will reduce the surface hardness and cause a residual stress condition, which will reduce wear resistance. Re-hardening burn will produce a hard, brittle surface layer, and cracks may begin in the tooth surface and result in low life due to pitting and fracture.

3) Axial cracking in through-hardened bearings, where the bearings are prone to cracking as they have inherent poor toughness and residual tensile stresses due to the heat treatment process. The cracks may lead to

the raceway slipping on the shaft, and potentially a catastrophic failure in the gearbox. (Crowther & Eritenel, 2012).

HFE techniques can help detect the faults caused by stress concentrations in design and machining processes before they can cause unscheduled downtime.

2.8. Hilbert Transformation

The Hilbert transformation is a mathematical variation of the Fast Fourier transform which demodulates a vibration signal and extracts the high frequency, low amplitude data of interest. The transform involves a phase shift of 90 degrees from the original signal. Following the transformation, the data consists of a complex signal comprised of a real (original signal) and imaginary (transform) aspect. It can be mathematically described as $F(t) = f(t) + j*h(t)$ where t is in the time domain, F is the analytic signal constructed from the input signal (f) and its Hilbert transform (h). If phase is a necessary component, then the expression becomes $F(t) = A(t)^{j*\theta(t)}$ where A is the envelope or amplitude of the analytic signal and ɵ represents the phase of this analytic signal (Johansson, The Hilbert transform, 1999). The Hilbert function is used to effectively construct a new waveform built from the original raw waveform that compiles all amplitude peaks from the raw wave, whether positive or negative, at a particular frequency and displays these peaks as positive amplitudes in the full wave rectified envelope waveform.

2.9. Summary

HFE processing can provide valuable information necessary for ascertaining true machinery condition. However, benefits can only come from implementing such early detection techniques properly. An introduction to the methodology behind high frequency enveloping was presented. Two LabVIEW™ based enveloping methods were chosen for study, and the value of HFE as it relates to rolling element bearings was explored.

CHAPTER 3. RESEARCH METHODOLOGY

3.1. Introduction and Experimental Setup

In order to gauge the performance of the enveloping algorithms chosen (in this case the Hilbert transform and OAT envelope detection), time waveform and power spectra data were generated and analyzed for both full frequency using FFT and mathematically transformed (enveloped) vibration signals. The goal of this experiment was to determine the effectiveness of the enveloping procedure using the two chosen forms of the enveloping technique in order to answer the first research question. A comparison of algorithm performance in detecting an induced fault in the cage, roller, and inner race of a pillow block rolling element bearing was developed. The bearing was one of two such bearings supporting the rotor shaft of an electric motor connected to a test stand designed to demonstrate two plane balancing procedures (see figure 3.1). The overall structure of the test stand was comprised of steel and aluminum framing and the motor speed was controlled by a frequency drive with rotational speed measured by a tripod mounted laser tachometer.

Figure 3.1. Two plane balancing test stand.

3.2. Research Design

When viewing an acceleration time waveform, the independent variable was time (seconds) and the dependent variable is acceleration amplitude; typically measured in decibels (dB) or gravitational units (g). Frequency was another variable measured in cycles per second (hertz). Vibration data was detected using a tri-axial AC accelerometer rigidly mounted to the pillow block bearing support structure attached to the shaft of an electric motor. The raw acceleration waveform from the horizontal, vertical, and axial directions was recorded for each enveloping method. The enveloping algorithm was applied using the appropriate signal processing functions in LabVIEW™ to create a "virtual instrument" (VI) for signal processing, and a comparison established to determine performance and consistency. This approach was implemented due to the fact that this particular form of enveloping looks only for the high-frequency, low-amplitude repetitive signals that are not routinely monitored. It should be noted that if impacts do

not exist, the envelope spectrum will be flat. Value was still gained from obtaining such an envelope spectrum as this was indicative of properly running equipment and was used as a baseline. Note: Since the testing setup used was not a continuously running or regularly operating machine, trending was not performed.

3.3. Experiment control

In order to establish an experimental control, the rolling element bearing chosen for this study was tested using each of the two proposed enveloping procedures. The testing consisted of two preliminary control steps followed by three phases of progressively more severe faults applied to the cage, a single roller, and inner race of the test bearing. First, an envelope analysis was performed on a new, unused, and unlubricated pillow block bearing at three different operating speeds: 325, 450, and 900 RPM. Vibration acceleration data was taken in the horizontal, vertical, and axial directions on the bearing housing and enveloping analysis was developed. The test bearing was then properly lubricated and another envelope analysis was developed. The lubricated bearing test and evaluation established a baseline control waveform as well as demonstrated the difference in vibration frequency response between unlubricated and lubricated bearings which can help to avoid a simple case of poor lubrication in the field. The first fault-induced phase of the experiment involved comparison of the baseline lubricated envelope spectra at each of the specified operating speeds to vibration data obtained from the same bearing but with ~~a~~ mechanically-induced cage, rolling element, and inner race faults. The faults were initially introduced by deliberately scratching the surface of these components as they connect in the same area. The second and third

phases analyzed data from the same bearing with progressively more severe cage, rolling element, and inner race faults induced by drilling into the same component connection that was scratched in phase I. Calculated bearing frequencies using the formulas found in Chapter 2 (see 2.4 Spectral Analysis) served as the criteria for fault localization from the enveloped spectra.

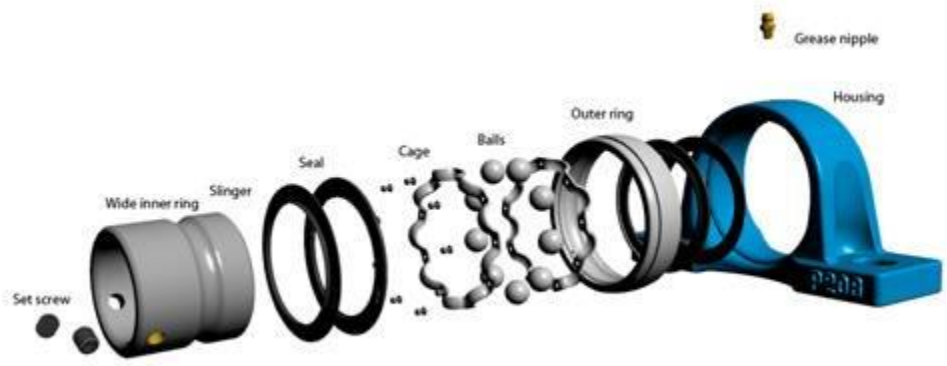

Figure 3.2. Pillow block bearing exploded view (FYH Bearing UCP205-16 1" Pillow Block Mounted Bearings, 2016)

3.4. Experimental Design

A balance test stand located in the Experimental Mechanics Lab, a part of Purdue University's Polytechnic Institute, was chosen as the motor-shaft system for this experiment. A 120V AC electric motor directly powered a rotating steel shaft. The bearing of interest was rigidly mounted and connected to the supporting steel frame substructure. Once secured, the bearing became part of the damped, forced vibration system. Using beeswax, the vibration transducer was mounted directly to the bearing housing to promote transmission of the low amplitude, high frequency repetitive vibration signals of interest. The transducer used was an AC tri-axial type connected to a

four channel in-line signal amplifier. Sampling rate was 1000 samples per second, while potential frequencies of interest were through 270 Hz for testing at 325 RPM and 370 Hz for testing at 450 RPM.

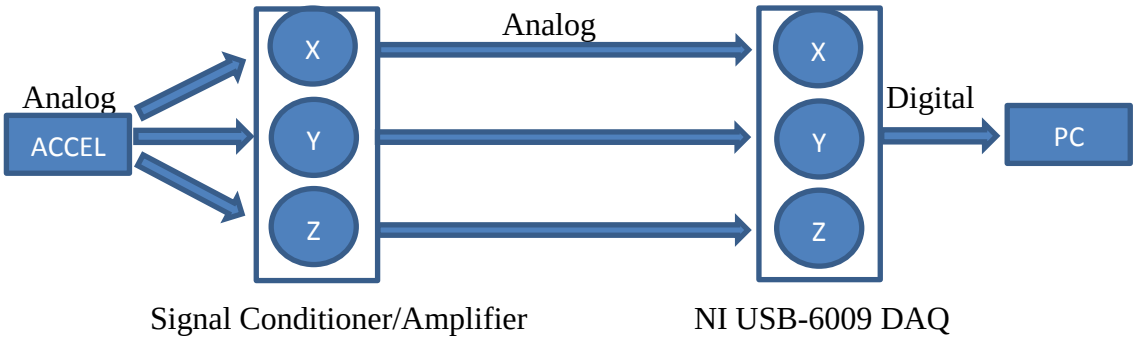

Figure 3.3. Vibration signal transmission path.

Some factors that can prove challenging during data collection and signal processing include accelerometer signal to noise ratio, operational noise, resonances, and harmonics. The above variability should be noted as part of the data reduction. Machine resonances were ascertained using a standard bump, start up, and coast-down test, and the enveloping procedure was carried out using LabVIEW™ signal processing software, specifically, the Hilbert transform and OAT envelope detection functions, respectively. Once baseline raw and enveloped waveforms were established from a new test bearing and shown to have a clean enveloped spectrum, the two enveloping methods were applied in an attempt to detect a fault in any of the purposely damaged bearing components. Data reduction includes graphical representations of the raw and enveloped waveforms, power spectra, and corresponding FFT analysis. The FFT analysis is used to show raw frequency spectra, showing any bearing defect frequencies if they exist. These bearing frequencies were then compared to calculated values to ascertain physical defect location

in the bearing. A performance analysis of each enveloping method with respect to FFT analysis results is also included in the data reduction to ascertain if enveloping can indeed be effective in locating faults earlier.

CHAPTER 4. RESULTS

4.1. Envelope Detection and Signal Processing Using LabVIEW™ 2012

There are many proprietary options for signal processing of machinery vibrations. The LabVIEW™ 2011 software package, with the supplementary Sound and Vibration Measurement Suite, provides the vibration analyst tools that allow signal processing of simple and complex waveforms obtained from a variety of sensor types. For this study, a PCB Piezoelectronics ICP triaxial 100mV/g accelerometer connected to a four channel, line-powered ICP sensor signal conditioner was used. The accelerometer unit was capable of linear sensitivity through 5 kHz and its voltage signal was routed to LabVIEW™ software through a National Instruments USB-6009 multifunction I/O DAQ unit where it was converted and scaled to the desired engineering units. A triaxial accelerometer senses acceleration in three perpendicular directions and has three corresponding output leads. The accelerometer was mounted to the test bearing's housing along the motor shaft centerline with the X (horizontal) oriented perpendicular and horizontal to the shaft, Y (axial) oriented parallel to the shaft, and Z (vertical) perpendicular and vertical to the shaft centerline (see figure 4.1). Use of LabVIEW™ for the fast Fourier transform (FFT) signal processing portion is accomplished through the built-in power spectrum function block. The following section provides an overview on steps required to program LabVIEW™ for high frequency acceleration enveloping (HFE)

data collection and presents results with a performance analysis between two commonly used enveloping algorithms. In addition, performance is evaluated to determine enveloping effectiveness in bearing fault detection versus the fast Fourier transform.

Figure 4.1. Test bearing with triaxial accelerometer mounted

4.1.1. Building a Virtual Instrument (VI)

In order to configure LabVIEW™ for signal acquisition, a virtual instrument (VI) program was created. This is the graphical programming environment, allowing a user to select various functions from a controls pallet and use pre-programmed sub-VI's connected by virtual wiring to process the incoming signal with the desired parameters, as well as develop custom programming functions.

The user begins by identifying the various parameters such as signal type, scan rate, number of input channels, input units, and maximum/minimum signal thresholds. This is accomplished using the 'DAQmx Create Channel VI' (see figure 4.2). This VI maps the physical channel configuration connected to the multifunction I/O unit to the

appropriate software channel. For the test experiment, three physical channels were used, one for each axis (horizontal, axial, vertical) and connected to the AI0, AI1, and AI2 ports on the NI-USB6009. Each channel type was set to voltage with a +/- 1V range.

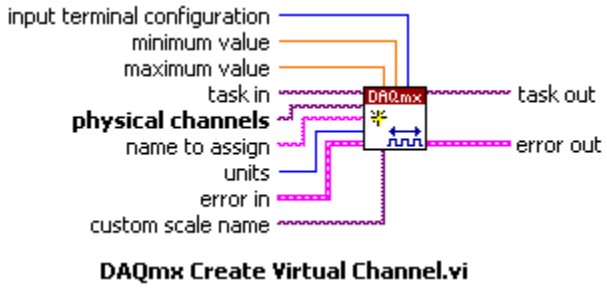

Figure 4.2. DAQmx create virtual channel virtual instrument

Each input signal was connected via virtual wire to the 'DAQmx Timing (Sample Clock) VI', shown in figure 4.3, which configures the number of samples and scan rate for a particular channel. These were set to 1000 samples per second for 10000 data points, allowing for an overall 10 second measurement time.

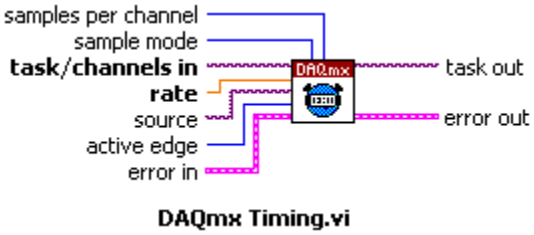

Figure 4.3. DAQmx timing virtual instrument

The function, 'DAQmx Read (Analog Waveform 1 Channels, N Samples)', was used to establish the signal as a raw waveform, one per channel and is shown in figure 4.4.

Figure 4.4. DAQmx read virtual instrument

4.1.2. Signal Scaling and Parameters

The type of signal and physical wiring configuration was defined in the previous steps, but the software still identifies the input as purely a voltage signal which must be converted to the proper engineering units using the 'Scale Voltage to EU' VI. For signal scaling, the sensor sensitivity was entered as 100mV/g. Acceleration was the measure of choice with a linear weighting filter and no pre-gain, in gravity units of g. Refer to figure 4.5 for the function block diagram.

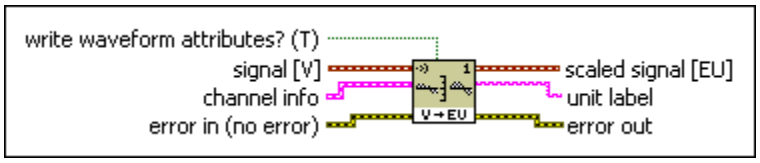

Figure 4.5. SVL scale voltage to EU virtual instrument

4.1.3. Raw Acceleration Waveform Recording

With proper scaling, the voltage signal could be recorded as a raw waveform with amplitude measured in gravity units versus the measurement time in seconds. The 'Write to Measurement File' function directly recorded 10000 data points per channel during the 10 second measurement time. A unique filename was entered as the desired storage location for each resulting spreadsheet data file.

4.1.4. Power Spectrum and FFT Analysis

The raw waveform (acceleration vs. time signal) is subsequently passed to a Power Spectrum function which uses Fast Fourier Transformation (FFT) to extrapolate the amplitudes at frequencies from 0 to 500 Hz as set by the bandpass filter. The standard Hanning window, which reduces amplitude uncertainty and frequency errors from energy leakage in the frequency spectrum, was used and the resulting acceleration amplitude (g) versus frequency (Hz) spectrum is displayed (LDS Dactron, 2003). These graphical representations of the acquired signal were designed to establish a baseline raw waveform and power spectrum before any enveloping algorithms were applied, allowing evaluation of the performance of each HFE method. Refer to figure 4.6 for the function block diagram.

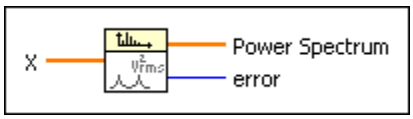

Figure 4.6. Power spectrum using fast Fourier transform

4.1.5. The Hilbert Enveloped Waveform and Spectrum

The first HFE method uses the fast Hilbert transformation function, h(t) mathematically defined as $h(t) = H\{x(t)\} = \frac{1}{\pi}\int_{-\infty}^{\infty}\frac{x(\tau)}{t-\tau}d\tau$, a variation of the typical fast Fourier transformation (FFT), where x(t) is the waveform at time t and τ is its period. The Hilbert function in LabVIEW™ performs the discrete implementation of the Hilbert transform and then displays both the enveloped waveform and enveloped power spectra by using FFT. The positive harmonics are multiplied by -(j), the imaginary component of

the complex signal, while the negative harmonics are multiplied by +(j). The new sequence, H(x), is inverted to obtain the Hilbert Transform of x. The function as it is represented in LabVIEW™ is shown in figure 4.7.

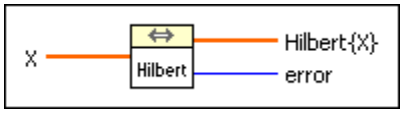

Figure 4.7. The Hilbert transform function

The resulting waveform can be described more clearly as a manipulation of an oscillating signal in such a way as to invert the negative components while preserving the overall magnitudes and frequencies. The positive amplitude components are subsequently graphed with the negative amplitude components to develop the enveloped waveform.

4.1.6. Order Analysis Toolkit (OAT) Enveloped Waveform and Spectrum

Another proprietary method for calculating the envelope of a raw waveform uses the Sound and Measurement Suite's Order Analysis Toolkit (OAT) function, which facilitates amplitude demodulation of a vibration signal. The function's input is a scaled signal. Given band specification parameters such as center frequency and span, the desired output is the enveloped signal. The OAT function icon is shown below in figure 4.8.

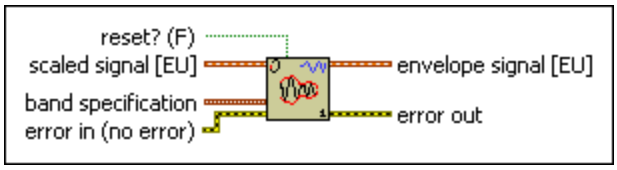

Figure 4.8. OAT envelope detection waveform output

4.1.7. LabVIEW™ Data Logging

The primary method for recording the bearing vibration data and preserving the various raw waveforms, power spectrums, enveloped waveforms, and enveloped spectrums from both the Hilbert and OAT techniques was through the data logging function built into the LabVIEW™ software. The data logging feature is located under the 'Data' menu and the log file binding must be established before the .DAT data file can be generated. The log file binding establishes the file names and directory locations into which collected data is to be saved. This feature allows any measurements recorded to be automatically stored and recalled at a later date.

4.2. Bearing Parameters

The following dimensional measurements were taken from the test bearing using a digital caliper. The contact angle could not accurately be measured and was assumed to be 0 deg because thrust loading is not part of the test stand's normal function. The speed was measured with a tachometer and the rolling elements counted.

1) Nb = number of rolling elements = 8

2) S = revolutions/second = 325RPM = 5.417 RPS

3) Bd = diameter of one rolling element = 0.3095”

4) Pd = pitch diameter = 1.3300”

5) Contact angle = 0 deg (assumed)

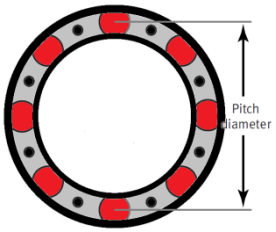

Figure 4.9. Pitch diameter

4.2.1. Operating Speed Ranges

Vibration acceleration data detected by the triaxial accelerometer taken from the bearing was recorded at three distinct, constant speeds provided by the 120V 6-pole electric motor controlled by variable frequency drive. The first speed, 325 RPM (5.4 Hz), was used to gather baseline data for a healthy bearing. The following two testing speeds, 450 RPM (7.5 Hz) and 900 RPM (15 Hz) were chosen to avoid any natural machine frequencies or resonances and remain with the motor’s speed range. Testing multiple speeds allowed the performance of the enveloping technique to be evaluated explicitly, and discrepancies due purely to the rotational speed of the bearing could be eliminated.

4.3. Rolling Element Bearing Calculations and Relevant Defect Frequencies

The next step in the enveloping process was to calculate the relevant bearing defect frequencies for fault identification. Information such as the ball diameter, pitch diameter, and number of rolling elements was obtained, and the contact angle estimated.

Calculations were then made to estimate the approximate frequencies of any bearing defects.

The fundamental train frequency (FTF) involves the frequency of the roller cage structure. Ball pass frequency inner race (BPFI) and ball pass frequency outer race (BPFO) are the vibration frequencies of defects of the inner and outer races based on a certain rotational speed. The ball spin frequency (BSF) is the defect frequency of the rollers themselves. If any of these calculated frequencies show up as peaks in enveloped spectrum plots, then a fault could be progressing in that bearing component. Sample calculations are shown in sections 4.3.1 through 4.3.4 for bearing fault frequencies at 325 RPM. Table 4.3 shows calculated fault frequencies at 450 RPM and 900 RPM.

(Dimensions in inches; angles in degrees)

4.3.1. Fundamental Train Frequency at 325 RPM

$$FTF = \frac{S}{2} * \left(1 - \frac{Bd}{Pd} * \cos(\emptyset)\right)$$

$$FTF = \frac{5.412}{2} * \left(1 - \frac{0.3095}{1.3300} * \cos(0)\right)$$

FTF = 2.706 *0.7673

FTF = 2.08 Hz

4.3.2. Ball Pass Frequency Inner Race at 325 RPM

BPFI = $\frac{Nb}{2} * S * (1 + \frac{Bd}{Pd} * \cos(\emptyset))$

BPFI = $\frac{8}{2} * 5.412 * (1 + \frac{0.3095}{1.3300} * \cos(0))$

BPFI = 21.648 * 1.233

BPFI = 26.69 Hz

4.3.3. Ball Pass Frequency Outer Race at 325 RPM

BPFO = $\frac{Nb}{2} * S * (1 - \frac{Bd}{Pd} * \cos(\emptyset))$

BPFO = $\frac{8}{2} * 5.412 * (1 - \frac{0.3095}{1.3300} * \cos(0))$

BPFO = 21.648 * 0.2015

BPFO = 16.61 Hz

4.3.4. Ball Spin Frequency at 325 RPM

BSF = $\frac{Pd}{2Bd} * S * (1 - \left(\frac{Bd}{Pd}\right)^2 * \cos(\emptyset)^2)$

BSF = $\frac{1.3300}{2*.3095} * 5.412 * (1 - \left(\frac{0.3095}{1.3300}\right)^2 * \cos(0)^2)$

BSF = 11.628 * (0.9458)

BSF = 11.00 Hz

Table 4.3. Calculated Bearing Fault Frequencies at 325, 450, and 900 RPM.

Bearing Fault Frequencies	325 RPM	450 RPM	900 RPM
Fundamental Train Frequency	2.08 Hz	2.87 Hz	5.75 Hz
Ball Pass Inner Race Frequency	26.69 Hz	36.98 Hz	73.96 Hz
Ball Pass Outer Race Frequency	16.61 Hz	23.01 Hz	46.03 Hz
Ball Spin Frequency	11.00 Hz	15.24 Hz	30.48 Hz

4.4. Bearing Testing Parameters with Traditional Raw Waveform and Power Spectrum (FFT) Analysis

During the course of the experiment, the bearing underwent five physical condition changes at 325 RPM, 450 RPM, and 900 RPM. The progression of these physical states can be described as dry or unlubricated, lubricated, and three phases of deliberately induced inner race faults with increasing levels of severity respectively. Phase three testing was only performed for the slower 325 RPM speed for safety reasons. An FFT analysis on the raw waveform and power spectrum is presented.

4.4.1. Unlubricated

The first physical state that the bearing experienced for testing was new and unlubricated. This test demonstrated how vibration signals might behave in the unlubricated (dry) or under-lubricated bearing condition. Figure 4.10 shows the overall raw vibration waveform and power spectrum at 325 RPM over a 10 second measurement time in all three axes. Note: Negative amplitudes in the time domain, when full wave rectified, show as positive components.

When examining the 325 RPM power spectra, the cyclical nature of the vibration signal can be seen in the horizontal (parallel to shaft centerline) and vertical (perpendicular to shaft centerline) directions, and seem to be almost identical in time duration, but with larger vertical axis amplitudes. The axial axis (horizontal and parallel to shaft centerline) signal measured a larger overall signal amplitude which carries over to the power spectrum, showing larger amplitudes than in the other two directions. At 325 RPM, the frequency distribution in the power spectrum is identical in the three directions with an interval of 50 Hz. In the horizontal axis, a small fundamental train frequency of 2.08 Hz is present at 0.00025g. Axial vibration at FTF is present at .00022g and vertical axis has a .0003g ball spin frequency (11 Hz) with a 0.0008g FTF.

At 450 RPM however, the 50 Hz interval seen at 325 RPM disappears and a small peak at 23 Hz ball pass outer race frequency (BPFO) is detected in both the horizontal and vertical axes with a larger peak at 38 Hz which is approximately ball pass inner race frequency. The calculated fundamental train frequency estimated as 2.87 Hz is not present, but the closest peak occurs with a large 1.75 Hz peak present in both the horizontal and vertical spectra. In addition, a peak at 46 Hz with sidebands is present which could represent 2x BPFO. This is interesting because once lubrication is applied, the amplitude decreases from 0.0004g to 0.0001g in the horizontal direction. It is important to note the possibility of false positive fault readings when operating under the unlubricated condition and the importance of inspecting bearings for proper lubrication as an important first step when applying traditional FFT.

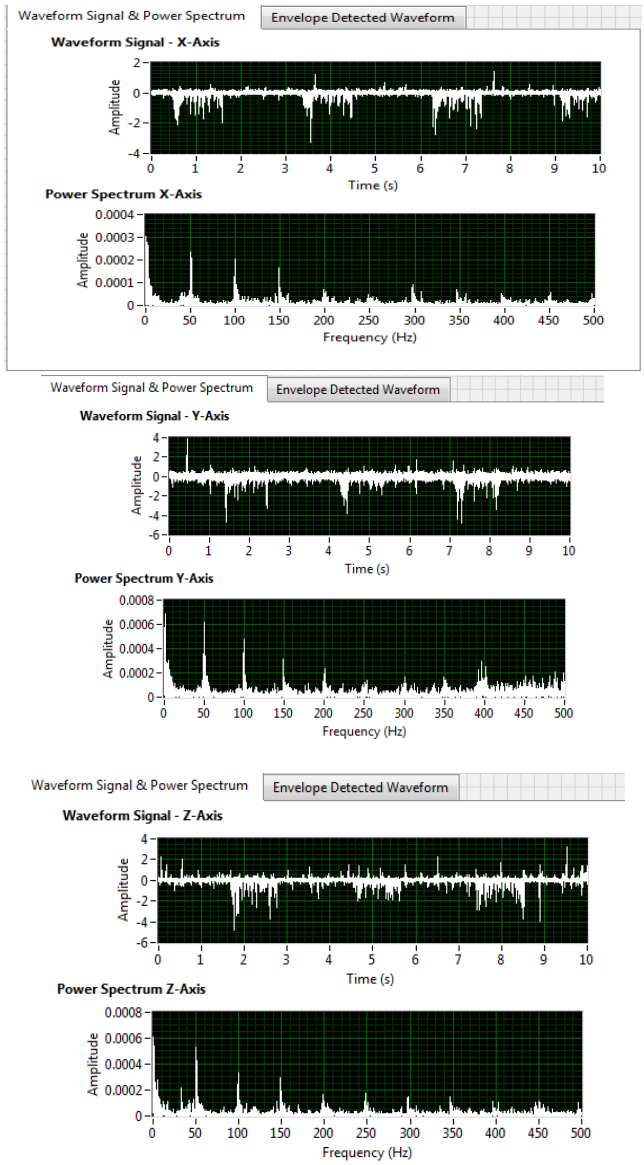

Figure 4.10. Raw waveform and power spectrum – unlubricated 325 RPM (horizontal, axial, vertical axes)

4.4.2. Lubricated

In order to establish a baseline vibration signature from the test bearing in its optimal operating condition, the bearing was lubricated using the recommended grease. Testing commenced using the same parameters as were outlined in the unlubricated state.

These signals were recorded at 325 RPM, 450 RPM, and 900 RPM respectively. Figure 4.11 shows the associated results at 325 RPM. Once the bearing was properly lubricated, the amplitudes in the time waveforms decreased slightly, while the power spectra show a measurable amplitude decrease. Also note line frequency (60 Hz) clearly shown in both the horizontal and axial axes in the overall frequency spectra. At 450 RPM, a large amplitude decrease is observed in the horizontal axis at 2x BPFO with other bearing frequencies showing small decreases or no change.

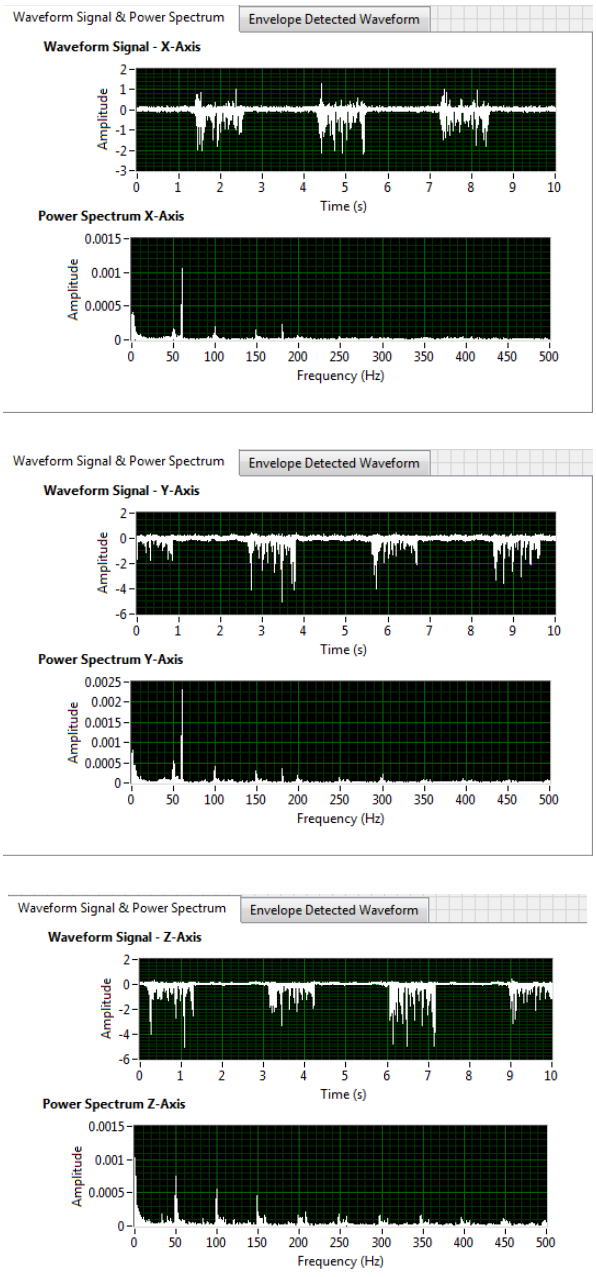

Figure 4.11. Raw waveform and power spectrum – lubricated 325 RPM (horizontal, axial, vertical axes)

4.4.3. Induced Component Faults Phase 1

The first phase of the induced cage and rolling element fault was achieved using a small drill bit to create a small imperfection on one of the eight rolling elements as well as the adjoining cage. The resulting vibration signatures at 325 RPM are shown in figure 4.12, with 450 and 900 RPM plots available in the appendices. It would be expected that a small imperfection on the inner race would not significantly change the raw waveform or the traditional FFT power spectrum values. Testing did confirm this assumption at all three test speeds, there were little, if any measureable differences between the purely lubricated and fault induced (phase I) states with regard to bearing fault frequencies. Further analysis is discussed in the envelope investigation included in section 4.5.

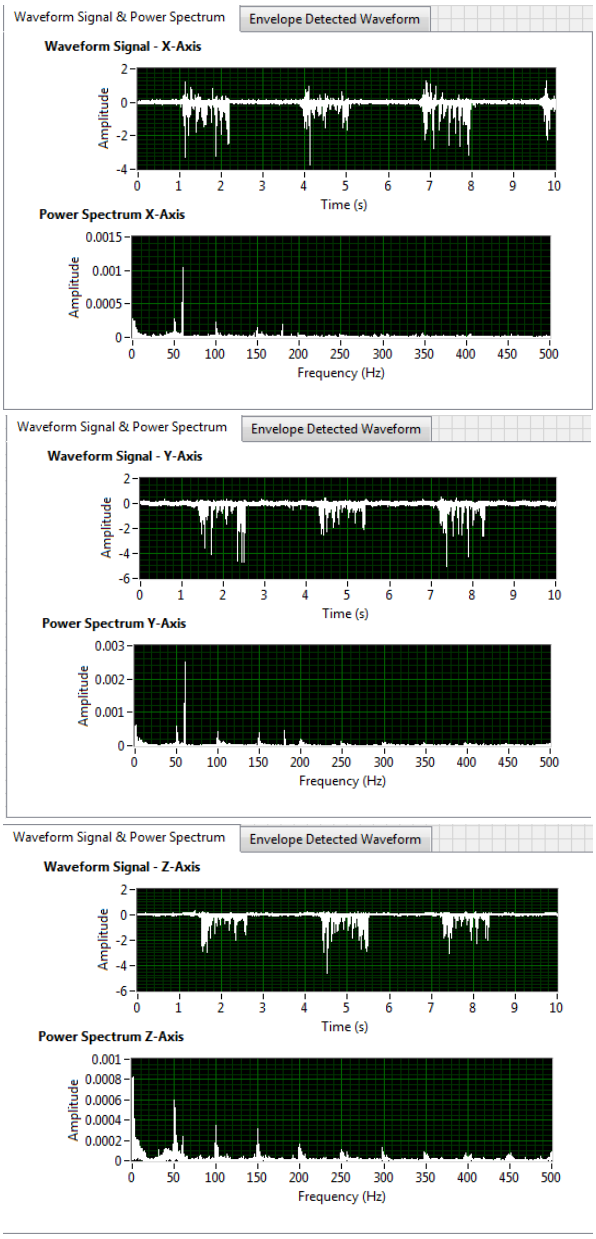

Figure 4.12. Raw waveform and power spectrum – induced fault (phase 1) at 325 RPM (horizontal, axial, vertical axes)

4.4.4. Induced Component Faults Phase 2

The second phase of induced fault testing involved further damage to the cage of the test bearing using a small reinforced drill bit. The added fault was applied to the same area as the scratch in phase one. Figure 4.13 shows the resulting waveform and spectrum plots at 325 RPM which show an increase in amplitude for raw waveform components from the horizontal and vertical directions when compared to phase one and lubricated spectra. At 100 Hz, the horizontal axis amplitude increases about 30% from 0.0025g to 0.0035g between phases one and two. The vertical axis amplitude at 100 Hz also increases 42% from 0.0035g to 0.006g. The axial direction component (at 100 Hz) did not show any significant changes between phases one and two at 325 RPM.

At 450 RPM in the 0 to 50 Hz frequency range, the phase two horizontal axis measured a peak of 0.00025g amplitude at approximately 3 Hz representing the fundamental train frequency (FTF) associated with the cage of the bearing is a 100% increase from 0.00012g in phase one. At 900 RPM, in the 0 to 100 Hz frequency range spectra, the phase two horizontal axis has a 0.00025g peak at 5 Hz FTF as well as a small 30 Hz ball spin frequency. The distinct 0.0011g peak at 48 Hz closely matches the calculated outer race ball pass frequency (BPFO) and confirms the small amplitude 23 Hz BPFO results seen at 450 RPM in the previous two phases. Although the increases in amplitude for FTF between phases one and two are anticipated, the outer race frequency was unexpected to see because the damage was applied to the rolling element, cage, and inner race directly, not the outer race.

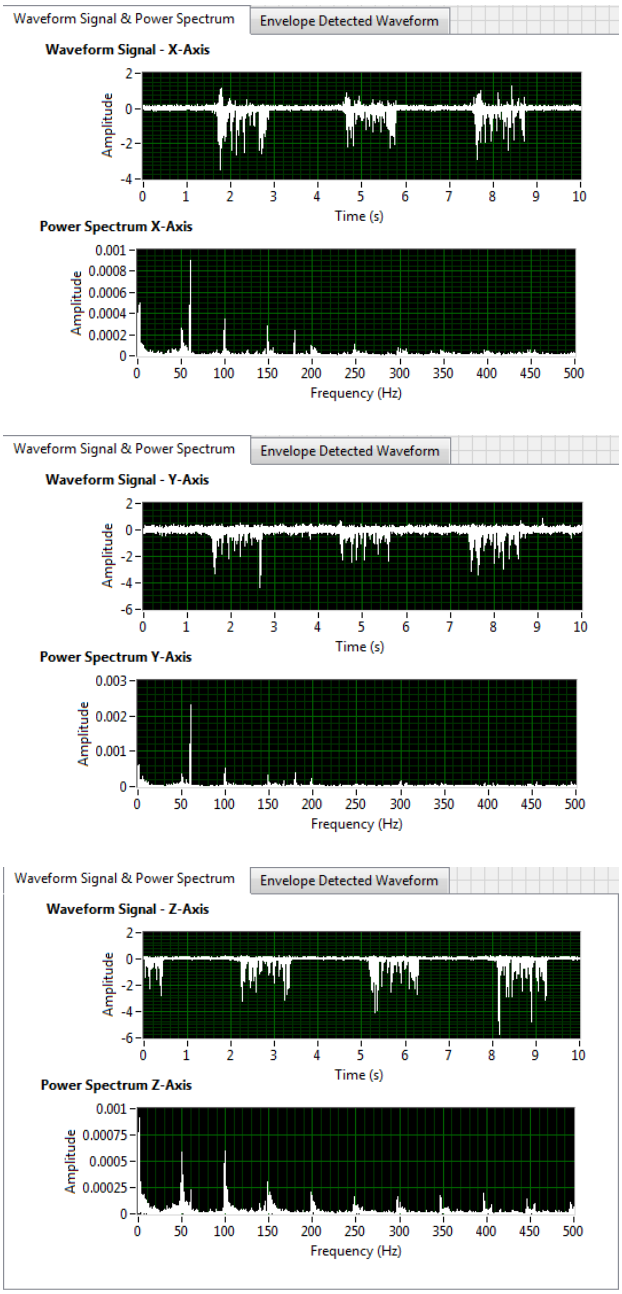

Figure 4.13. Raw waveforms and power spectrum – induced fault (phase 2) at 325 RPM (horizontal, axial, vertical axes)

4.4.5 Induced Component Faults Phase 3

The third and final phase of fault induced testing was used to demonstrate a bearing's vibration signature when the minor fault has progressed, or when a larger initial fault is present. Figure 4.14 displays these results at 325 RPM. The horizontal axis waveform showed an approximately 10% increase in signal noise floor with repetitive impacts occurring on a 3-second cycle. In the power spectrum plot, the fault progression is clearly seen as amplitude increases in the lower end of the frequency spectrum around running speed (5.4 Hz) as well as at line frequency (60 Hz) and 3X line frequency (180 Hz). The axial axis waveform component shows the signal transforming from the cyclical pattern towards one with larger overall signal magnitude and amplitude extremes. The vertical axis components in the time waveform retained the 3-second cyclical pattern, but decreased slightly in overall amplitude when compared to phase two plots.

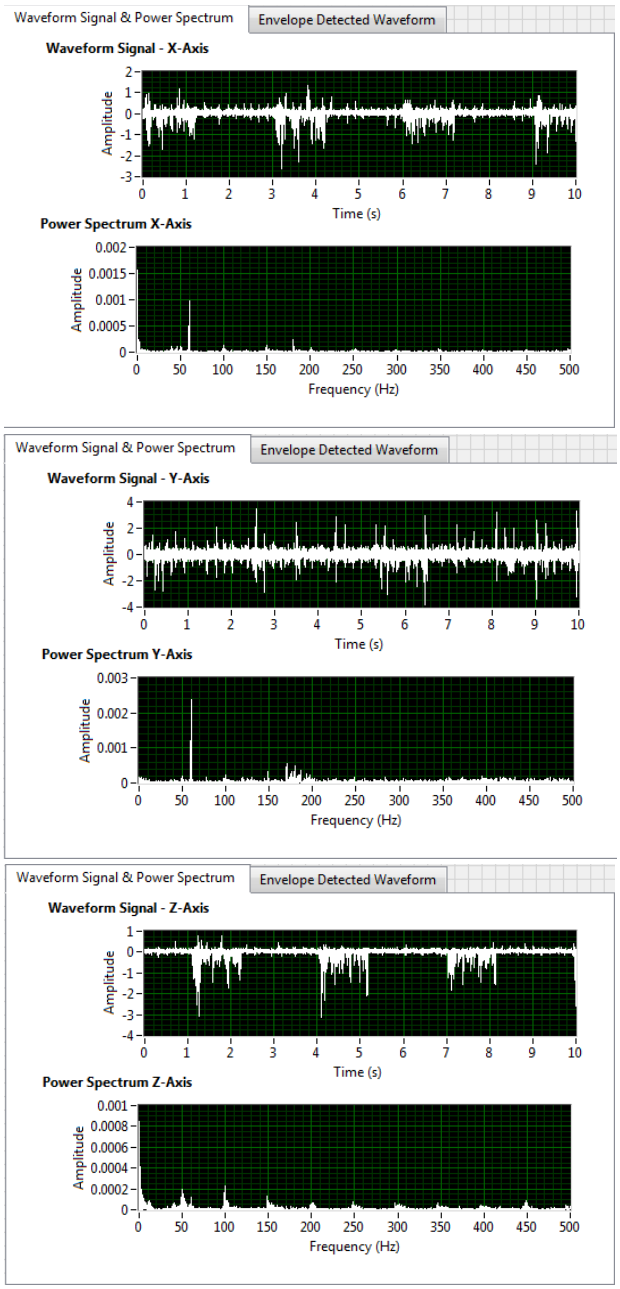

Figure 4.14. Raw waveform and power spectrum – induced fault (phase 3) at 325 RPM (horizontal, axial, vertical axes)

4.5. Envelope Data Reduction

This section of chapter four develops the analysis relating to the vibration signature after passing the signal through the enveloping process and interpreting it from enveloped waveform and spectrum plots. The analysis is based on vibration waveforms at operating speeds of 325 RPM, 450 RPM, and 900 RPM. 325 RPM waveforms appear throughout the chapter; 450 RPM and 900 RPM plots are shown in appendix A.

4.5.1. Enveloping through the Hilbert Transformation Method (325 RPM)

One of two enveloping methods discussed in section 2.8, the Hilbert transformation function, found in LabVIEW™, will be presented in this section and an envelope analysis performed on vibration data from the test bearing through five physical states ranging from unlubricated to lubricated followed by three phases of intentionally induced component faults designed to demonstrate fault progression.

4.5.1.1. Unlubricated Bearing Hilbert Envelope Analysis

The raw waveform from the unlubricated bearing was shown in figure 4.15. The enveloping process involves full wave rectification of the waveform where negative components are inverted and the envelope is developed. The red portion of the plot represents the envelope built from the raw waveform through the Hilbert transformation. The envelope spectrum is established using FFT analysis on the enveloped waveform and filtered from zero to 250 Hz. The third and final plot is a scaled version of the envelope spectrum showing details from zero to 50 Hz. Above 250 Hz, the amplitudes become

close to zero and are therefore omitted from the plot to better display the spectra in the lower zero to 250 Hz range.

The unlubricated state is included in this study to demonstrate what the vibration signature might look like if there is a lack of lubrication. With the goal of avoiding any residual damage, the newly installed bearing was exposed briefly to the unlubricated service condition at 325 RPM and 450 RPM for only the 10 second time intervals necessary to collect vibration data. The bearing was not tested at 900 RPM to avoid any permanent damage. The results are displayed in figure 4.15. The amplitudes in the time waveform plots, FFT spectra, and enveloped spectra generated during testing are compared to the lubricated state results (figure 4.16) and evaluated in further detail in the subsequent section.

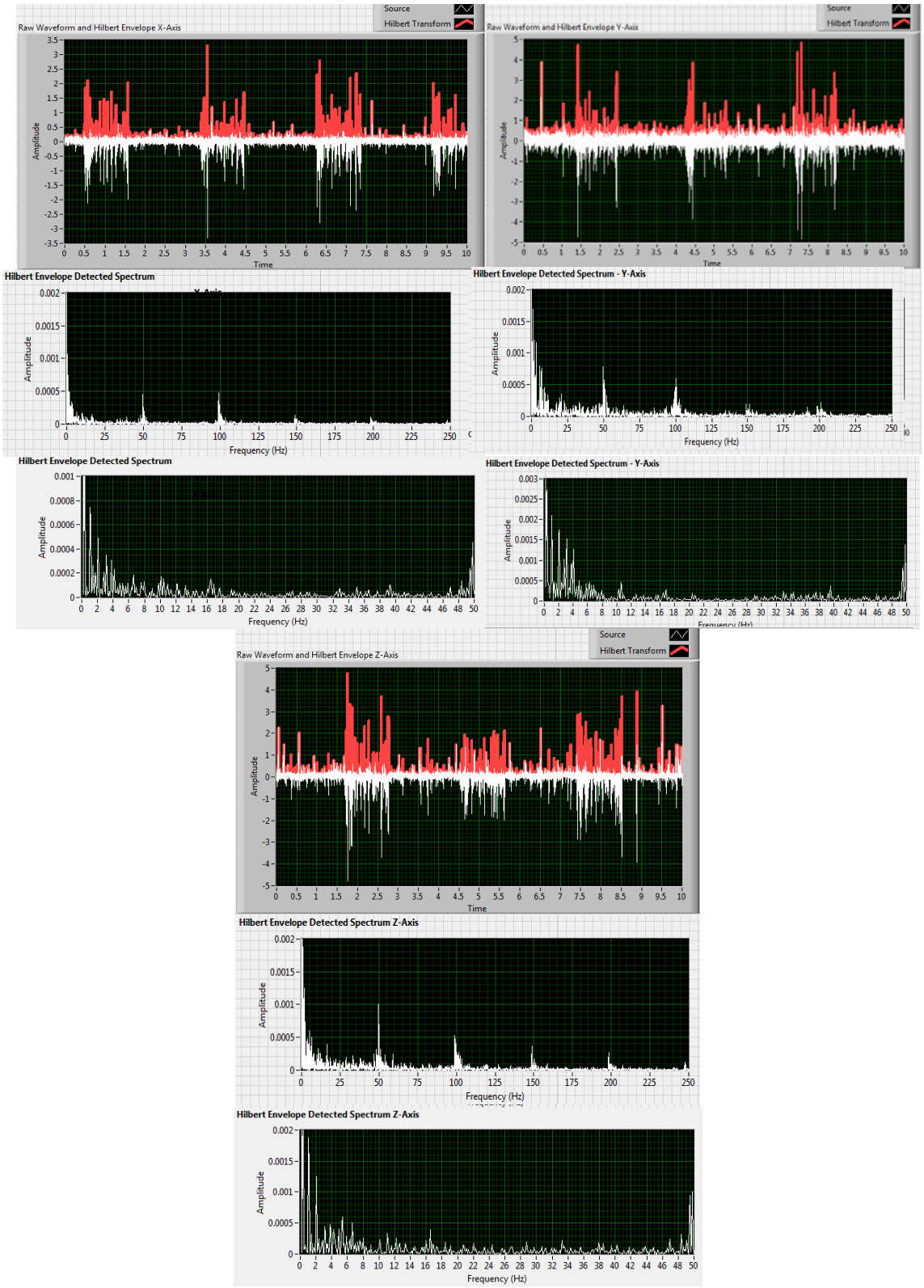

Figure 4.15. Hilbert envelope waveform and frequency spectrum (unlubricated at 325 RPM) - horizontal, axial, vertical axes

4.5.1.2. Lubricated Bearing Hilbert Envelope Analysis

When comparing the unlubricated and lubricated enveloped spectra, the expectation is to see "cleaner" or lower vibration amplitudes in the spectral plots of the lubricated state. The vibration signature between the two states is interesting as it does show an amplitude reduction at some frequencies, while other frequencies have an amplitude increase (see figure 4.16).

Taking a look at the horizontal axis raw waveforms between this and the previous state, the highest peak was 3.25g for the unlubricated state while the max peak registered in the lubricated state was only 2.75g. Other peaks in the horizontal axis were between 2g and 3g (unlubricated) and between 1g and 2g (lubricated). Examining the enveloped waveform plots, the lubricated state clearly shows smaller overall amplitude vibration signatures confirmed by a lower noise floor. The lubricated plots show a cyclical vibration pattern. While this pattern is still somewhat present in the unlubricated waveforms, it is obscured by the added vibrations caused from looseness due to lack of lubrication as the rolling elements have excessive clearance without the specified grease.

Comparing the bearing vibration at 325 RPM in the unlubricated to lubricated states, the horizontal axis enveloped spectrum plot shows slight increases in low frequency amplitude around fundamental train frequency (FTF) when lubrication was applied with the rest of the bearing fault frequency range showing no faults as shown in figure 4.15. The time waveform plots, however indicate the expected large decreases in noise floor and overall amplitude across the fault frequency range. At 450 RPM, the axial axis enveloped spectra results show a significant decrease in amplitude in the 0-50

Hz bearing fault frequency range as shown in figure 4.15. This variation in enveloped spectra is an example of the importance of using all of the information available to the analyst when determining overall bearing condition. In this case the time waveform plots contributed the most value to determining bearing condition. One must also be aware that the enveloping method is an extraction of very low amplitude vibrations obscured by larger amplitude, lower frequency peaks in the traditional FFT spectrum. During bearing testing, the amplitude demodulation process was observed to have minutely different amplitude results when each ten second test sample was taken consecutively however, frequency extraction was highly consistent.

325 RPM unlubricated

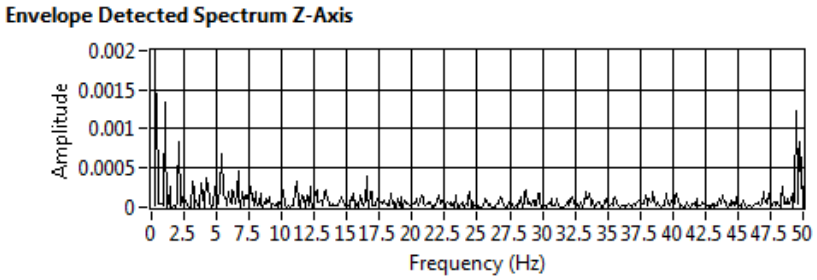

325 RPM lubricated

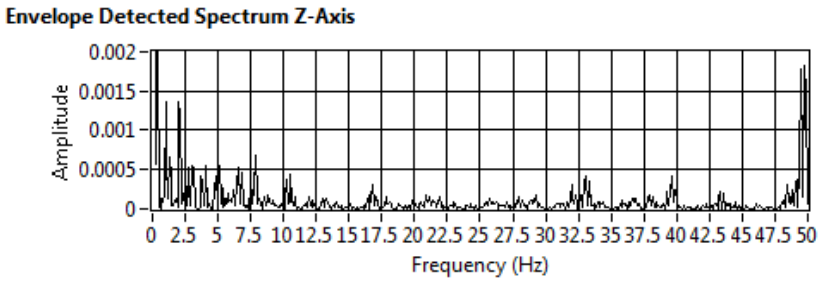

450 RPM unlubricated

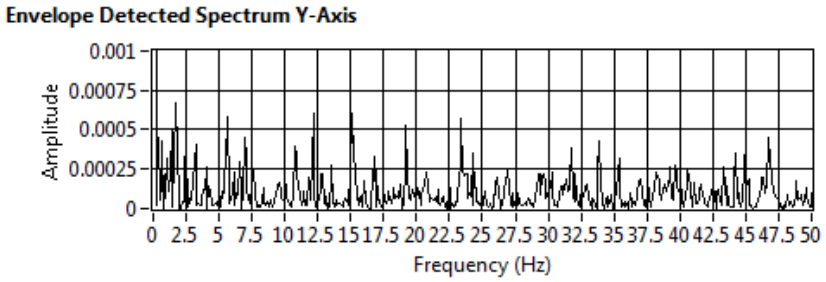

450 RPM lubricated

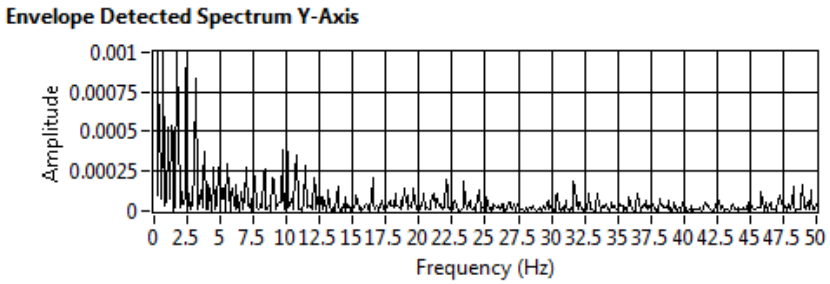

Figure 4.16. Unlubricated to lubricated results at 325 RPM and 450 RPM

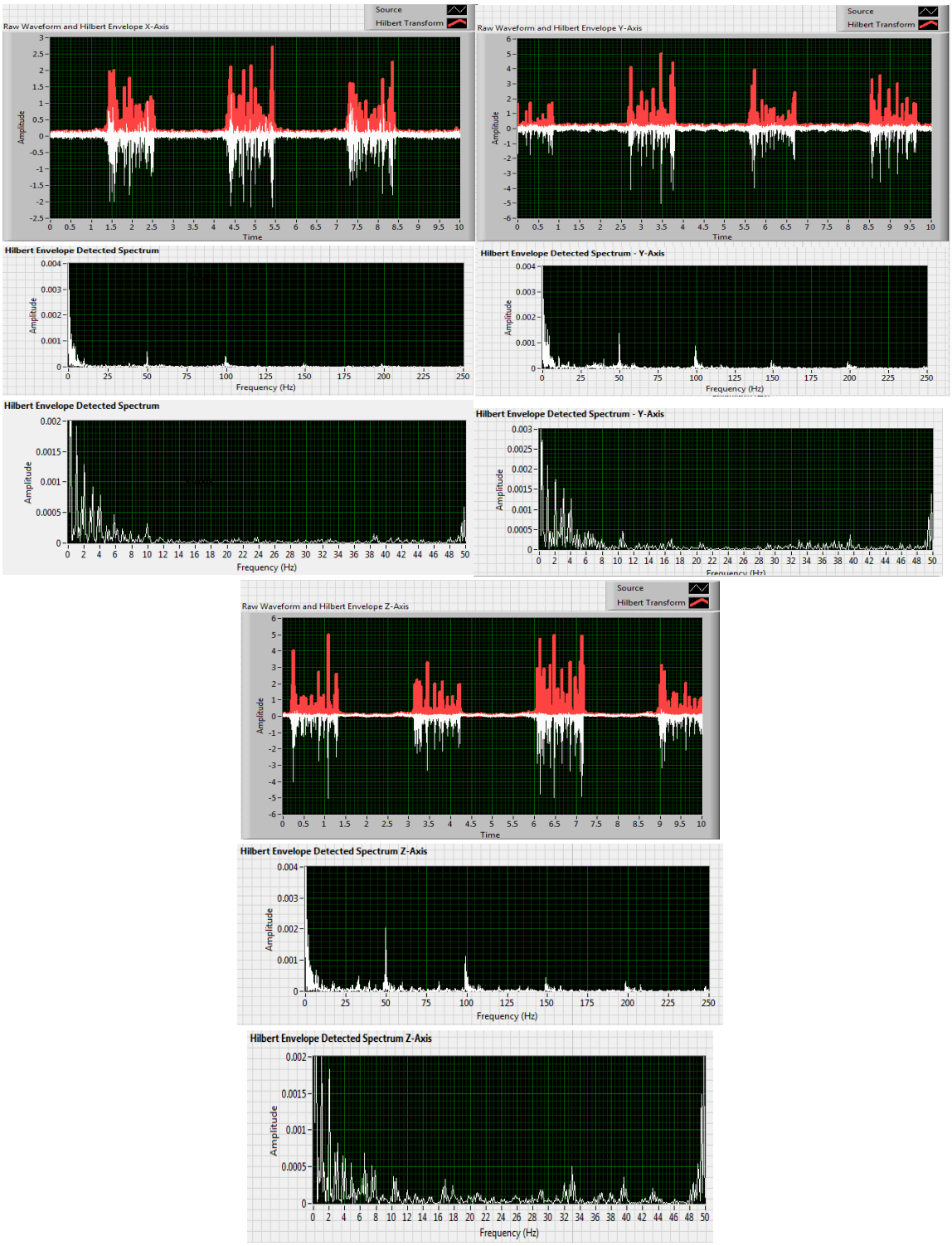

Figure 4.17. Hilbert envelope waveform and frequency spectrum (lubricated, 325 RPM) - horizontal, axial, vertical axes

4.5.1.3. Phase I: Component Fault Hilbert Envelope Analysis

The next phase of the bearing test was an intentionally induced fault to the cage, rolling element, and inner race of the bearing using a small drill bit to introduce imperfections to the surfaces. The resulting enveloped plots are shown in figure 4.17. It is important to note that the signal noise floor has a tendency to obscure the bearing fault frequencies in the initial fault stage, but fault frequencies can still be identified. This issue is minimized as the fault severity is increased or the operating speed is increased. The lubricated and fault phase one plots can now be compared.

At 325 RPM, the enveloped spectrum plot for the horizontal axis at fundamental train frequency at 0.0015g is an increase from 0.0010g. The vertical axis at the same frequencies showed very slight increases in gravity units from the lubricated to phase one states while the axial vibration slightly decreased from 0.0014g to 0.0011g. It is feasible that small amplitude measurement variability from sample to sample can be an artifact of the filtering process or a result of not enough induced damage to be detectible. However, when looking at the enveloped time waveform plots for the horizontal and axial axes, it is possible to visually confirm that phase one peaks are generally higher in amplitude than in the lubricated state. The vertical axis results are the exception with lower vibration amplitudes in both waveform and spectrum plots. This change in direction of the vibration amplitudes at the frequencies of interest is intriguing as the component fault is introduced.

At 450 RPM, the vertical axis in the phase one state had a small 0.0003g amplitude spike around the calculated inner race fault frequency. The fundamental train

frequency was recorded slightly higher than the calculated value but was present at 3.1 Hz in all three axes. Also, as seen earlier in the Fast Fourier Transform analysis (see sections 4.4.2 and 4.4.3), the outer race and 2x outer race frequencies are present the enveloped spectra, however the amplitude is very small at 0.0005g, and did not increase from the lubricated state.

At 900 RPM phase I, the horizontal axis only has a 0.0002g at fundamental train frequency. The rest of the spectrum up to 100 Hz is clean of bearing fault frequencies. The axial direction confirmed a 0.0004g at the same frequency. The vertical axis had a clean spectrum with no noticeable faults.

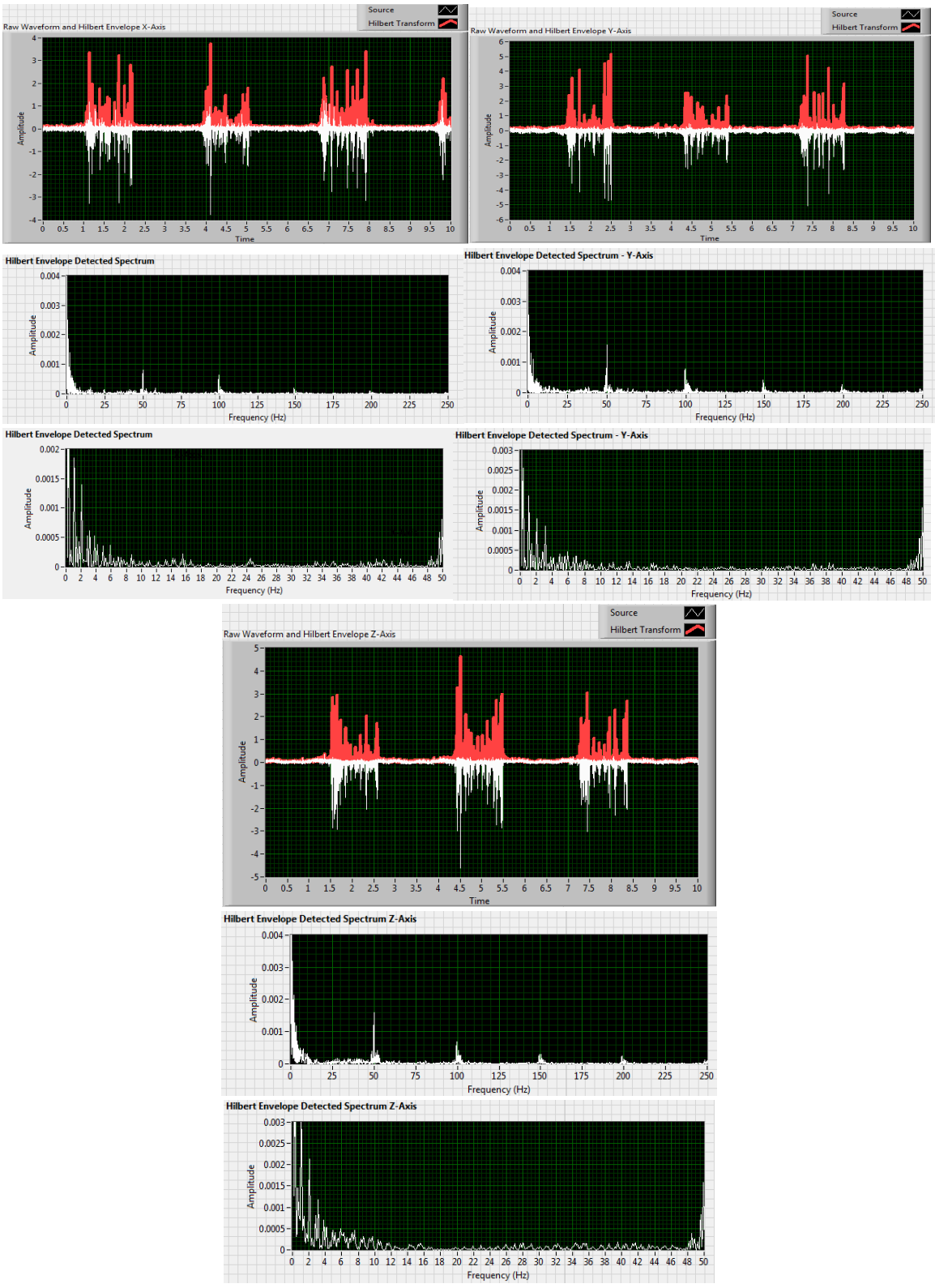

Figure 4.18. Hilbert envelope waveform and frequency spectrum (phase 1 fault at 325 RPM) - horizontal, axial, vertical axes

4.5.1.4. Phase 2: Component Fault Hilbert Envelope Analysis

For the second phase of induced fault vibration testing, more surface damage was added to the bearing cage and rolling element with a small drill bit at the same physical location as phase one. The previously defined data acquisition parameters continued to be applied with the resulting waveforms and spectra plotted in three directions.

At 325 RPM and in the horizontal direction, the fundamental train frequency (2 Hz) at 0.0014g is the only bearing fault frequency shown and did not change in amplitude when compared to phase one. However, in the vertical axis, the fundamental train frequency increased in amplitude from 0.0015g to 0.0024g in the enveloped spectra. This almost doubling in amplitude is an indication of the progression of a cage fault.

At 450 RPM, the horizontal axis spectra recorded a marginal increase from 0.0006g to 0.0007g for fundamental train frequency (3 Hz) in addition to a very small 16 Hz peak, which is close to the calculated ball spin frequency. This increase was confirmed by a vertical axis FTF amplitude doubling in intensity from 0.0005g to 0.001g. The inner race fault frequency of 37 Hz is now present at 0.00025g. In the axial direction, a 0.0003g ball spin frequency is present but not an increase from phase one.

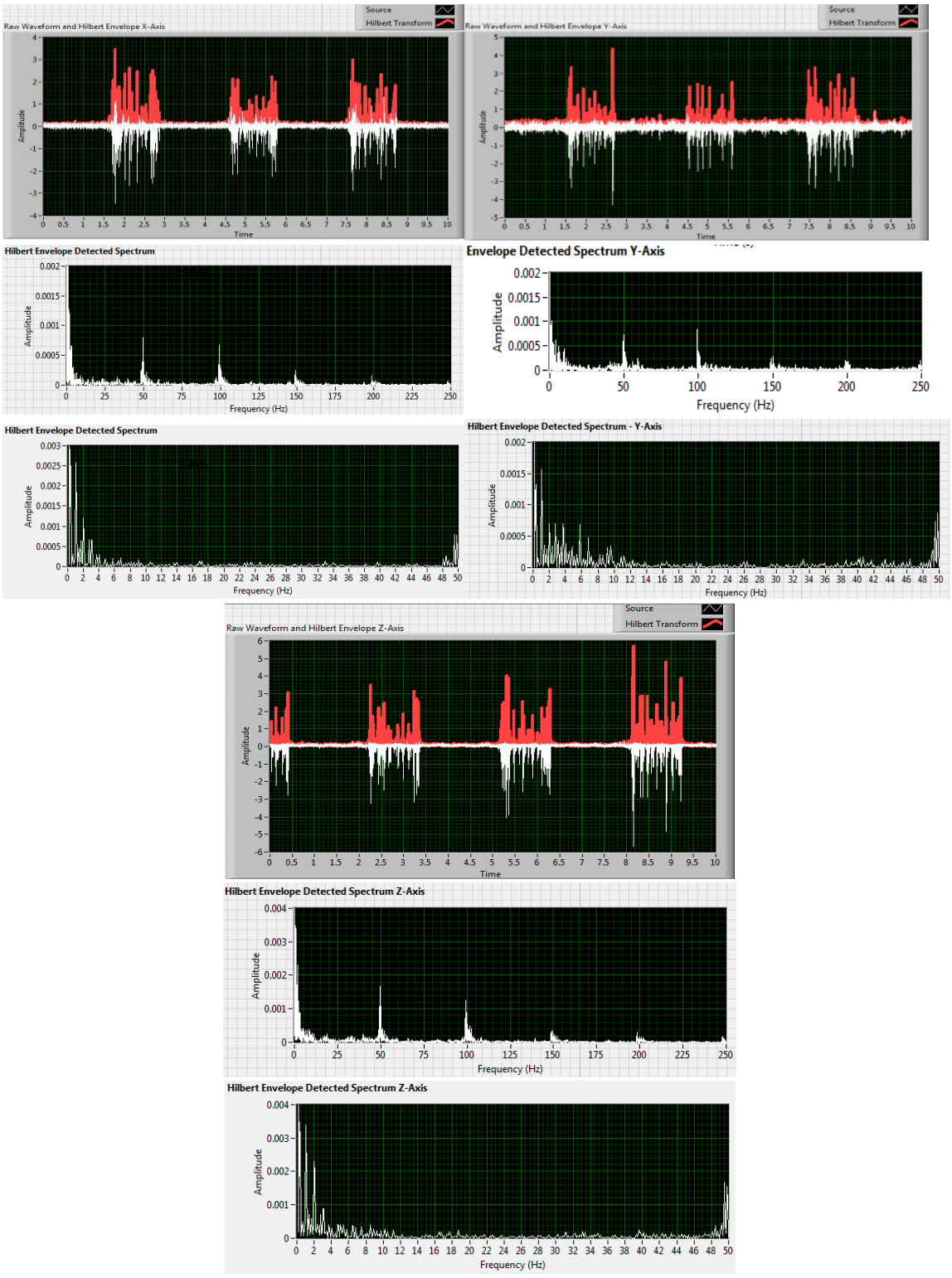

Figure 4.19. Hilbert enveloped waveform and frequency spectrum (phase 2 fault at 325 RPM) - horizontal, axial, vertical axes.

4.5.1.5. Phase 3: Component Fault Hilbert Envelope Analysis

For phase III, further damage to the bearing's cage and a chosen rolling element was applied carefully at the same physical location to attempt to simulate a fault that is progressing in severity. The horizontal axis enveloped waveforms do not appear to show much amplitude deviation from phase II, but the enveloped spectra indicate a significant reduction in vibration amplitude.

At 325 RPM, the axial axis enveloped time waveform shows a large amplitude increase in the noise floor with many impulses, including multiple amplitudes above 3g. The axial axis enveloped spectrum differs significantly from the previous phases and can be described as multiple peaks of running speed (5.4 Hz) varying from 0.0008g to 0.0024g, with diminishing amplitudes as frequency increases. A large 0.0016g peak at 11 Hz ball spin frequency is a sure sign of fault progression as it was not present during phase two.

At 450 RPM, the vertical axis confirms a small 36 Hz inner race fault frequency present at 0.006g is a significant increase from phase two indicating fault progression. Vibration signature changes between the three phases confirm that as fault severity increases, vibration energy is concentrated within a particular axis, and this energy concentration appears to cause a reduction of amplitude in the other axes. The increase in fault severity is also indicated by the multiple peaks and harmonics of running speed.

A visual assessment of the damage induced for phase 3 can be seen in figures 4.19 through 4.23. The faults can be seen directly as imperfections in the inner race and cage parts of the assembly. The rolling elements themselves did not show any visual signs of

contact surface scratching or galling. The heat treatment of the metal combined with extremely fine surface finish and round shape of the rolling elements posed a significant challenge to induce a fault directly with the chosen drilling tool. The outer race was not targeted in this study and as expected, showed no signs of damage.

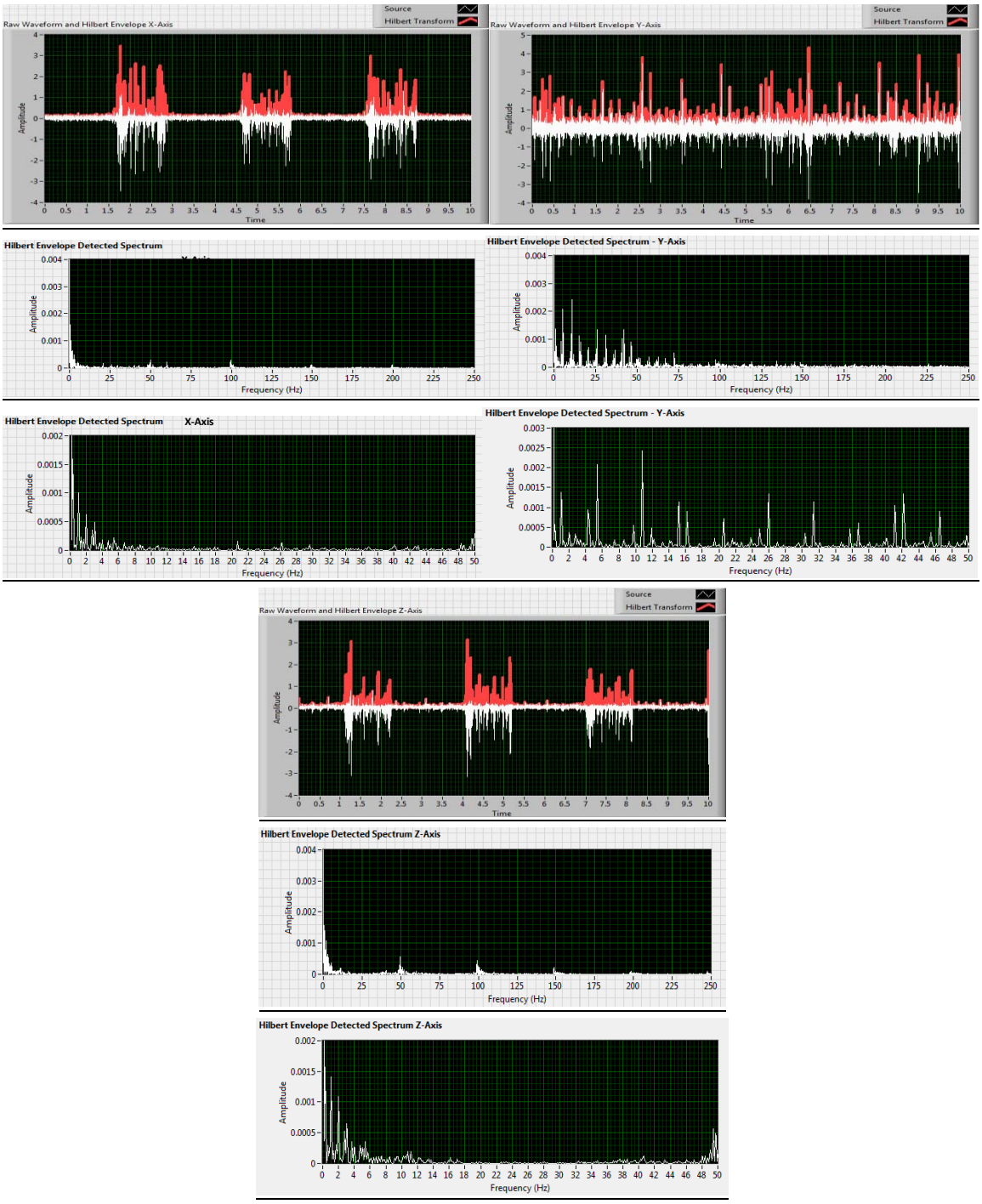

Figure 4.20 Hilbert envelope waveform and frequency spectrum (phase 3 fault at 325 RPM) - horizontal, axial, vertical axes

Figure 4.21 Test bearing exploded view.

Figure 4.22 Test bearing outer race (phase 3 fault).

Figure 4.23 Test bearing inner race (phase 3 fault).

Figure 4.24. Test bearing cage damage (phase 3 fault)

4.5.2. Order Analysis Toolkit Acceleration Enveloping (325 RPM)

A second algorithm developed by National Instruments, called the order analysis toolkit (OAT), extracts the modulating signal from the overall amplitude-modulating signal. Some types of mechanical faults exhibit this type of modulating signal pattern, and are therefore detectible through this signal processing technique. The OAT virtual instrument envelope waveforms and spectral plots will be presented in the following sections. Envelope analysis parallel to that completed for the Hilbert transformation will be done, including comparisons to the Hilbert transformation results. A formal performance analysis is discussed in section 4.6.

4.5.2.1. Unlubricated Bearing OAT Envelope Analysis at 325 RPM

The unlubricated phase data was used again with OAT Enveloping Analysis to demonstrate the enveloped signal from an undamaged bearing strictly under an inadequate lubrication condition. Vibration data was collected in three perpendicular directions. Corresponding envelope waveforms and frequency spectral plots were generated, shown in figure 4.24. The zoomed frequency spectrum plot of the enveloped signal is shown directly below the unscaled plot, better displaying the lower zero to 50 Hz range where a majority of the vibration signature exists.

The horizontal axis OAT envelope waveform exhibits the same 3-second cyclical pattern as, the Hilbert method waveform, with amplitude maximums of 3.4g and 2.8g. The spectra show some subtle differences in amplitudes at 50 Hz and 100 Hz. Axial axis envelope waveforms were also very similar, but spectra showed variations in amplitudes

at 50 Hz and 100 Hz with amplitudes being about 0.002g smaller on the OAT plots. The vertical axis spectrum showed the opposite effect at 50 Hz; its Hilbert amplitude was approximately 0.002g smaller than the OAT plot. At other frequencies, both methods appeared to have nearly identical amplitudes.

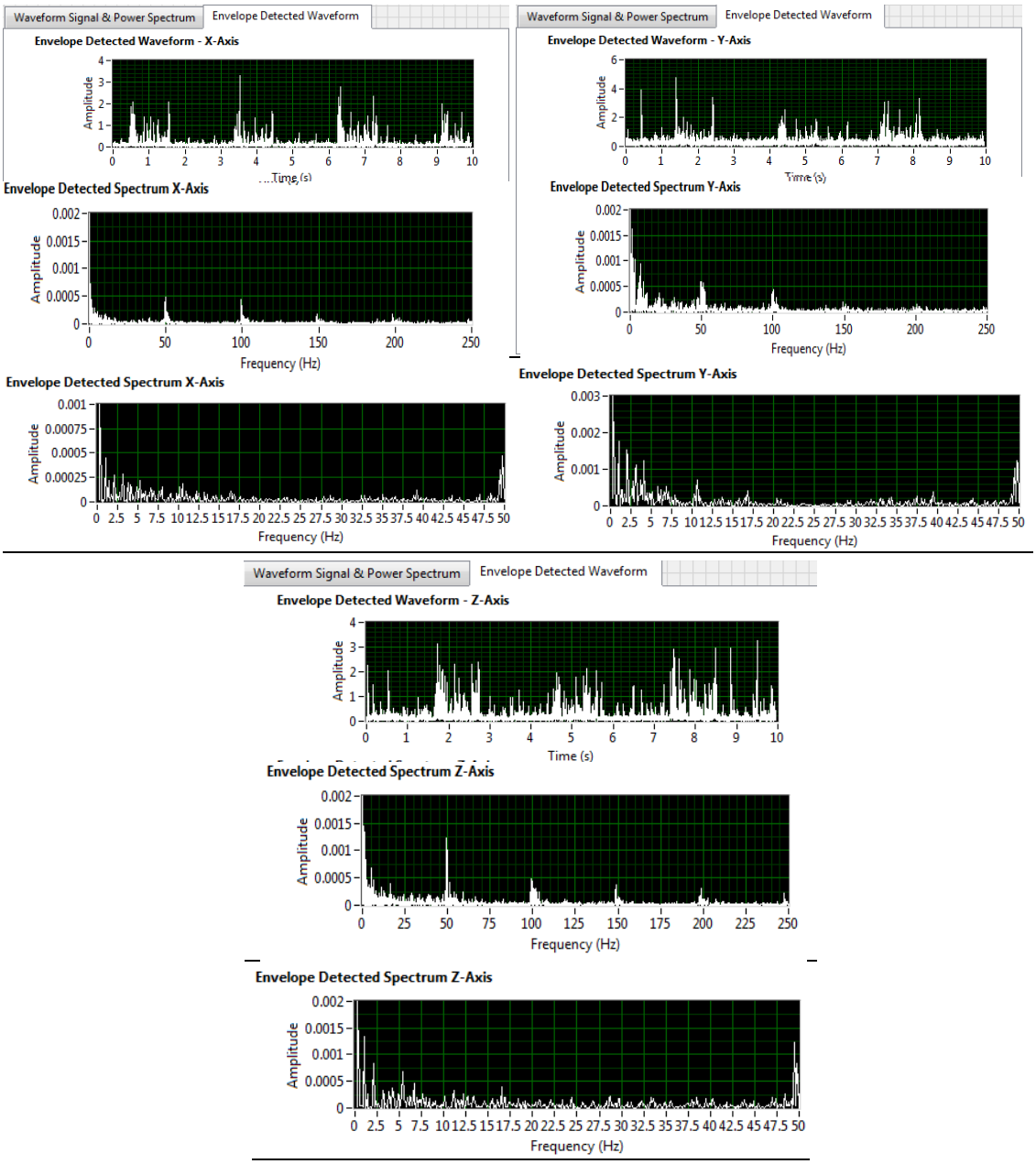

Figure 4.25. OAT envelope waveform and frequency spectrum (unlubricated at 325 RPM) - horizontal, axial, vertical axes.

4.5.2.2. Lubricated Bearing OAT Envelope Analysis at 325 RPM

The lubricated phase demonstrates the vibration signature from a bearing that is in good mechanical condition and operating as designed. This signal represents a baseline with which future measurements could be compared. Figure 4.25 displays the enveloped waveforms and spectra from the three directions.

In the 325 RPM unlubricated state, the axial and vertical axes enveloped waveforms show a significantly higher noise floor, and the 3-second cyclical pattern of the lubricated state is overcome by the added lower amplitude vibrations. The spectra in the lubricated state have lower overall amplitudes throughout the 0-250 Hz frequency band (with the exception of 50 Hz and 100 Hz peaks). When compared to the enveloped waveforms and spectra from the Hilbert transformation, there were slight variations in amplitudes. The horizontal, axial, and vertical axis 50 Hz peak from OAT was about 0.0002g lower in amplitude while the OAT axial axis 11 Hz peak was about 0.0004g higher than the Hilbert spectrum.

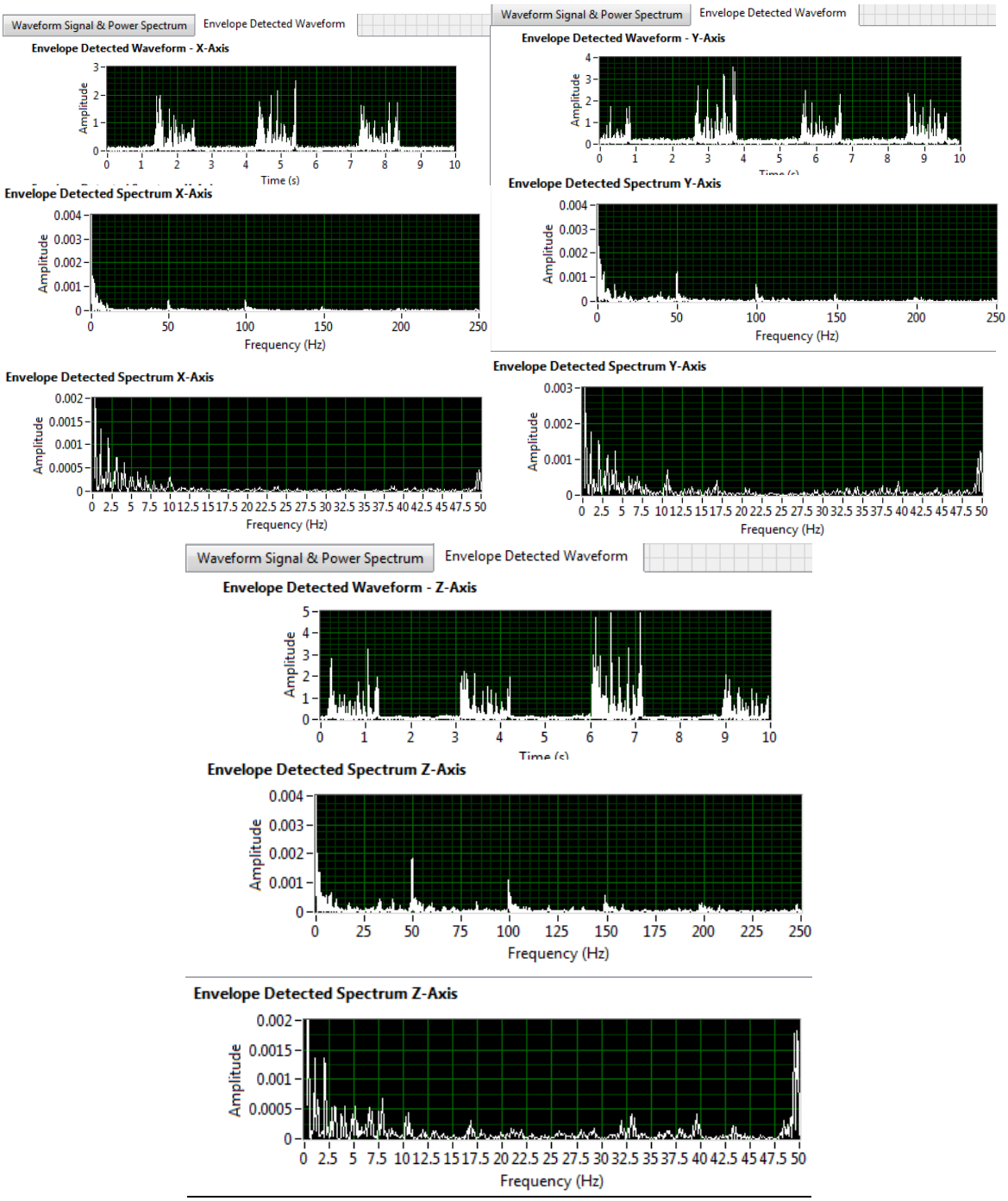

Figure 4.26. OAT envelope waveform and frequency spectrum (lubricated bearing at 325 RPM) - horizontal, axial, vertical axes.

4.5.2.3. Phase I: Component Fault OAT Envelope Analysis at 325 RPM

A fault on the cage of the test bearing was induced by introducing a local surface imperfection in three phases; each with increasing severity. For the first phase, a drilling tool was utilized, between the cage and rolling element to induce small imperfections. These imperfections can be detected as amplitude escalation at frequencies of interest.

The enveloped horizontal axis spectrum from the lubricated stage at 50 Hz displays an amplitude of 0.0005g while the phase one fault induced results (see figure 4.26) show an amplitude of 0.00075g. The axial axis spectrum also shows a slight increase in amplitude at 50 Hz in the spectrum plot. The vertical axis envelope spectrum showed an amplitude decrease at both 50 Hz and 100 Hz. This can also be seen in the enveloped waveform spectrum as reduced amplitude across the entire 0-250 Hz frequency band. This phenomenon suggests the possibility of a directional shift in the vibration signal due to the induced fault. Comparing the Hilbert transform results to the OAT spectrum plots, the axial axis at 50 Hz shows a difference of 0.00025g with some variations in the enveloped time waveforms as well.

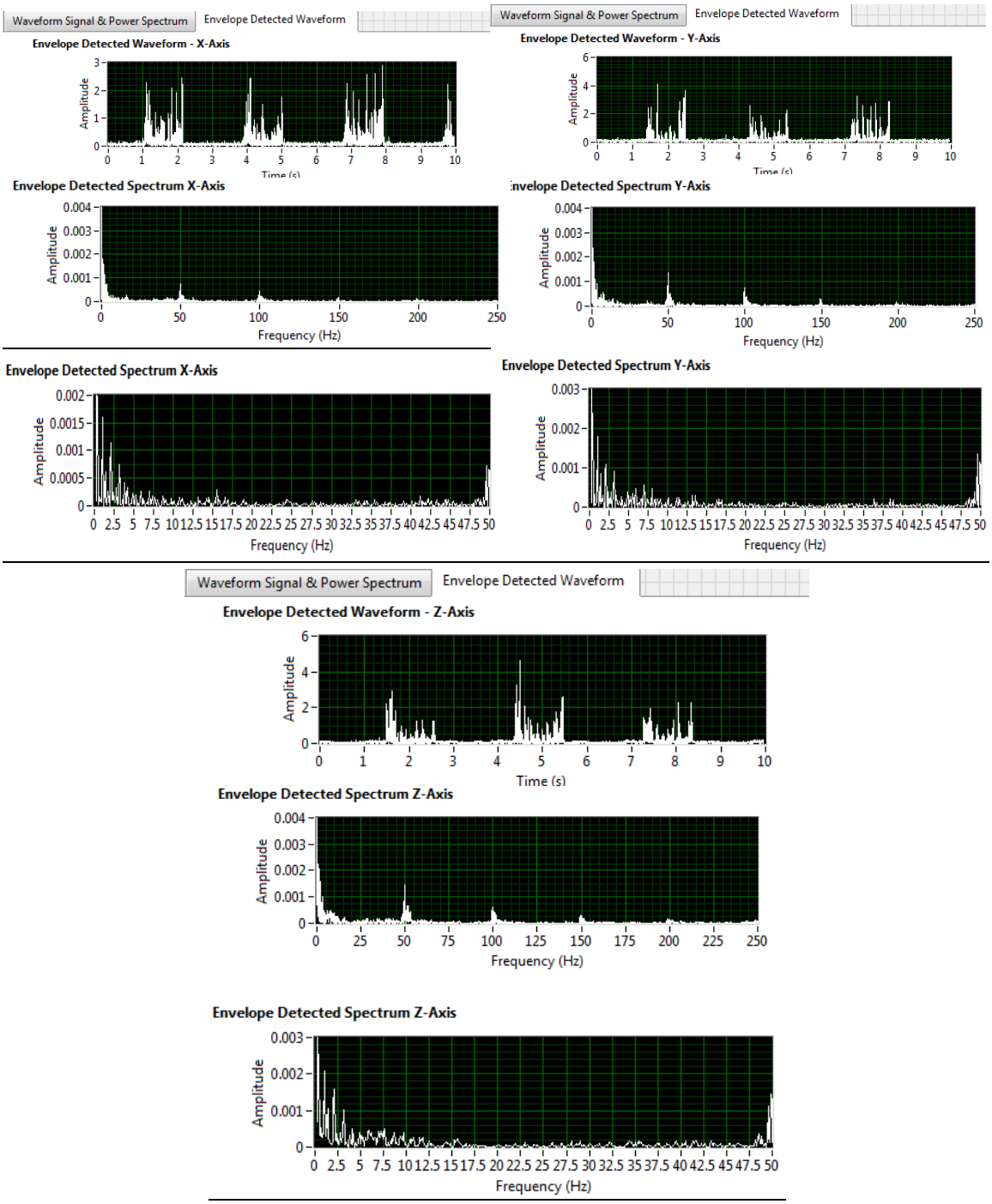

Figure 4.27. OAT Envelope waveform and frequency spectrum (phase 1 fault at 325 RPM) - horizontal, axial, vertical axes.

4.5.2.4. Phase 2: Bearing Component Fault OAT Envelope Analysis at 325 RPM

The second phase increased the fault severity by removing some more material from the cage and rolling element surface as compared to just scratching the surfaces in phase I. The resulting plots are shown in figure 4.27. Interestingly enough, the amplitude at 50 Hz from the axial axis spectrum decreased by a factor of two, while the vertical axis spectrum plot resulted in an amplitude increase of 0.0004g or about 25% at 50 Hz.

In comparison to the Hilbert enveloping method, there were some variations in amplitudes. The 50 Hz peak from Hilbert was 0.0003g higher than the OAT spectrum plot. The enveloped waveforms appeared very similar with some slight variations between the two algorithms especially in the vertical axis.

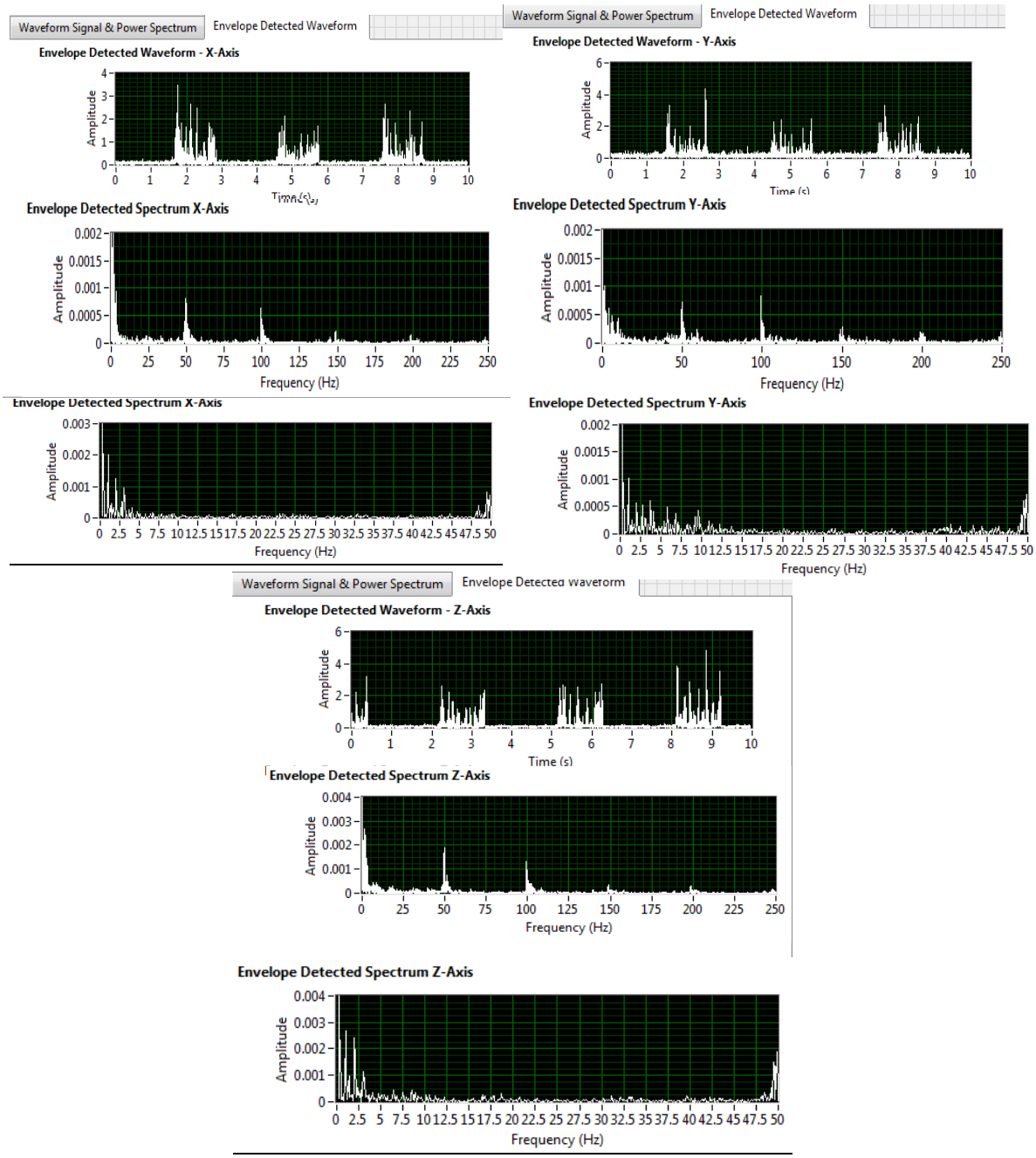

Figure 4.28. OAT envelope waveform and frequency spectrum (phase 2 fault at 325 RPM) - horizontal, axial, vertical axes.

4.5.2.5. Phase 3: Bearing Component Fault OAT Envelope Analysis at 325 RPM

In the third and last phase of the test experiment, a higher level of damage to the cage and rolling element was induced in the same location as in the previous two phases. This phase demonstrates the vibration signature from a cage/rolling element fault further into its progression. Figure 4.28 shows the resulting waveform and spectral plots from the test bearing utilizing the same parameters.

The horizontal axis and axial axis waveform plots display an increased noise floor that is starting to obscure the original bearing signature. Axial axis waveforms are significantly changed in phase three with higher overall amplitude and noise floor as well. The vertical axis waveform plot retains the original machine signature with slightly decreased overall amplitude. This could indicate that there was less excitation from the fault in this plane or that the fault caused the vibration energy to decrease in that direction while increasing elsewhere.

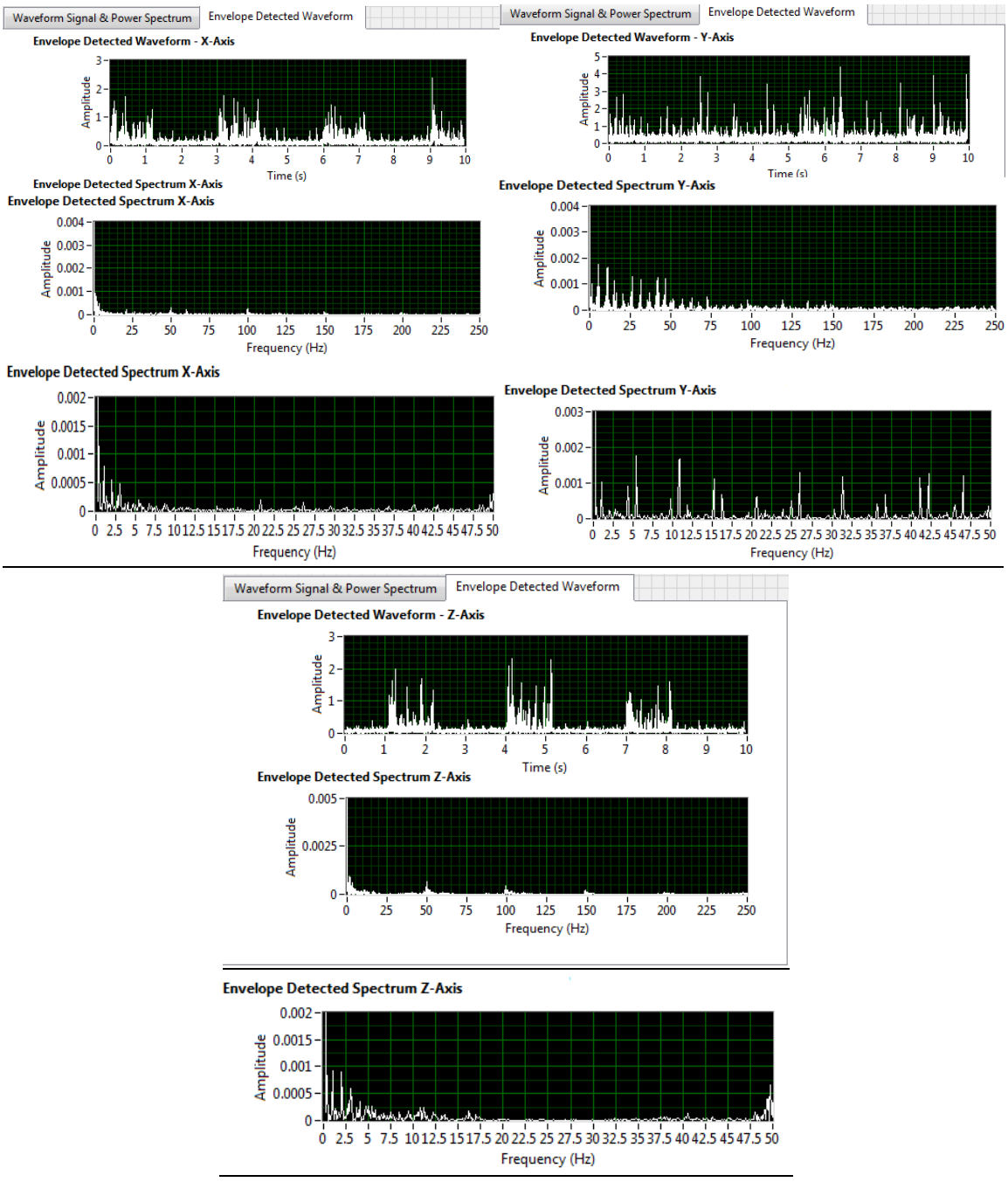

Figure 4.29. OAT envelope waveform and frequency spectrum (phase 3 fault at 325 RPM) - horizontal, axial, vertical axes.

4.6. Performance Analysis of Hilbert and OAT Enveloping Methods at 325 RPM

Using the calculated frequencies in section 4.5, a performance comparison between the two enveloping algorithms can be performed. The enveloped waveform and spectrum plots are evaluated between the traditional Hilbert transform and the LabVIEW™ OAT methods to reveal any differences in fault detection capabilities. This examination will focus on the bearing physical states (at 325 RPM) presented in chapter four.

4.6.1. Raw Waveform Enveloping Performance at 325 RPM

A visual comparison of the enveloping performance of the raw waveforms between the Hilbert and OAT methods is shown below (for triaxial data collected at 325 RPM). The data is phase (time) matched so comparisons can be made directly. This portion of the analysis will focus on differences between the two methods and not on the ability of each algorithm to extract the signals of interest (i.e. bearing fault frequencies). In section 4.6.2, bearing defect frequencies extracted by each method of envelope spectrum analysis will be compared.

Observing the horizontal axis graphs in Figure 4.29, in nearly all of the Hilbert plots (left), the peak amplitudes across the ten second time interval were higher overall than from the OAT plots (right), however the shape of the signal was similar in both cases. The Hilbert portion (red) of the plot appears to display more noise and less signal definition than is present using OAT, but this could be an effect of overlaying the enveloped signal portion over the raw waveform. As expected, the overall amplitudes

decrease from the unlubricated to the lubricated states, and then increase again as the phase I fault is introduced. Similarly, amplitude increases occur with faults in phases II and III, respectively.

From the axial and vertical axis plots (see figures 4.30 and 4.31 respectively), the Hilbert amplitudes are again higher overall than the OAT amplitudes, and there are subtle differences in the resulting waveforms. Both algorithms accomplish the goal of drawing an envelope of the amplitude versus time plot, however, the resulting minor variability in the mathematical processing is apparent. (Hilbert on left, OAT on right).

Unlubricated 325 RPM (Horizontal Axis)

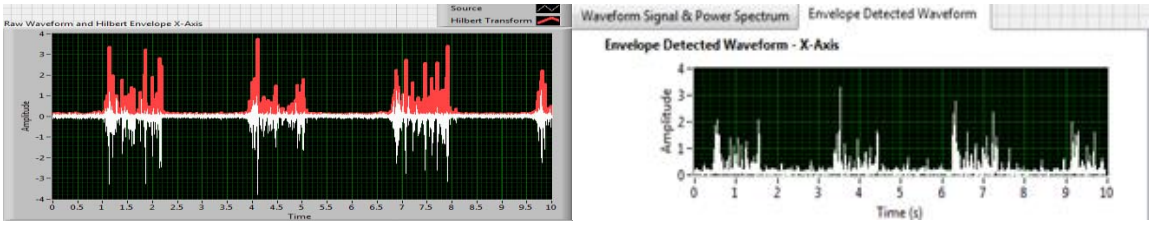

Lubricated 325 RPM (Horizontal Axis)

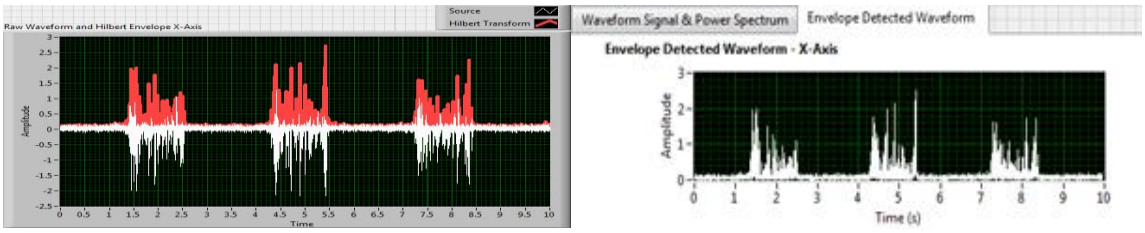

Phase I Fault, 325 RPM (Horizontal Axis)

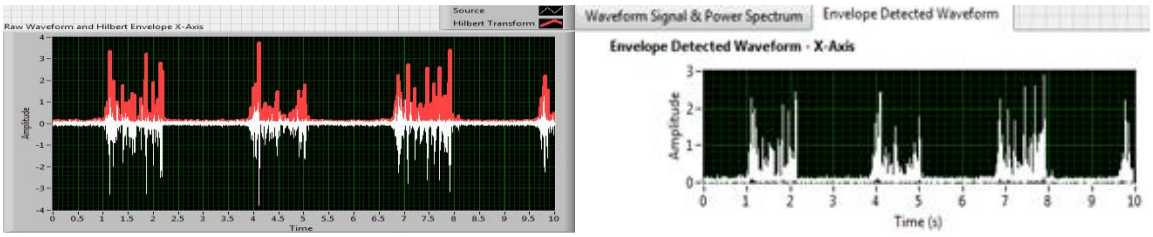

Phase II Fault, 325 RPM (Horizontal Axis)

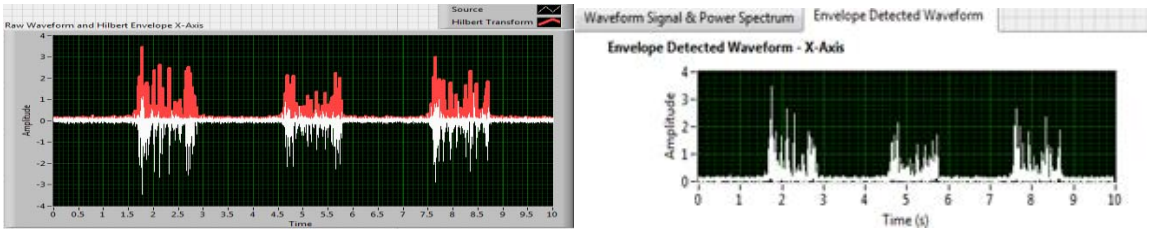

Phase III Fault, 325 RPM (Horizontal Axis)

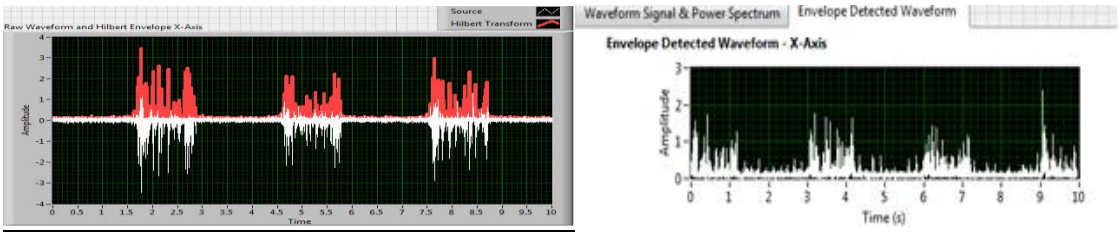

Figure 4.30. Horizontal axis enveloped waveform data: Hilbert (left) OAT (right).

Unlubricated (Axial Axis)

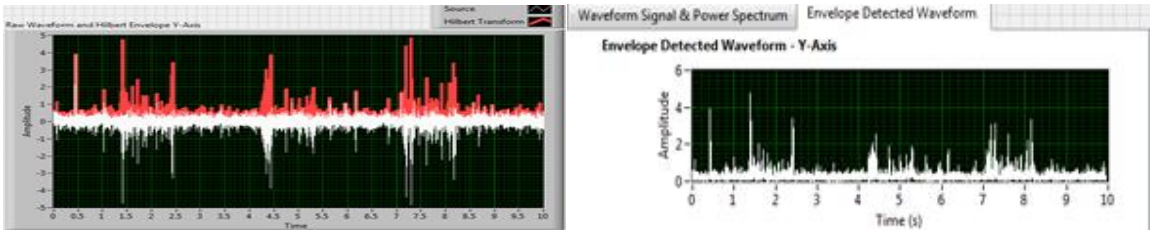

Lubricated (Axial Axis)

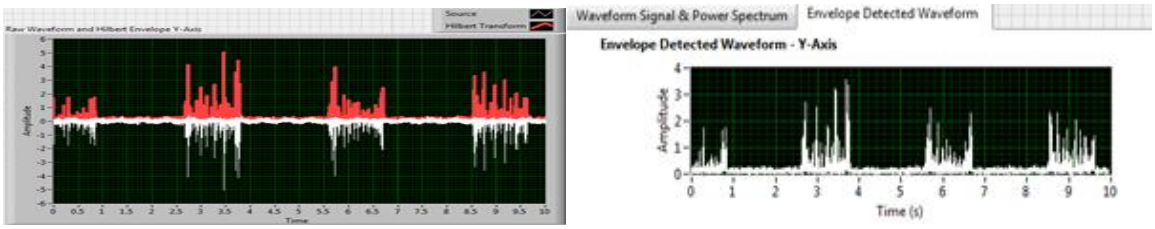

Phase I Fault, 325 RPM (Axial Axis)

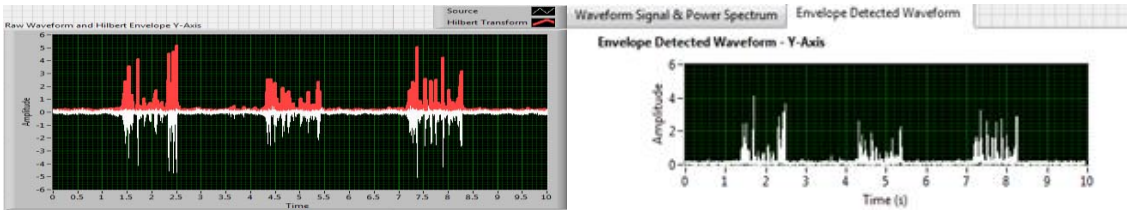

Phase II Fault, 325 RPM (Axial Axis)

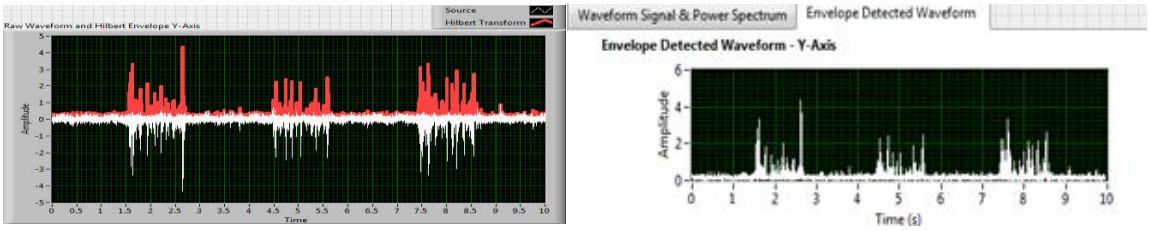

Phase III Fault 325 RPM (Axial Axis)

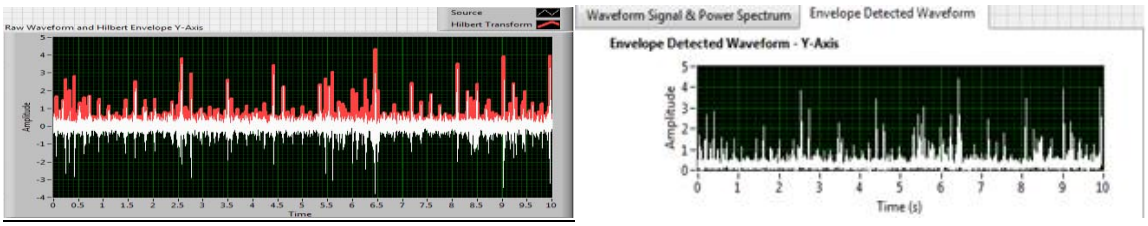

Figure 4.31. Axial axis enveloped waveform data: Hilbert (left) OAT (right).

Unlubricated (Vertical Axis)

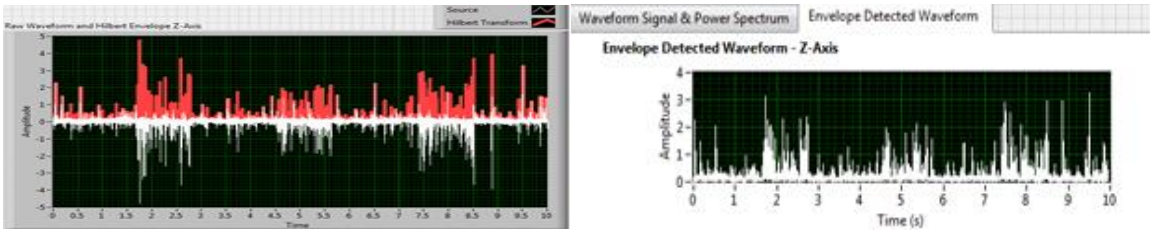

Lubricated (Vertical Axis)

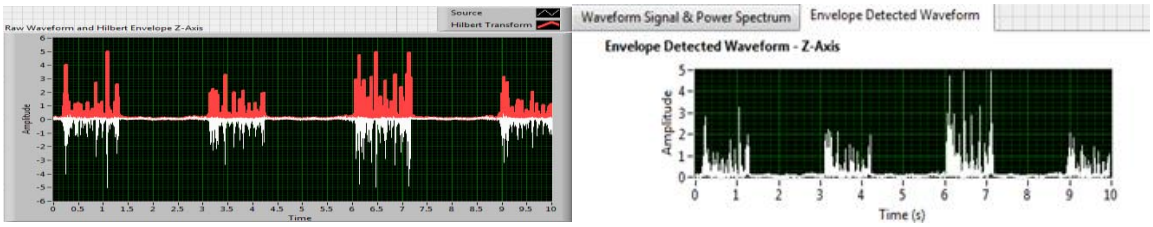

Phase I Fault, 325 RPM (Vertical Axis)

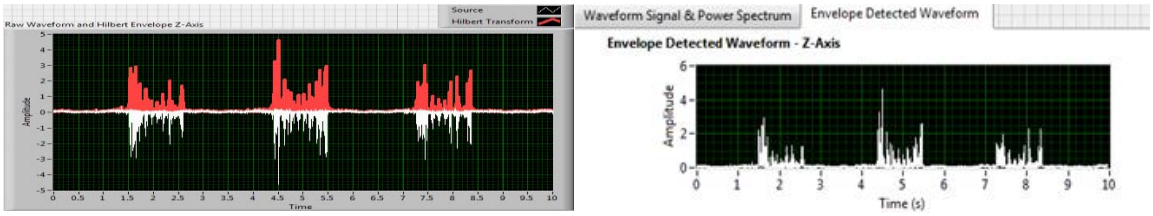

Phase II Fault, 325 RPM (Vertical Axis)

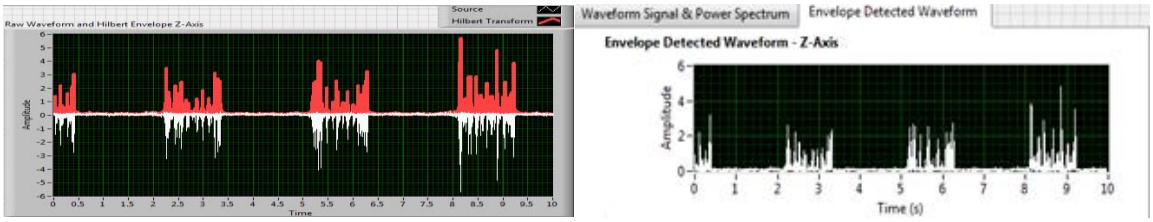

Phase III Fault, 325 RPM (Vertical Axis)

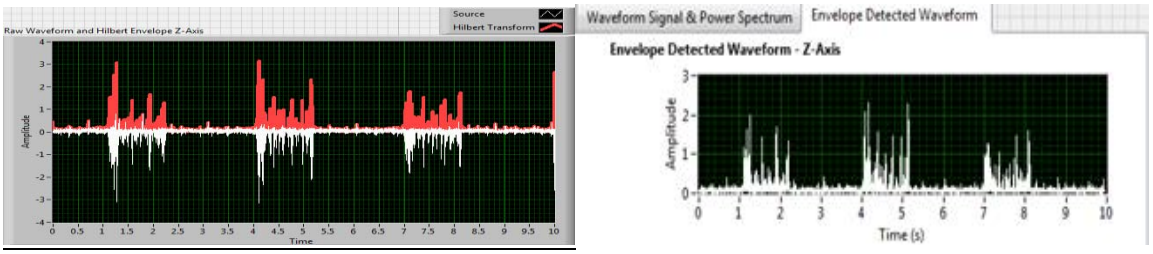

Figure 4.32. Vertical axis enveloped waveform data: Hilbert (left) OAT (right).

4.6.2. Envelope Spectrum Performance at 325 RPM

The bearing frequencies calculated in section 4.5 represent physical locations or parts of the bearing that contribute those frequencies. From horizontal axis unlubricated data, a large fundamental train frequency (2.08 Hz) peak, smaller ball spin frequency (11 Hz), and ball pass frequency outer race (16.61 Hz) are all present in both Hilbert and OAT plots with similar amplitudes. As expected, the graphs of the lubricated bearing generally have lower amplitudes than unlubricated and show that the Hilbert method generates slightly higher amplitudes at the same frequencies as the OAT method. Hilbert enveloping was slightly more sensitive with higher extracted amplitude, but had a false positive on the outer race frequency in phase two while OAT did not pick up BPFO until phase three.

Both phase one and two envelope spectrum graphs have the fundamental train frequency (2 Hz) present in all three axes corresponding to damage located in the cage of the bearing, which is consistent with the actual induced physical damage. In addition, phase three (axial axis) spectrum plots show a small ball pass inner race frequency peak at 27 Hz as well as ball spin frequency at 11 Hz. This tends to point towards damage beginning to occur to one or more rolling elements as further drilling has begun to scratch those surfaces. (Hilbert on left, OAT on right).

Unlubricated 325 RPM (Horizontal Axis)

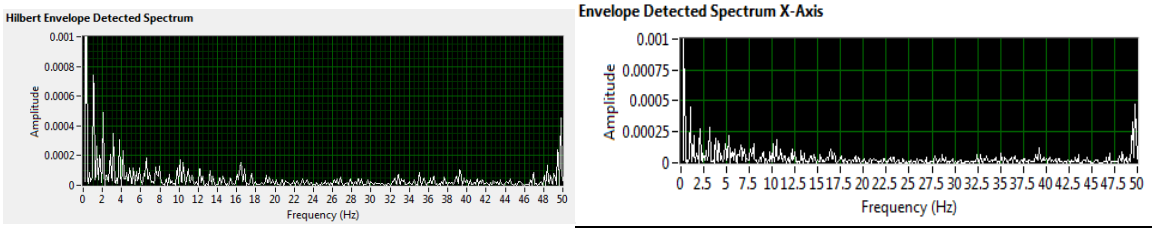

Lubricated 325 RPM (Horizontal Axis)

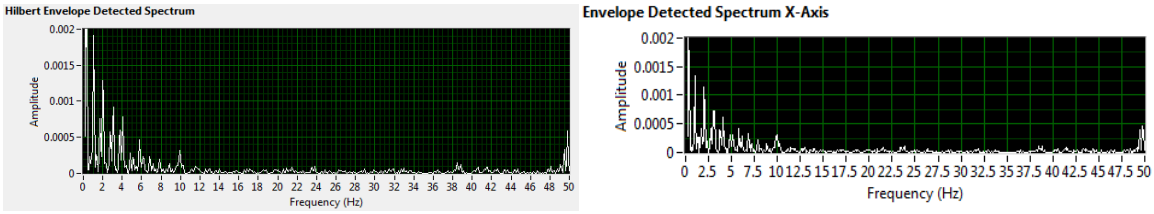

Phase I Fault, 325 RPM (Horizontal Axis)

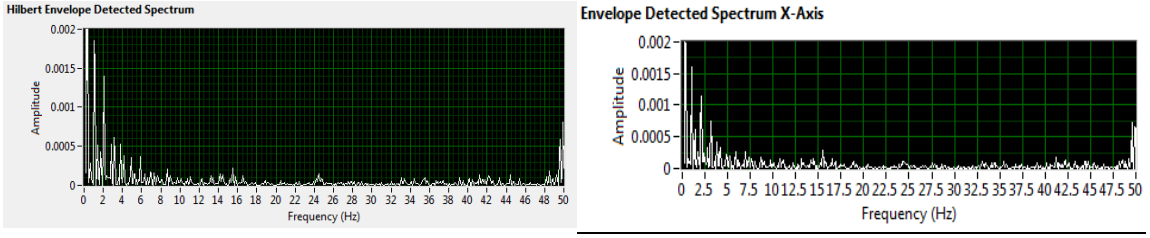

Phase II Fault, 325 RPM (Horizontal Axis)

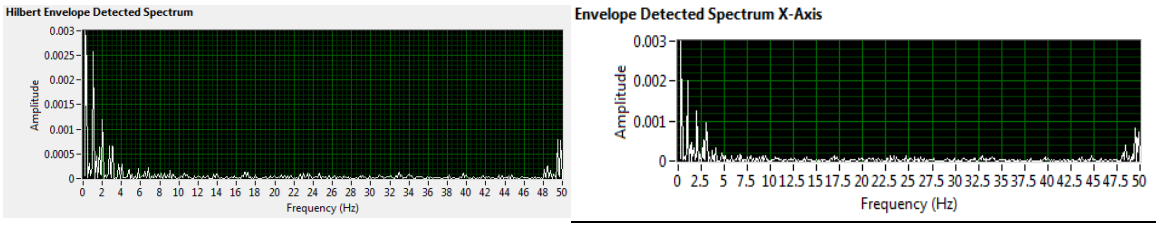

Phase III Fault, 325 RPM (Horizontal axis)

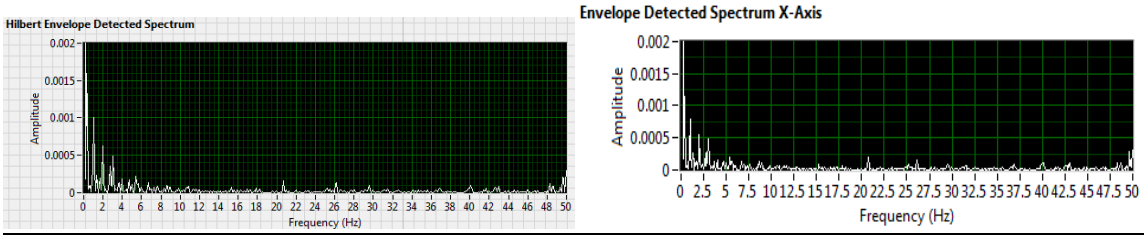

Figure 4.33. Horizontal axis enveloped spectra data 0-50 Hz: Hilbert (left), OAT (right).

Unlubricated 325RPM (Axial Axis)

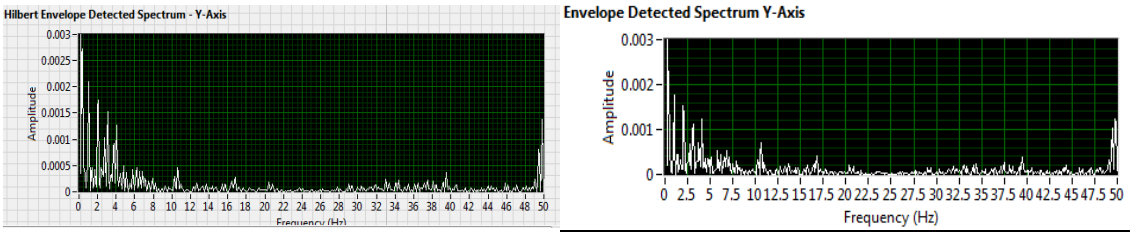

Lubricated 325RPM (Axial Axis)

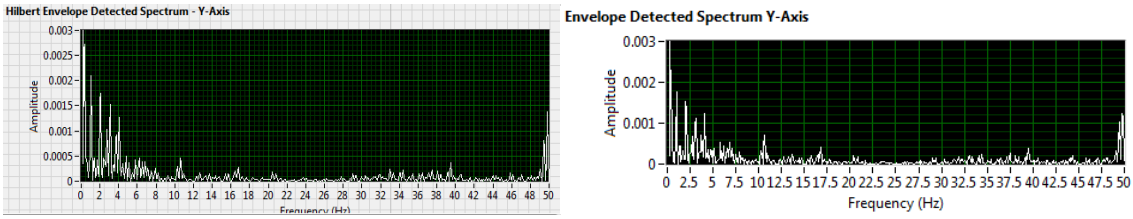

Phase I Fault, 325 RPM (Axial Axis)

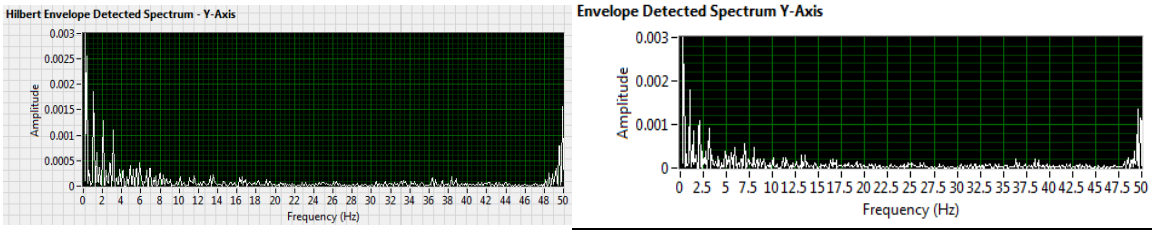

Phase II Fault, 325 RPM (Axial Axis)

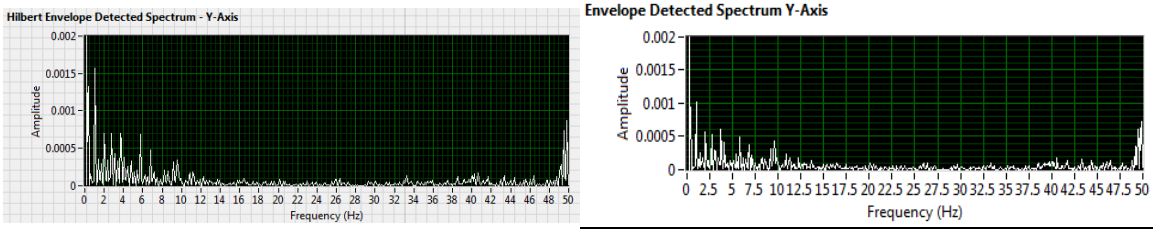

Phase III Fault, 325 RPM (Axial Axis)

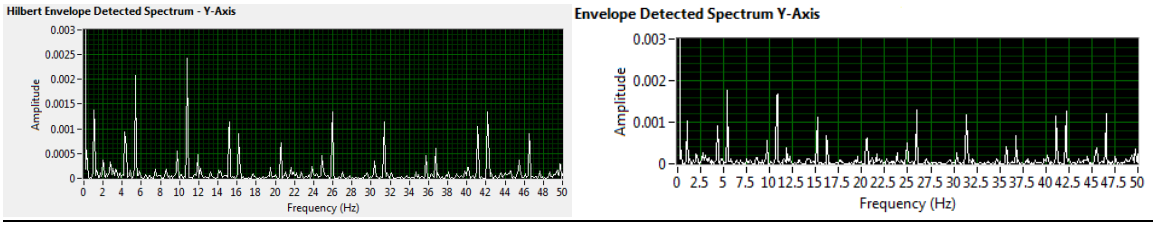

Figure 4.34. Axial axis enveloped spectra data 0-50 Hz - Hilbert (left), OAT (right).

Unlubricated 325RPM (Vertical Axis)

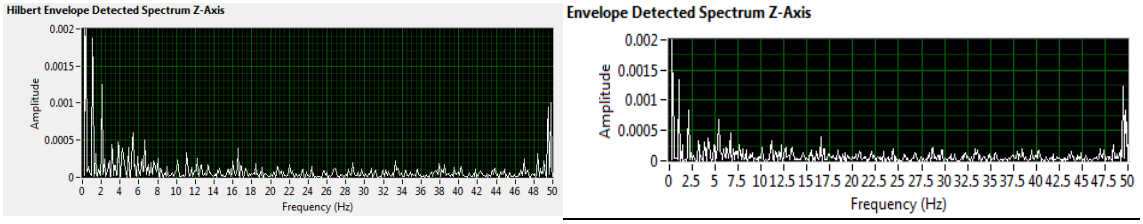

Lubricated 325RPM (Vertical Axis)

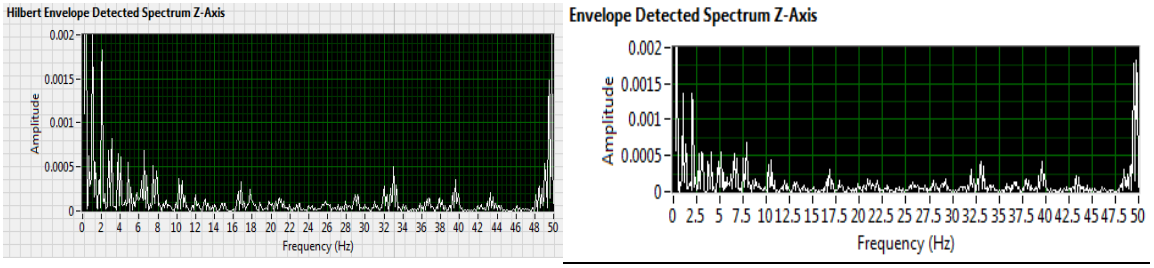

Phase I Fault, 325 RPM (Vertical Axis)

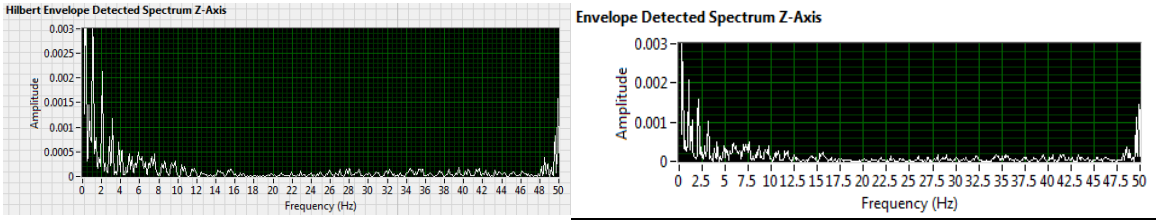

Phase II Fault, 325 RPM (Vertical Axis)

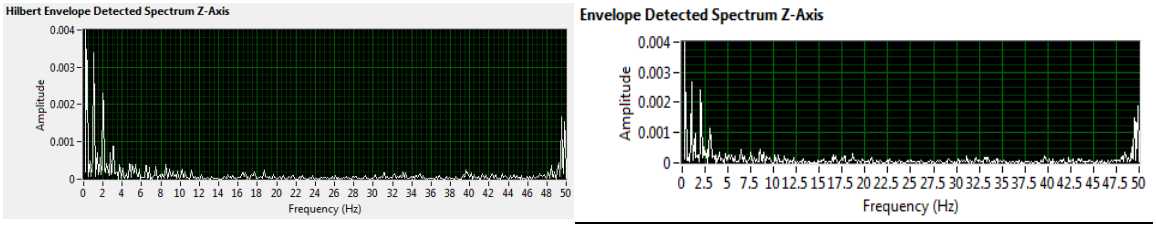

Phase III Fault, 325 RPM (Vertical Axis)

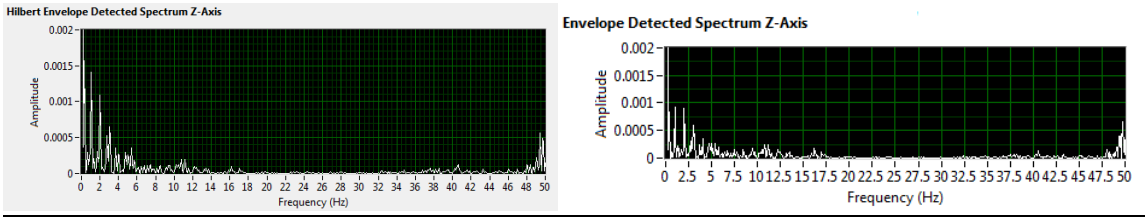

Figure 4.35. Vertical axis enveloped spectra data 0-50 Hz: Hilbert (left), OAT (right).

4.7. Performance Analysis of Fast Fourier Transform (FFT) with the Hilbert Enveloping Method at 325 RPM

In order to address the questions posed in section 1.2 fully, a performance analysis was developed to compare traditional FFT fault detection techniques against enveloping (using the Hilbert transformation method). Spectra plots from both FFT (left) and Hilbert enveloping (right) are presented below and used to illustrate performance difference at each stage in the study (sorted by axis location). As a reminder, the amplitudes between FFT and enveloping cannot be compared directly. The top left and right graphs (for each phase) shown in figures 4.35 to 4.37 are scaled from 0-500 Hz in order to illustrate the overall signal spectrum, while the second row of graphs represents the spectrum from 0-50 Hz, which is used to highlight bearing frequencies of interest (see section 4.3).

Beginning with the unlubricated bearing state, the horizontal axis FFT spectrum in Figure 4.35 shows a higher noise floor from 0-500 Hz, but very similar plots from 0-50 Hz with both methods showing a prominent peak around 2 Hz (fundamental train frequency) which could be attributed to the vibration generated by the metal to metal contact of the rolling elements to the race and cage surfaces without lubrication. Also worth mentioning, the enveloping spectrum picked up a slight peak around 17 Hz (BPFO). The axial axis overall signal from FFT was noisier towards the higher end of the frequency spectrum with the 2 Hz FTF frequency peak present in the enveloping spectrum, but missing from the FFT graph for both axial and vertical axes. In the vertical axis, both techniques show a small peak at BPFO but only enveloping picked up a slight spike at 11 Hz ball spin frequency (BSF). However, the enveloping technique tends to

reveal more defects due to the lack of lubrication by the ability to reduce the masking effect present when using the full spectrum raw waveform signal without Hilbert transformation for generating spectra. Even though enveloping needs to be used cautiously with regard to lubrication, the enveloping results provide value to overall machine condition.

Under lubricated conditions with no induced damage, a baseline amplitude can be established. Horizontal axis overall FFT power spectrum is much different than the unlubricated state with a prominent 60 Hz peak corresponding to 120V line frequency. Both FFT and HFE spectra have a peak amplitude at the fundamental train frequency as well as a small one at ball spin frequency in the horizontal and axial axes. It is important to remember that amplitudes in an enveloped spectrum cannot be directly compared to the FFT spectrum amplitudes, but only to other enveloped spectra when other factors remain constant (mounting location/method, forcing frequency, transducer model etc.). Therefore, the amplitude scale is adjusted so that the vibration signature fully encompasses the graphing space to allow for easier comparisons between fault phases across the same method, not explicitly between FFT and enveloping. For example, when only examining enveloping graphs, the enveloping amplitudes could be progressively compared from unlubricated to lubricated to phase I through phase III faults. The same is true for FFT spectra. In addition, the frequency scales for power spectra encompass 0-500 Hz in order to include any orders of vibration outside the calculated bearing frequency values.

Examining the horizontal axis in fault phase I, which introduced a small fault in the cage, inner race, and rolling element intersection, the amplitudes at the fundamental train frequency for FFT decreased from 0.00035g to 0.00025g while the same frequency for HFE, the amplitude increased slightly from 0.0013g to 0.0014g. Line frequency is again only present in both the horizontal and axial axes in the unscaled fast Fourier transform. The axial spectrum shows a steady 2 Hz fundamental train frequency at 0.0013g for enveloping, but no bearing frequencies whatsoever in FFT power spectra. Vertical axis train frequency for enveloping increased in amplitude from the lubricated state by 0.0003g.

The phase II horizontal axis FFT power spectrum shows a factor of two amplitude increase from 0.00025g to 0.0005g at the train frequency while no amplitude change exists in the enveloping spectra. The axial axis HFE amplitude at 2 Hz actually decreased from phase I with no other defect frequencies appear to be present. As in phase I, the FFT technique doesn't show any bearing frequencies of interest in the axial direction. The vertical acceleration measured showed no change in amplitude for fundamental train frequency between phase I and II for either technique.

In Phase III, the fault progressed even further, but the horizontal axis spectra show reduced train frequency amplitudes for both methods. However, HFE displays a very slight amplitude increase at the inner race ball pass frequency (BPFI) which has not been seen yet at 325 RPM until this point in the study. The axial axis shows significantly higher noise floor in both methods with a high peak at ball spin frequency as well as BPFI for HFE, while FFT had a slight amplitude increase at FTF with no other

frequencies of interest present. The vertical amplitude at the train frequency for HFE dropped by a factor of two from phase II. A very small peak at ball spin frequency is present in both FFT and HFE for the vertical axis.

Based on this performance study, it is easy to see that neither FFT or HFE alone provided a complete picture of the bearing's condition at any point in time. In combination however, more information about the fault could be ascertained to provide a more concrete analysis of bearing condition. Enveloping, however, was able to catch the progression of the induced fault earlier than Fast Fourier Transform for all bearing frequencies of interest, bringing significant value to the end user. This is especially true during such testing in real world scenarios by aiding in the earlier detection of defects, and when used with FFT, confidence in correct diagnosis of overall bearing condition.

Unlubricated 325 RPM (Horizontal Axis)

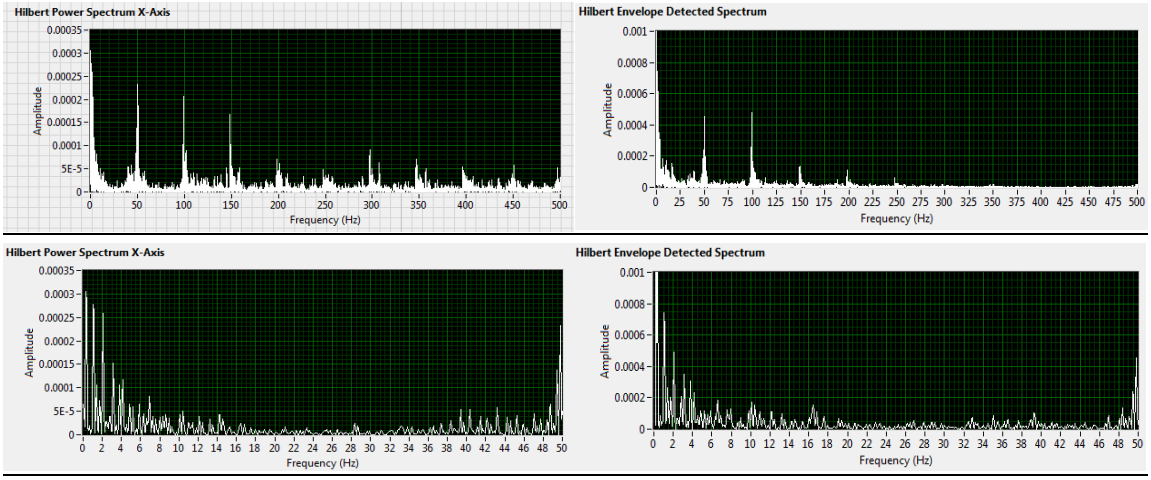

Lubricated 325 RPM (Horizontal Axis)

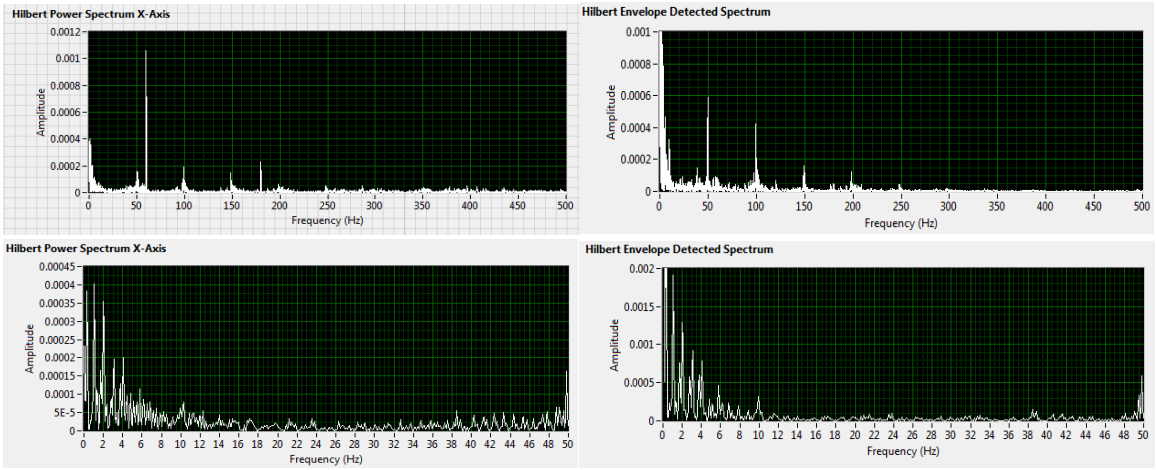

Phase I Fault 325 RPM (Horizontal Axis)

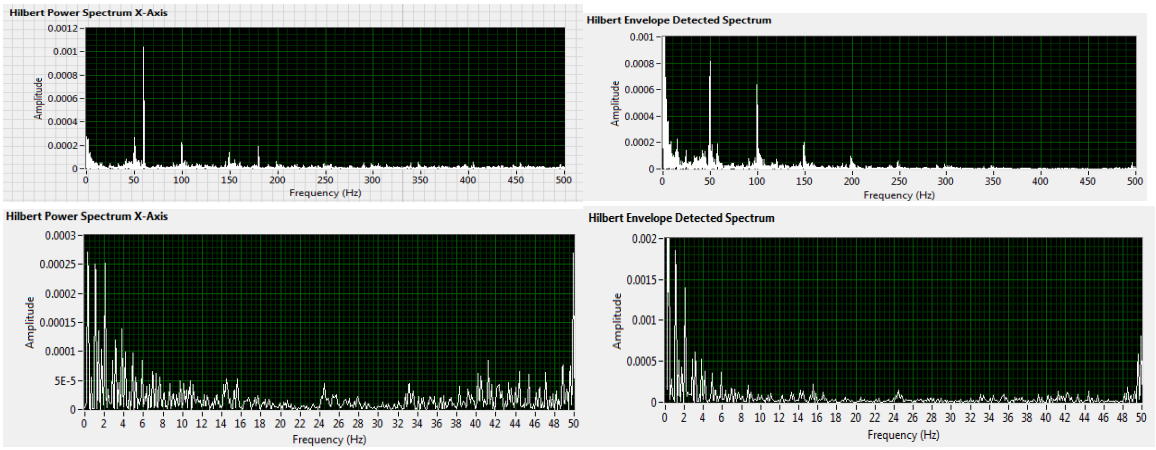

Phase II Fault 325 RPM (Horizontal Axis)

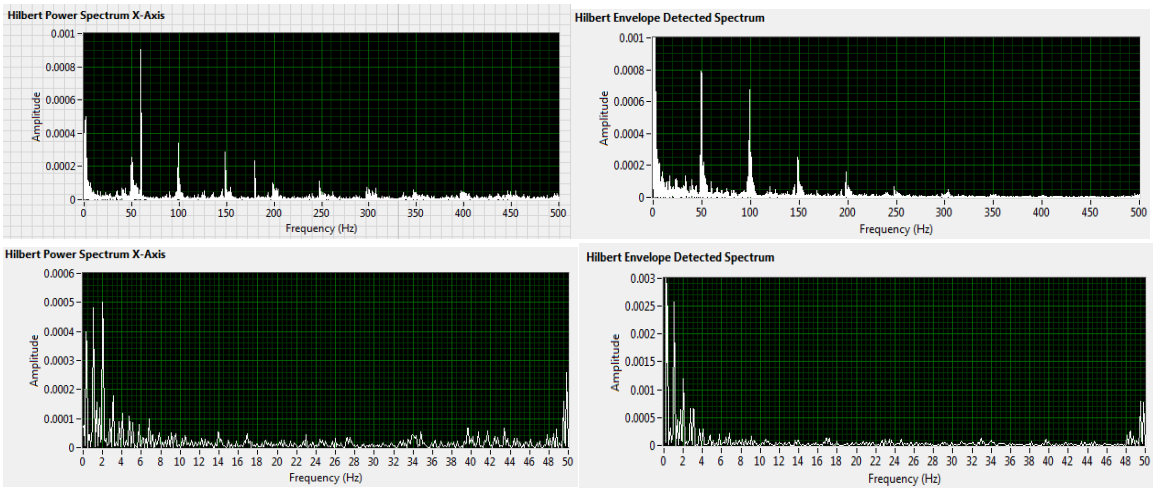

Phase III Fault 325 RPM (Horizontal Axis)

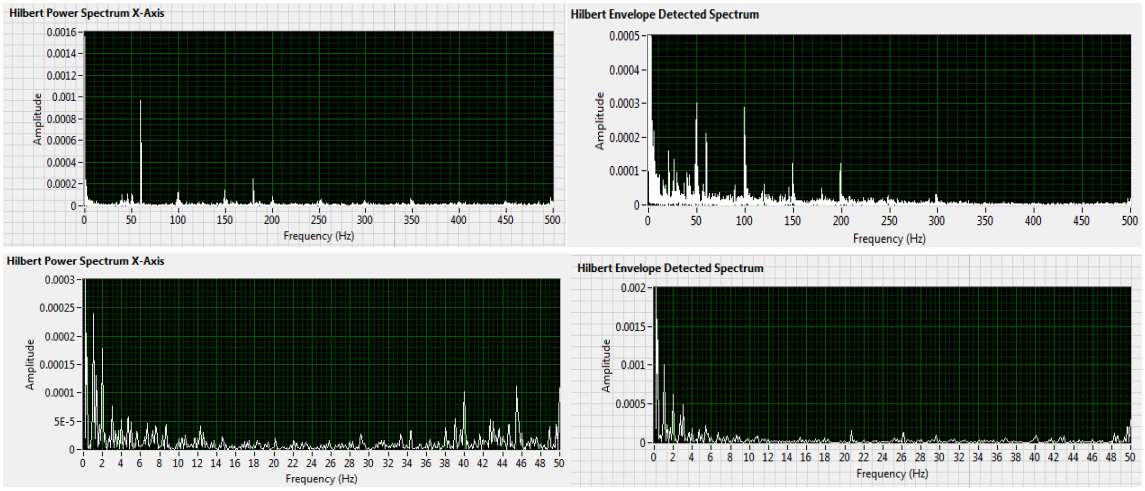

Figure 4.36. Horizontal axis power spectrum data – FFT (left), HFE (right).

Unlubricated 325 RPM (Axial Axis)

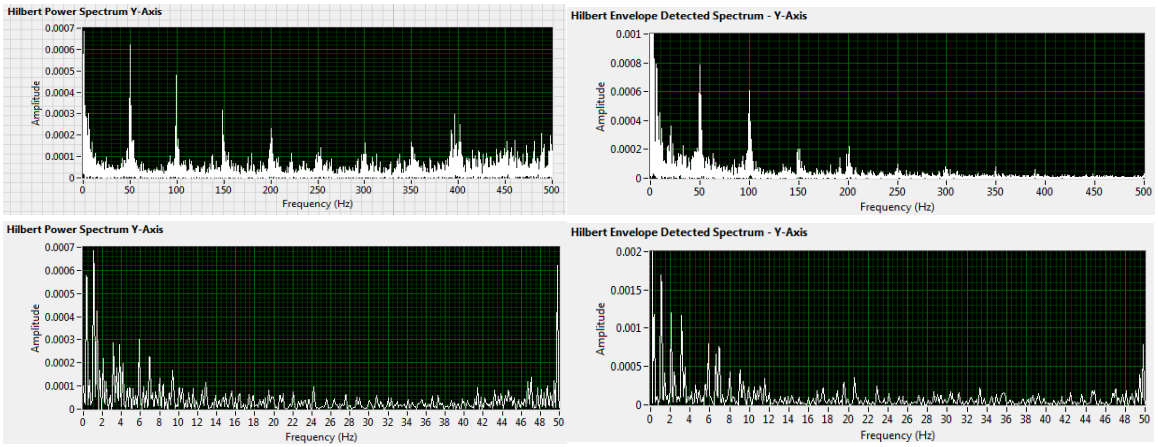

Lubricated 325 RPM (Axial Axis)

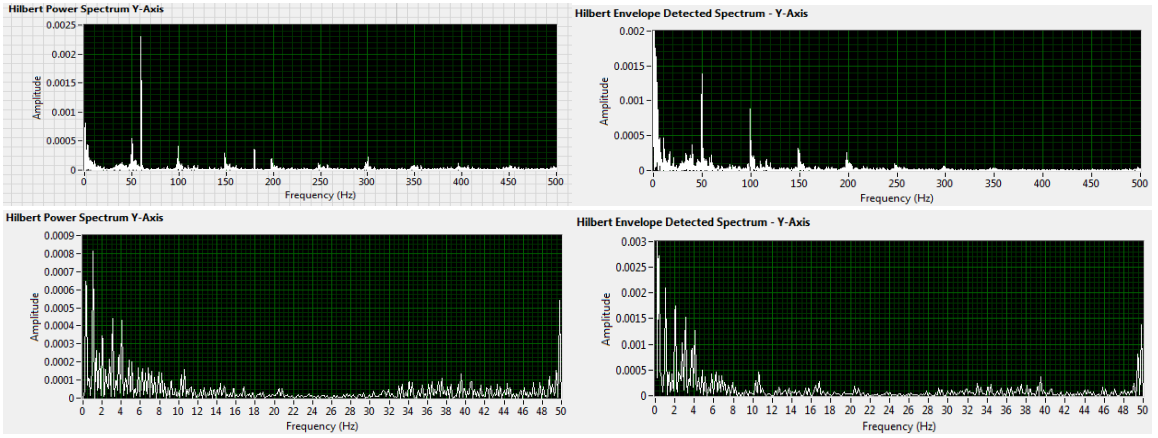

Phase I Fault 325 RPM (Axial Axis)

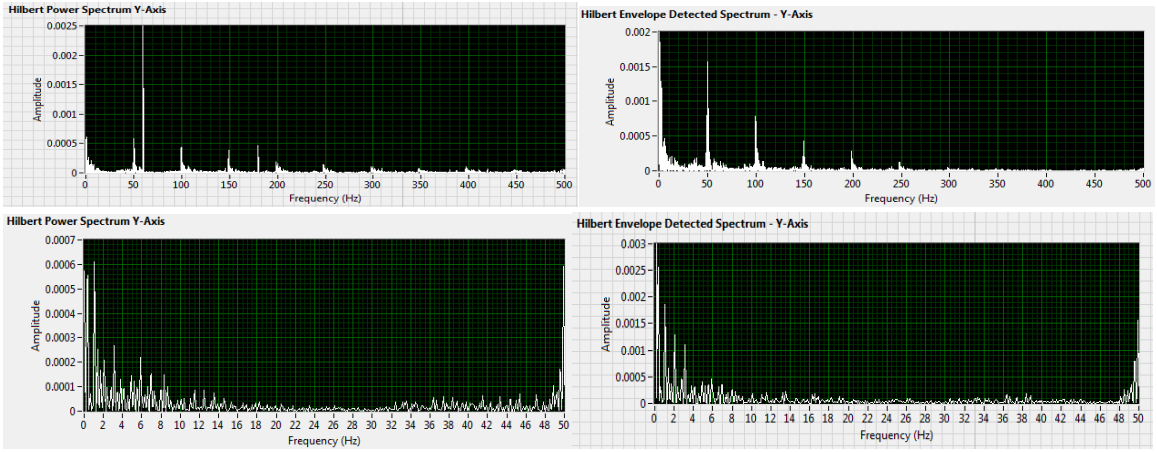

Phase II Fault 325 RPM (Axial Axis)

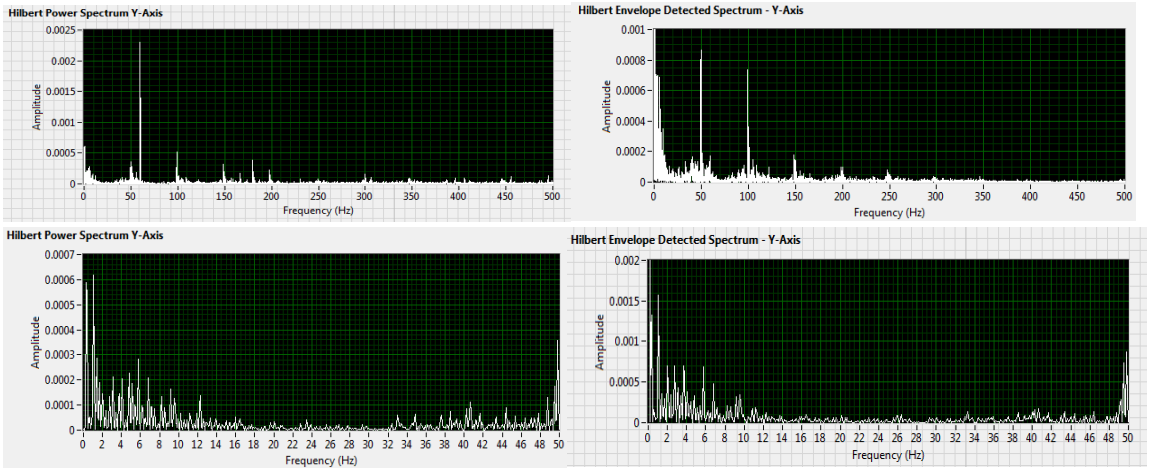

Phase III Fault 325 RPM (Axial Axis)

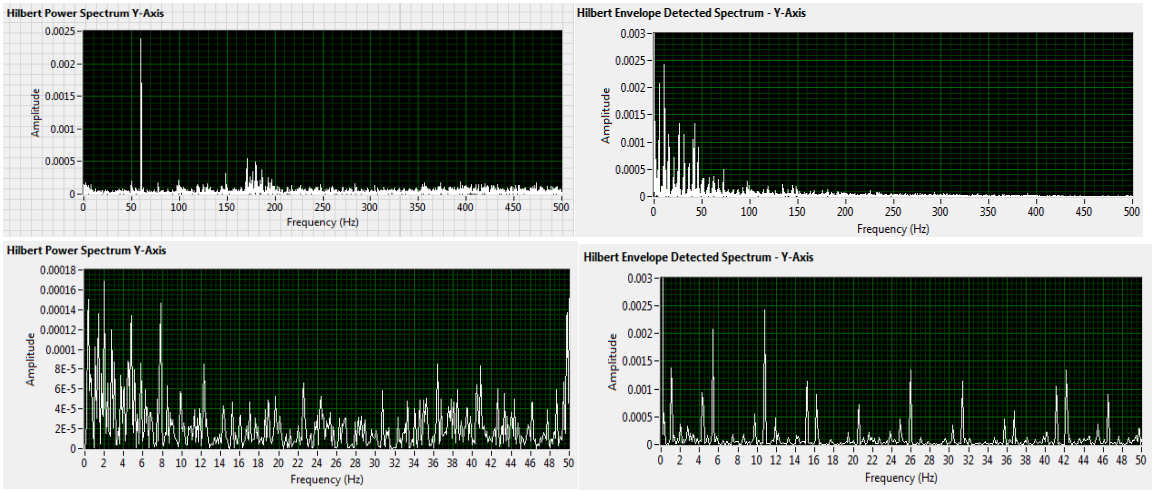

Figure 4.37. Axial axis power spectrum data – FFT (left), HFE (right)

Unlubricated 325 RPM (Vertical Axis)

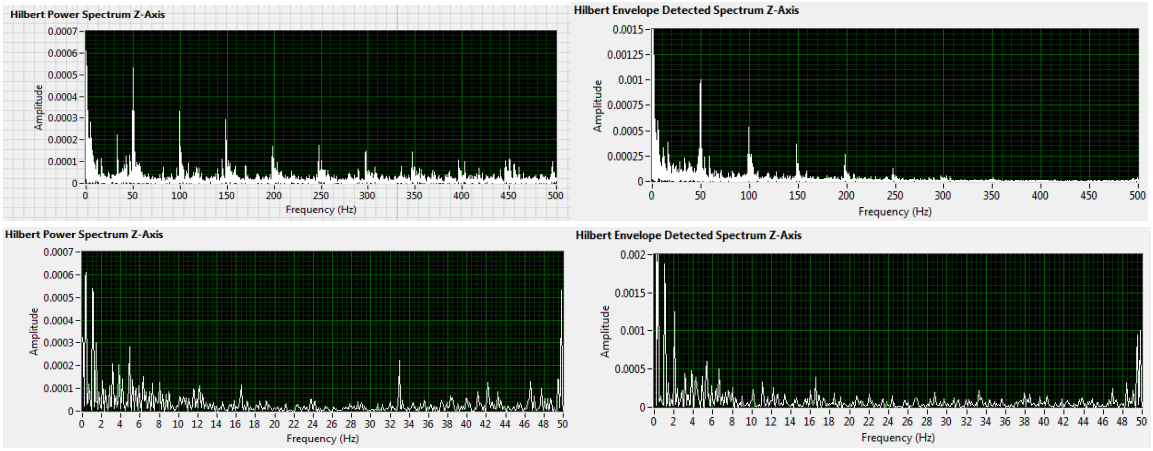

Lubricated 325 RPM (Vertical Axis)

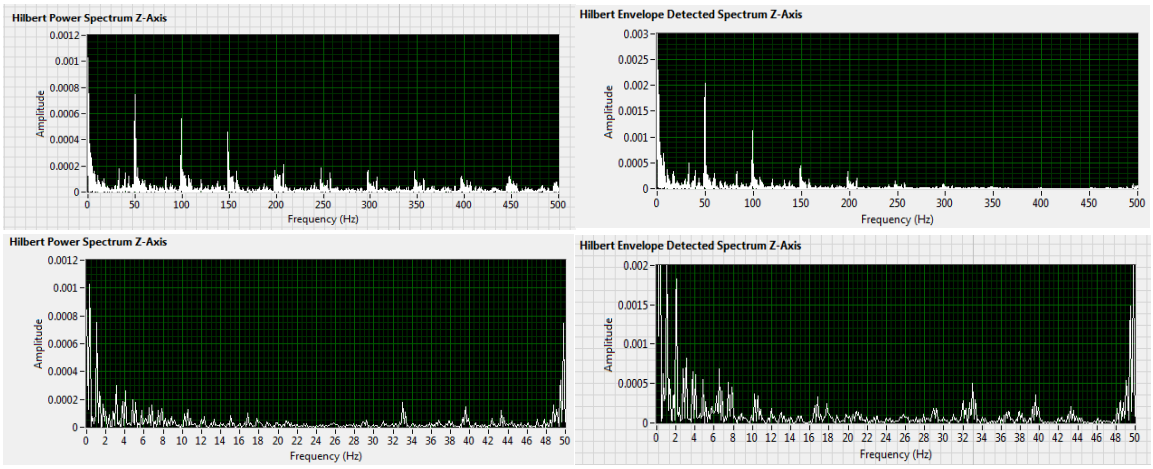

Phase I Fault 325 RPM (Vertical Axis)

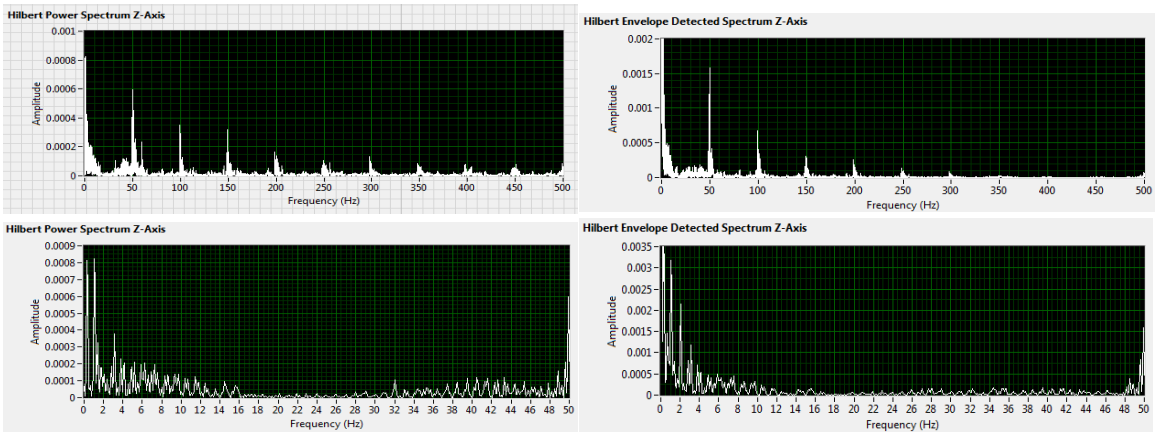

Phase II Fault 325 RPM (Vertical Axis)

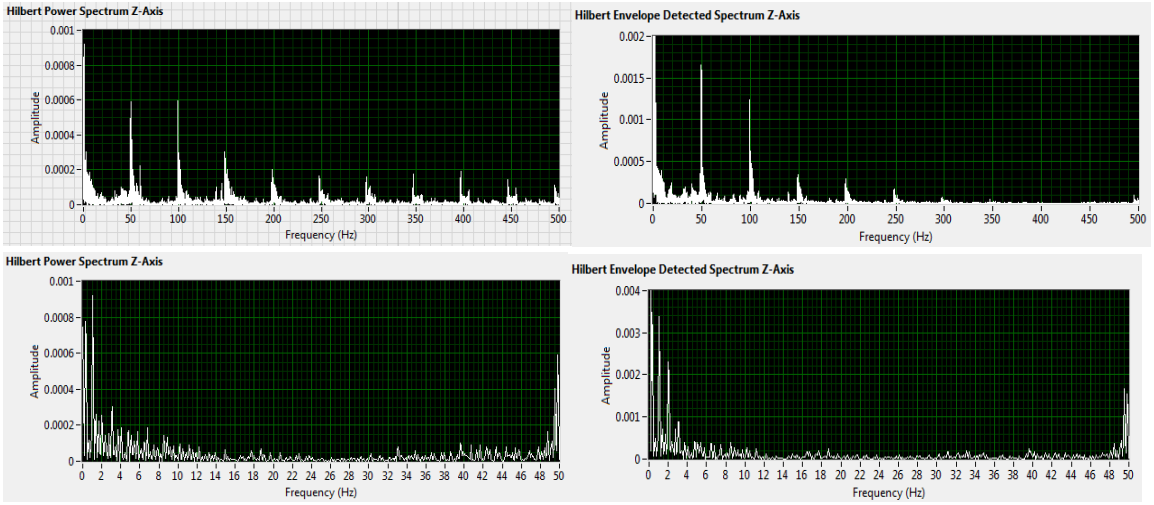

Phase III Fault 325 (Vertical Axis)

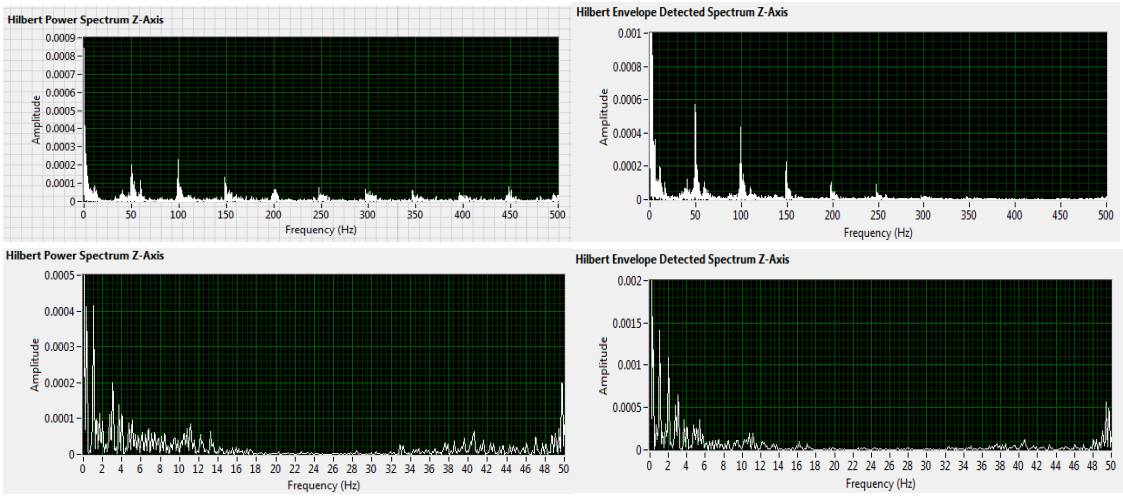

Figure 4.38. Vertical axis power spectrum data – FFT (left), HFE (right).

4.8. Summary

Chapter 4 presents an introduction to envelope detection using National Instrument's LabVIEW™ software and provides an overview of the enveloping process, followed by the steps required to set up the proposed bearing vibration experiment. These steps include building the virtual instrument and configuring the relevant process parameters to display desired waveform and spectrum plots used for envelope analysis and FFT.

Two processing algorithms provided with LabVIEW™ to mathematically extract the signals of interest were presented and tested in this experiment; the Hilbert Transformation and Order Analysis Toolkit. Each algorithm was used to develop the enveloped signal for a specific rolling element bearing undergoing three progressive stages of damage to a localized area at the intersection of the cage, inner race, and a single rolling element. The enveloped waveforms and associated spectra were presented graphically and reviewed individually followed by a performance comparison between the two methods. The individual analysis includes a raw waveform and power spectrum examination before and after the enveloping process for the various bearing physical conditions (unlubricated, lubricated, etc.) tested. The relevant bearing frequencies were calculated, and frequency evaluation was conducted to identify the physical location of the bearing fault as well as any processing variations between the two algorithms. The induced cage and rolling element damage was detected in the enveloped spectra as bearing frequencies of 1 x BSF and 1 x FTF. In addition, a very small amplitude 1 x BPFI was found which could be attributed to the damaged rolling element repeatedly contacting the damaged inner race during rotation. These enveloped spectra were then

compared to power spectra results from FFT. A fault detection performance analysis for HFE and FFT was presented and conclusions drawn in section 5.1.

CHAPTER 5. SUMMARY, CONCLUSIONS, and RECOMMENDATIONS

5.1. Summary and Conclusions

In summary, high frequency acceleration enveloping has been proven to be an effective tool in the early detection of bearing faults in rolling element bearings and the two HFE methods presented here are both suitable for processing the envelope of a raw waveform with subtle differences in performance between the two algorithms. In conjunction with FFT analysis, enveloping can aid in the identification of localized faults earlier than FFT analysis alone and provide a more complete analysis of bearing condition.

Based on the experimental development within this work, the following research questions presented herein have been explored:

1) Can high frequency acceleration enveloping help detect impending faults in rolling element bearings earlier than traditional FFT analysis?
2) How does the performance of traditional high frequency enveloping methodology compare to a proprietary envelope processing technique from National Instruments?

Based on the results in section 4.7, high frequency acceleration enveloping can help detect impending faults in rolling element bearings earlier than traditional FFT analysis. Based on results in 4.6, the newer proprietary high frequency enveloping

methodology, Order Analysis Toolkit from National Instruments, produces results similar to those obtained using the traditional envelope processing technique of Hilbert transformation. Although there has been some focus in enveloping methodology in past research publications, performance analysis between different mathematical methods as well as between enveloping and FFT analysis has development potential. Future work for research and practice are presented below.

5.2. Recommendations for Future Research Work

The data generated for this study has been used to further research in evaluating the performance of two enveloping methods. However, an appropriate next step in the research path would be to observe any changes in fault detection performance when variables such as transducer mounting, higher operating speeds, different bearing styles, etc. are changed. In addition, research into the performance of other enveloping methods would provide a more complete picture and value to the end user.

5.3. Recommendations for Future Practice Work

In practice, the performance of both Hilbert Transform and OAT envelope detection are similar enough when applied in conjunction with FFT that either will aid in the detection of rolling element bearing faults earlier than FFT alone. However, there are numerous other methodologies from other industry sources that have not been tested such as DEWESoft (DEWESoft® , 2016) and Ascent (General Electric, 2016). Using other

algorithms could potentially yield a larger performance increase. Exploring other related software and experimentation with other enveloping algorithms is recommended.

LIST OF REFERENCES

LIST OF REFERENCES

FYH Bearing UCP205-16 1" Pillow Block Mounted Bearings. (2016, Feb 12). Retrieved from VXB.com Ball Bearings: http://www.vxb.com/FYH-Bearing-UCP205-16-1-Pillow-Block-Mounted-p/kit8803.htm

Anaheim Automation. (2016, October 5). AC Motor Guide. Anaheim, California, USA. Retrieved from http://www.anaheimautomation.com/manuals/forms/ac-motor-guide.php#sthash.c3K7Q6MW.dpbs

Berry, J. (1996). High frequency envelopling and demodulation techniques. *Vibration Institute 20th Annual Meeting* (pp. 39-78). St. Louis: Technical Associates of Charlotte, Inc.

BINDT. (2012, October). *British Institute for Non-Destructive Testing*. Retrieved from Condition Monitoring: http://www.bindt.org/Certification/General_Information/Condition_Monitoring.html

Costinas, S., Diaconescu, I., & Fagarasanu, I. (2009). Wind power plant condition monitoring. *Energy Problems and Environmental Engineering* (pp. 71-76). La Laguna: WSEAS.

Crowther, A., & Eritenel, T. (2012, January). *Monitoring rotating machinery.* Retrieved September 4, 2012, from Romax Technology Inc.: www.romaxtech.com/wind

DEWESoft® . (2016, June 5). *Dewesoft® X2 Software*. Retrieved from Dewesoft® : http://www.dewesoft.com/products/dewesoft-x

Dictionary.com. (2016, June 5). *Forcing Frequency*. Retrieved from Dictionary.com: http://www.dictionary.com/browse/forcing-frequency

Dunn, S. (2009, August). *Condition Monitoring in the 21st Century.* Retrieved from www. plant-maintenance.com: http://www.plant-maintenance.com/articles/ConMon21stCentury.shtml

Engdahl, C. (2011, Oct-Dec). New tools for vibration condtion monitoring. *Hydrocarbon Asia*, pp. 44-49. Retrieved from www.hcasia.safan.com/mag/hca1011/t44.pdf

Eshleman, R. L. (2010). Condition Monitoring of Machinery. In A. G. Piersol, & T. L. Paez, *Harris' Shock and Vibration Handbook* (p. Chapter 16). McGraw Hill.

General Electric. (2016, June 05). *Ascent Software*. Retrieved from GE World Leaders in Machinery Health Information Systems : http://www.commtest.com/products/ascent

Hatch, C. (2004). Improved wind turbine condition monitoring using acceleration enveloping. *Orbit*, pp. 58-61. Retrieved October 2012, from www.ge-mcs.com/download/orbit.../2q04windturbcondmon.pdf

Hatch, C., Weiss, A., & Kalb, M. (2010). Cracked Bearing Race Detection In Wind Turbine Gearboxes. *Orbit, 30*(1), 40-47. Retrieved from GE Energy: http://www.ge-mcs.com/download/case-studies/bently-nevada/Hatch-Cracked-Race-Detection.pdf

Johansson, M. (1999). *The Hilbert transform.* Retrieved October 24, 2012, from http://w3.msi.vxu.se/exarb/mj_ex.pdf

Johansson, M. (1999). *The Hilbert Transform.* Retrieved October 24, 2012, from http://w3.msi.vxu.se/exarb/mj_ex.pdf

Kim, K., Parthasarathy, G., Uluyol, O., Shuangwen, S., & Fleming, P. (2011). Use of SCADA data for failure detection in wind turbines. *Energy Sustainability Conference and Fuel Cell Conference* (pp. 1-9). Washington D.C.: NREL.

Konstantin-Hansen, H. (2003, February). *Envelope Analysis for Diagnostics of Local Faults in Rolling Element Bearings.* Retrieved from Brüel & Kjær: http://www.bksv.com/doc/bo0501.pdf

Kschischang, F. R. (2006, October 22). The Hilbert Transform. Toronto, Ontario, Canada.

LDS Dactron. (2003). *Understanding FFT Windows.* Retrieved from University of Wrzburg Physics and Astronomy: www.physik.uni-wuerzburg.de/~praktiku/Anleitung/Fremde/ANO14.pdf

Lu, B., X., W., & Yang, Z. (2009). A Review of recent advances in wind turbine condition monitoring and fault diagnosis. *IEEE Power Electronics and Machines in Wind Applications* (pp. 109-115). Lincoln: PEMWA.

Manfred Weber. (2016, October 5). Triaxial Accelerometers. Radebeul, Germany. Retrieved from http://www.mmf.de/triaxial_accelerometers.htm

Mignano, F. (1996). Envelope Detection. *20th Annual Meeting* (pp. 55-60). St. Louis: Vibration Institute.

National Instruments. (2007, December). *Fault Detection (Sound and Vibration Measurement Suite).* Retrieved from NI Support: http://zone.ni.com/reference/en-XX/help/372416A-01/svtconcepts/fault_detection/#Envelope_Detection

National Instruments. (2007, December). *OAT Envelope Detection*. Retrieved from www.ni.com: http://zone.ni.com/reference/en-XX/help/372416A-01/lvoat/oat_envelope_detection/

National Instruments. (2007, December). *Performing Constant-Speed Bearing Fault Detection.* Retrieved February 2013, from zone.ni.com/reference/en-XX/help/372416A-01/svtconcepts/cst_speed_brg/

National Instruments. (2013, July 09). *FFT Analysis*. Retrieved from http://www.ni.com/white-paper/3342/en/

National Instruments. (2015, May 04). *Understanding FFTs and Windowing*. Retrieved from National Instruments: http://www.ni.com/white-paper/4844/en/

PCB. (2016). *Introduction to Piezoelectric Accelerometers*. Retrieved from PCB Piezotronics: http://www.pcb.com/techsupport/tech_accel

Sheen, Y. (2007, June 20). An analysis method for the vibration signal with amplitude modulation in a bearing system. *Journal of Sound and Vibration, 303*(3-5), 538-552. Retrieved from http://www.sciencedirect.com/science/article/pii/S0022460X0700106X

Sheen, Y. (2008, August). An envelope detection method based on the first-vibration-mode of bearing vibration. *Measurement, 41*(7), 797-809. Retrieved from http://www.sciencedirect.com/science/article/pii/S0263224107001212

Sinclair Knight Merz. (2006). *Condition monitoring of wind turbines.* Glasgow: SKM. Retrieved from http://www.evaluationsonline.org.uk/evaluations/Browse.do?ui=browse&action=show&id=441&taxonomy=BSK

SKF Group. (2012, August 30). *Glossary of Maintenance Terms*. Retrieved from SKF: http://www.skf.com/aptitudexchange/glossary.html

SKF Reliability Systems. (2012, August 30). *Frequently asked questions about enveloping, using an accelerometer transducer.* Retrieved from SKF: http://www.skf.com/skf/access/securefiles/867864.pdf

Truax, B. (1999). *Simon Frasier University*. Retrieved from Handbook for Acoustic Ecology: http://www.sfu.ca/sonic-studio/handbook/Rectification.html

Tse, P. W., Peng, Y. H., & Yam, R. (2001). Wavelet Analysis and Envelope Detection For Rolling Element Bearing Fault Diagnosis - Their Effectiveness and Flexibilities -. *Journal of Vibration and Acoustics*, 303.

Weller, N. (2004). *Acceleration enveloping - higher sensitivity, earlier detection.* Retrieved August 30, 2012, from GE Energy: http://www.ge-mcs.com/download/orbit-archives/2001-2005/2nd_quarter_2004/2q04accelenvel.pdf

Yan, R., & Gao, R. (2009, February). Multi-scale enveloping spectrogram for vibration analysis in bearing defect diagnosis. *Tribology International, 42*(2), 293-302. Retrieved from http://www.sciencedirect.com/science/article/pii/S0301679X08001400

Yang, W., Jiang, J., Tavner, P., & Crabtree, C. (2008). Monitoring Wind Turbine Condition by the Approach of Empirical Mode Decomposition. *Electrical Machines and Systems* (pp. 736-740). Wuhan: ICEMS.

APPENDICES

Appendix A. Vibration Data at 450 RPM

Test Bearing Vibration Data (450 RPM)

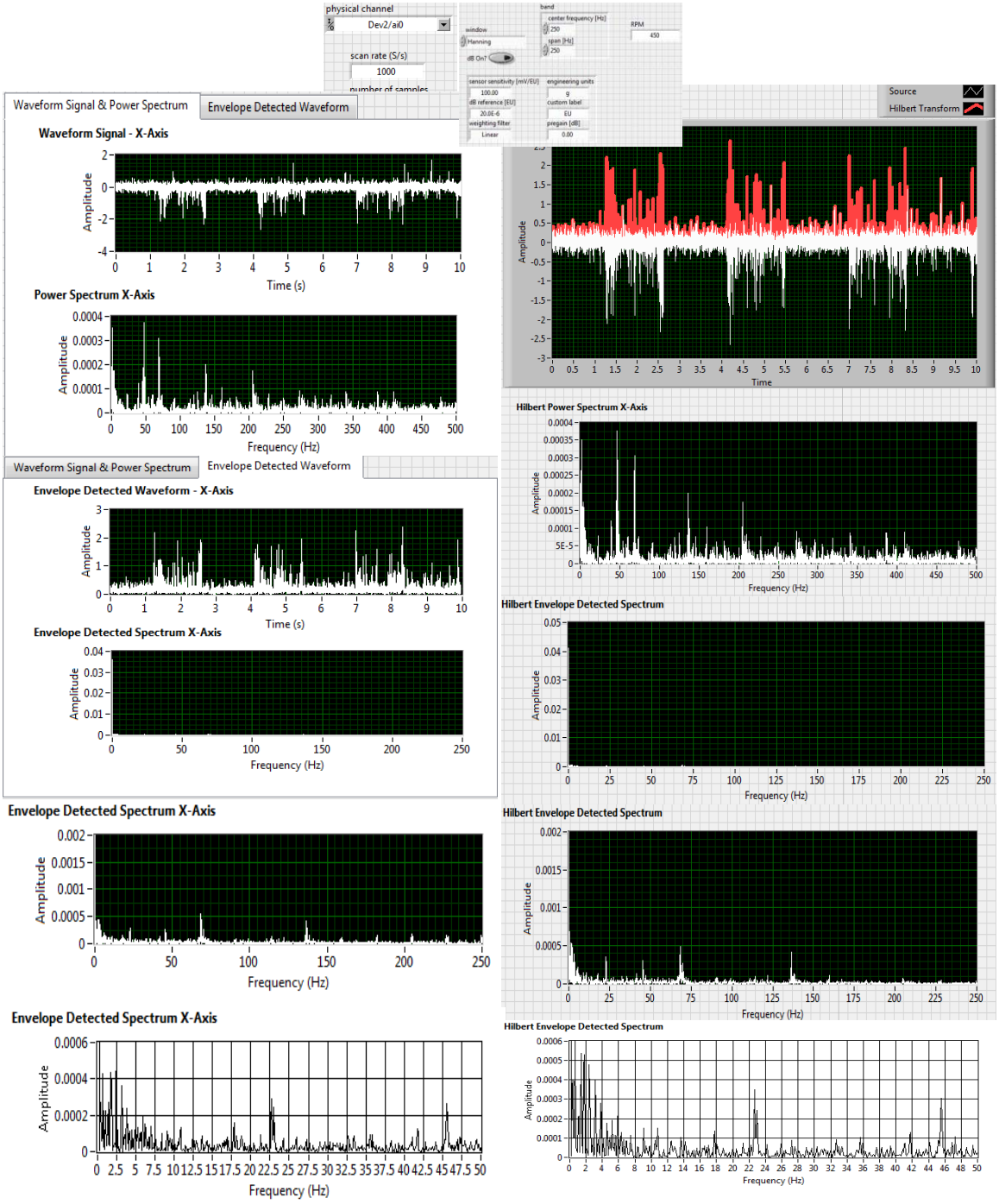

Figure A.1. Unlubricated bearing 450 RPM (horizontal axis)

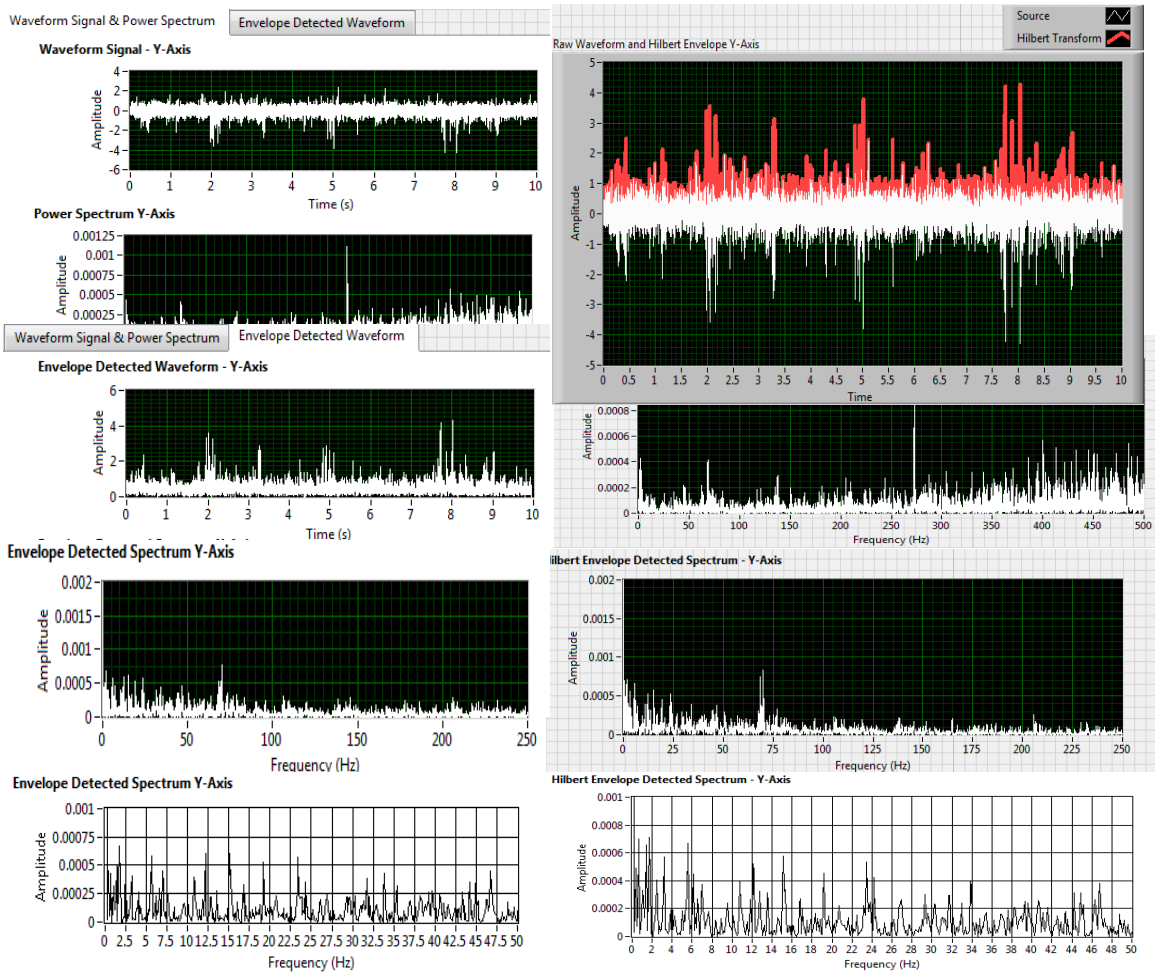

Figure A.2. Unlubricated bearing 450 RPM (axial axis)

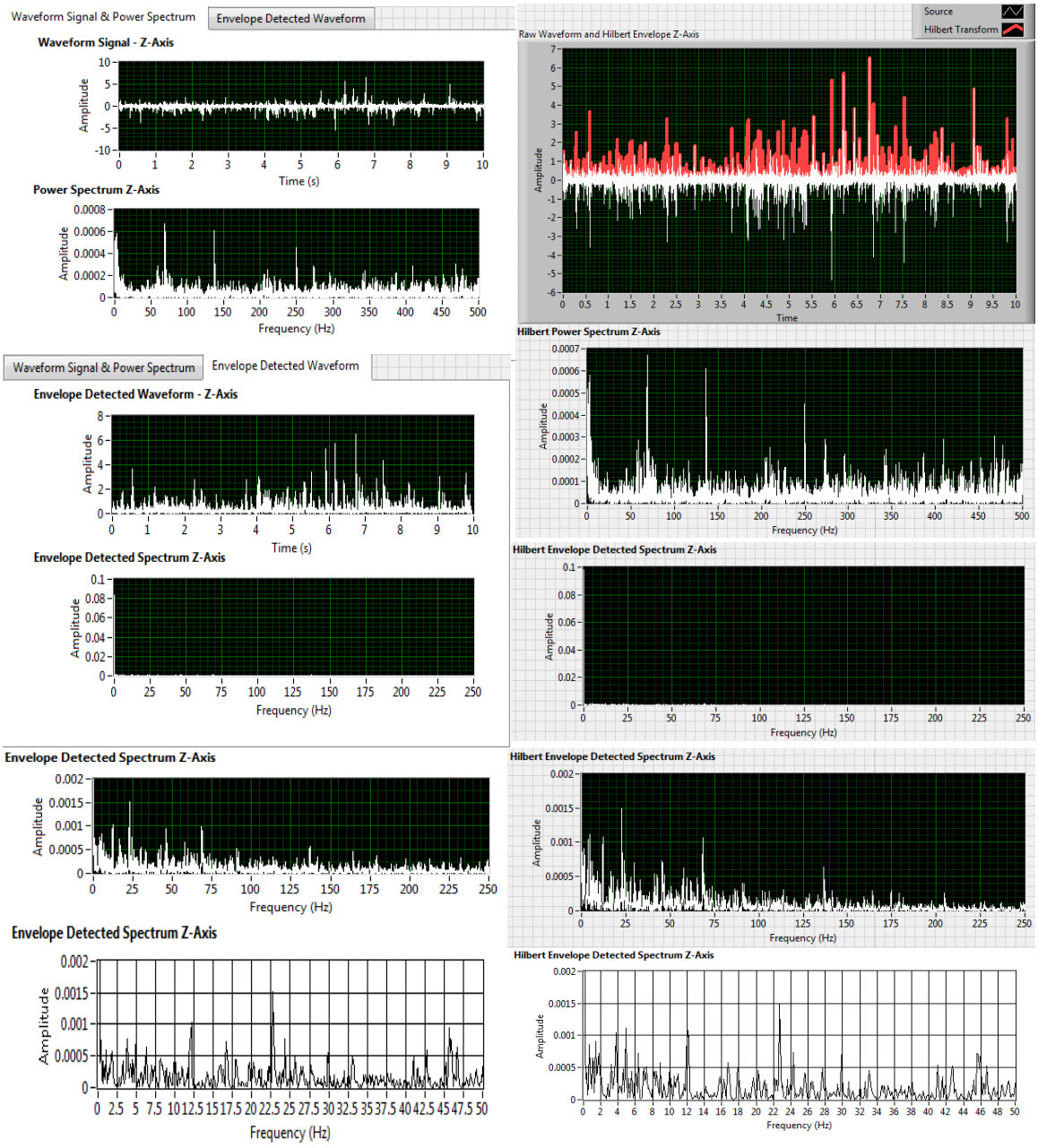

Figure A.3. Unlubricated bearing 450 RPM (vertical axis)

Lubricated Bearing 450 RPM (Horizontal Axis)

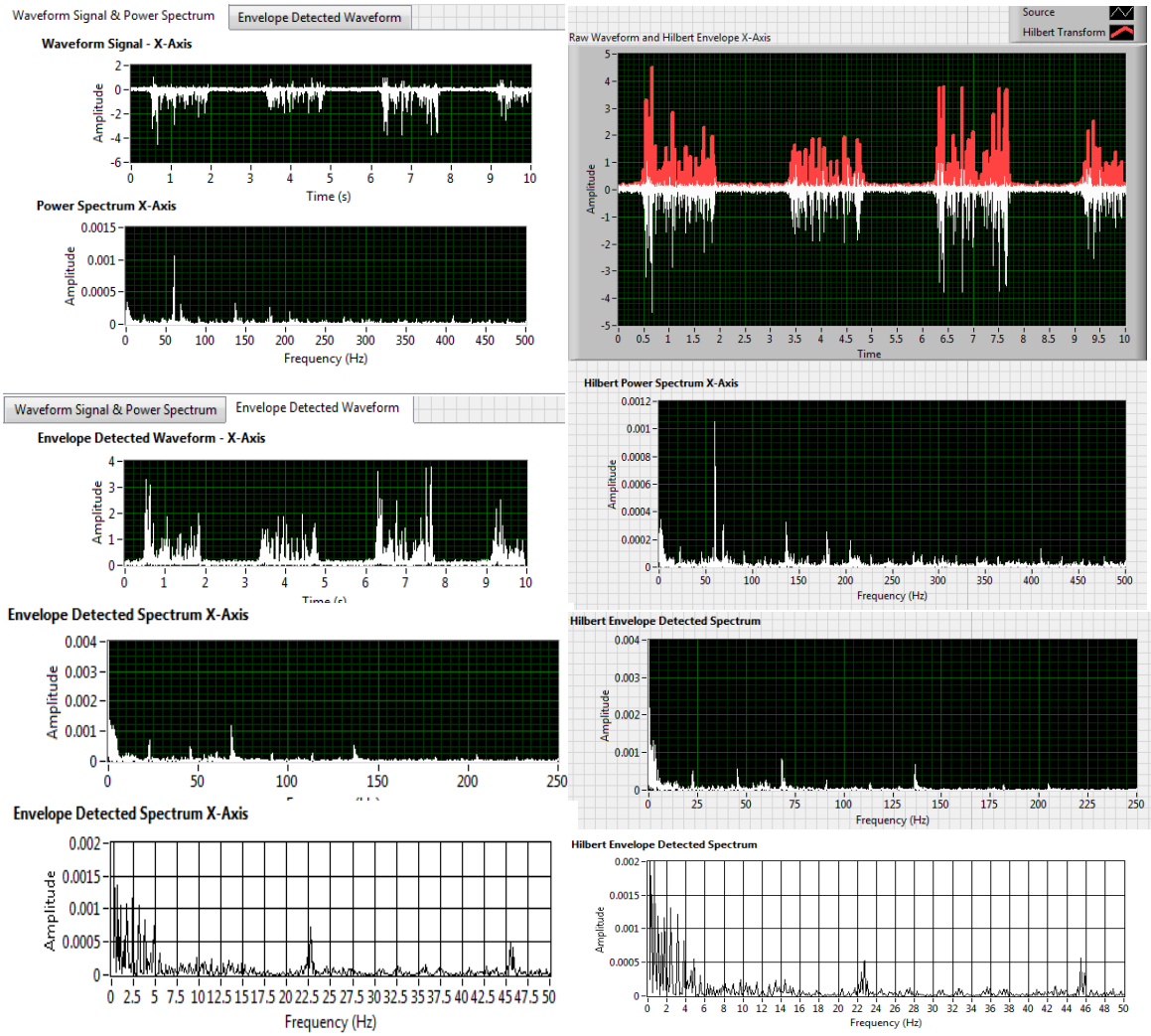

Figure A.4. Lubricated bearing 450 RPM (horizontal axis)

Lubricated Bearing 450 RPM (Axial Axis)

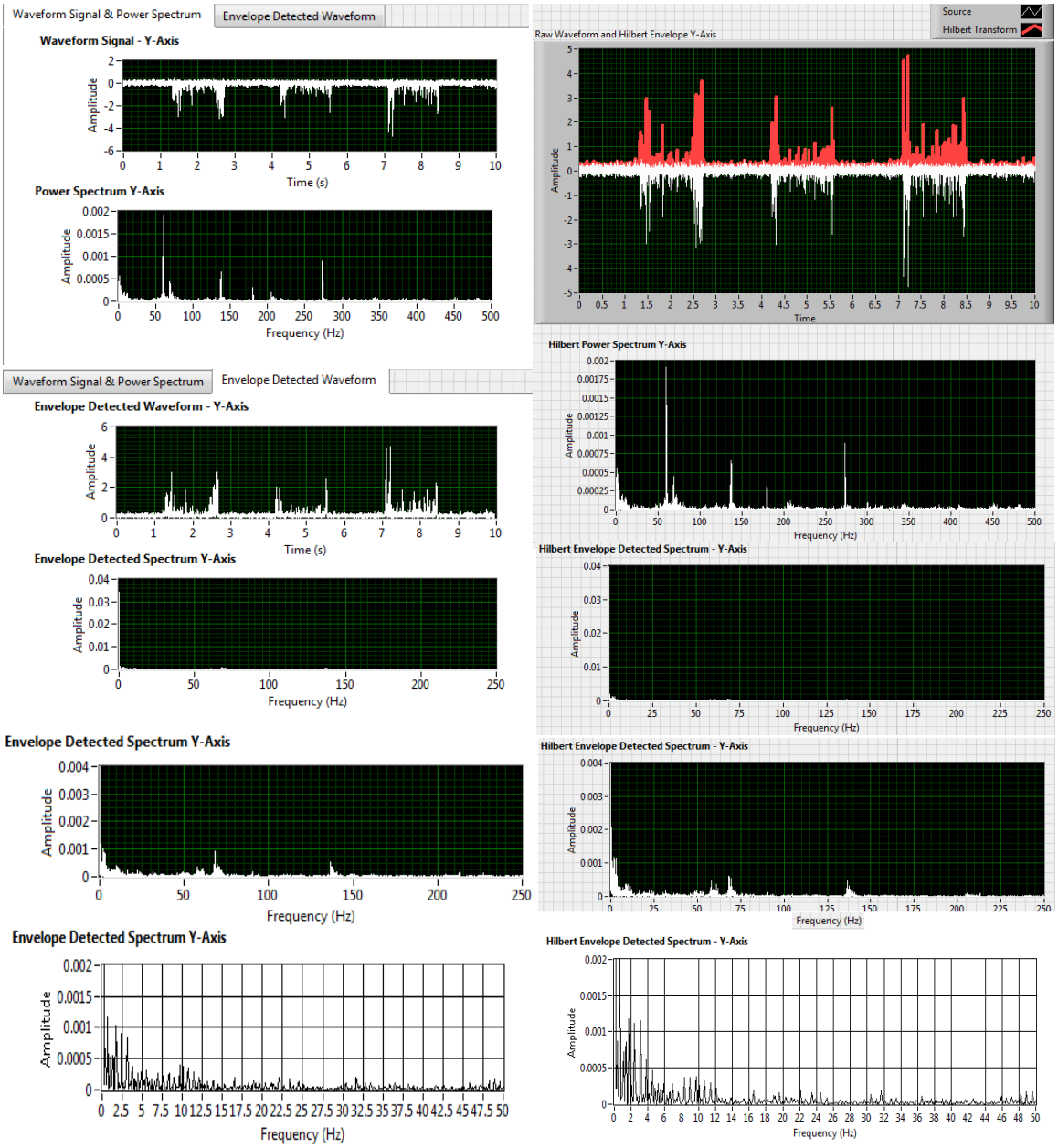

Figure A.5. Lubricated bearing 450 RPM (axial axis)

Lubricated Bearing 450 RPM (Vertical Axis)

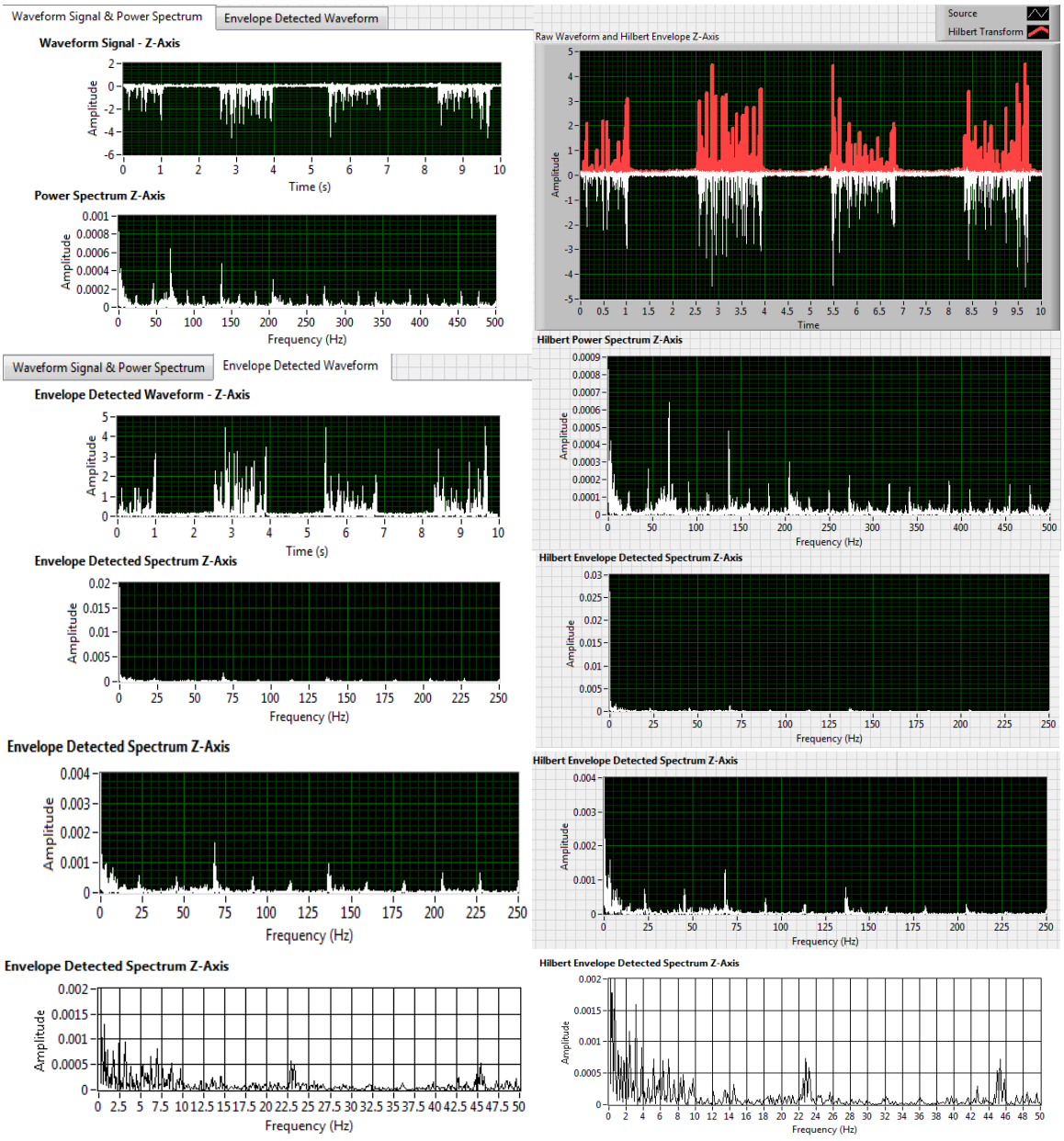

Figure A.6. Lubricated bearing 450 RPM (vertical axis)

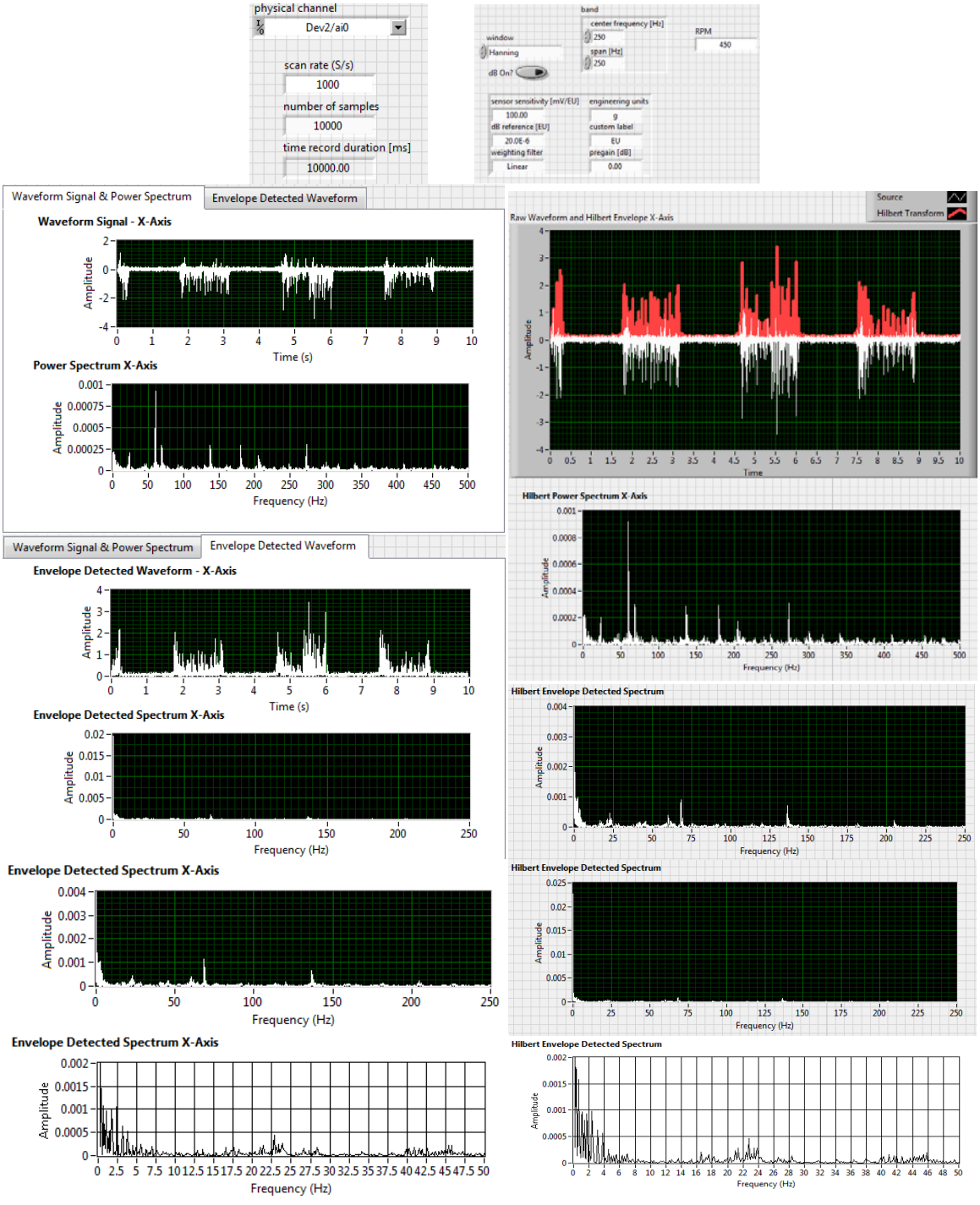

Figure A.7. Phase I induced fault 450 RPM (horizontal axis).

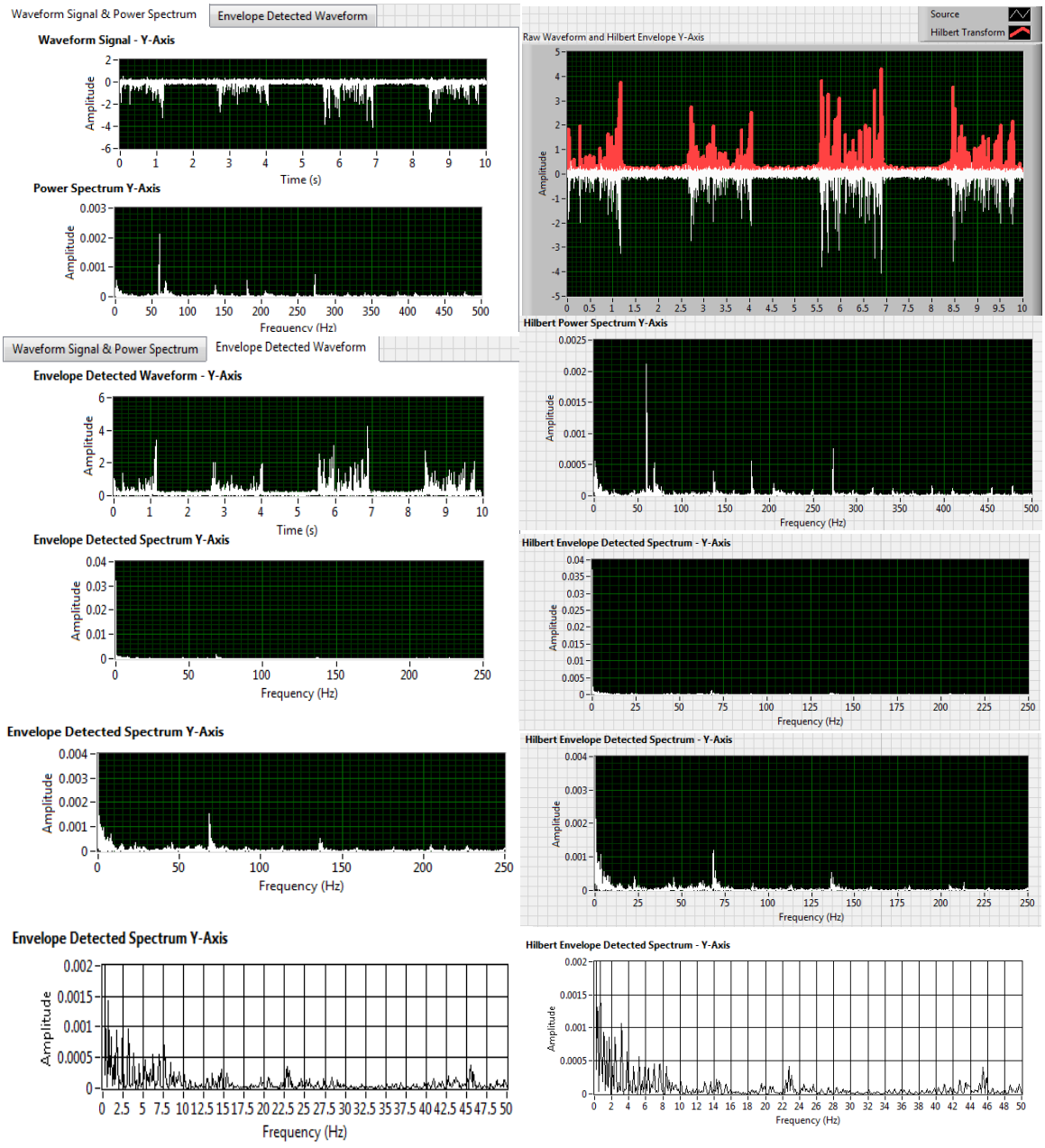

Figure A.8. Phase I induced fault 450 RPM (axial axis).

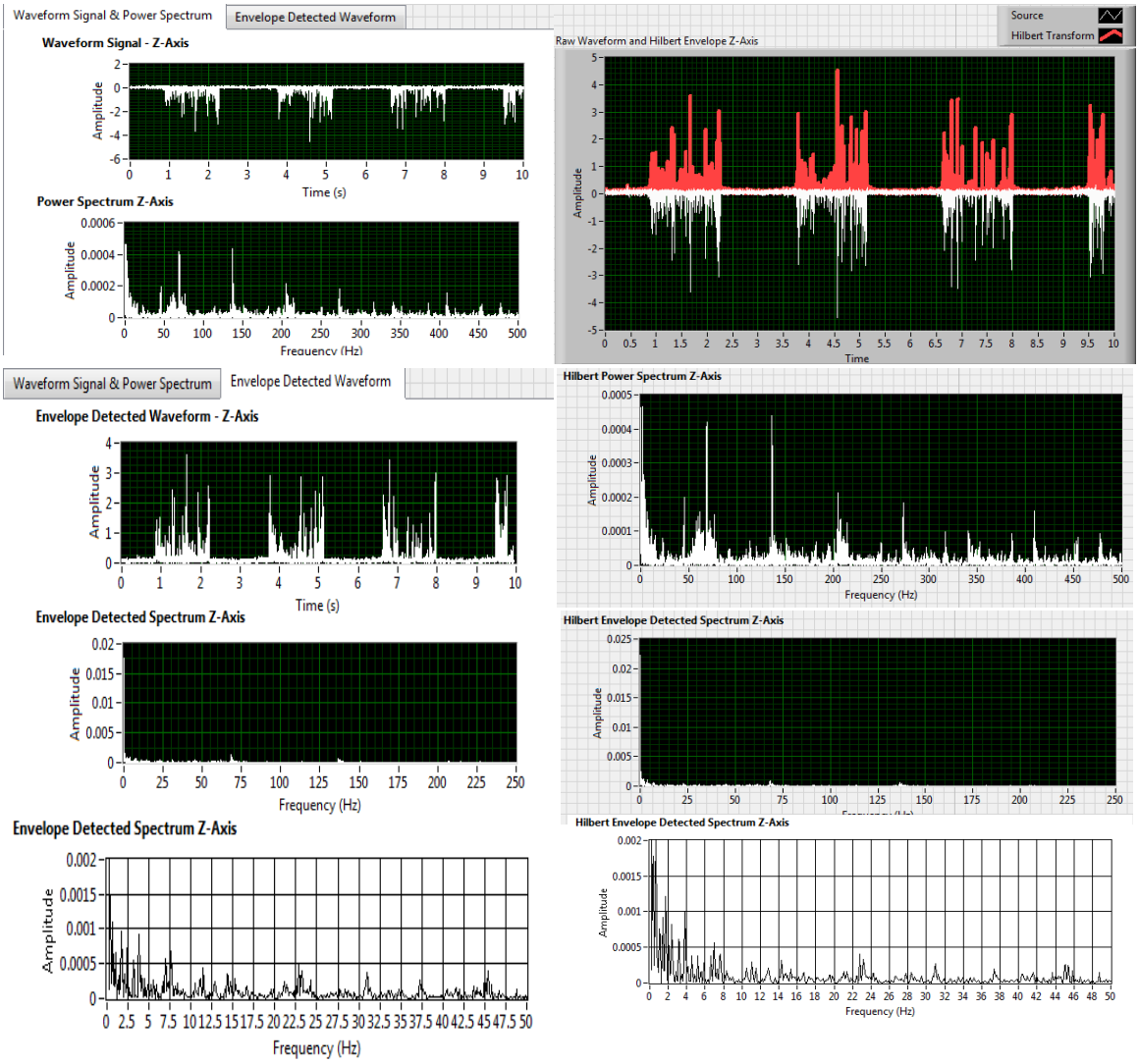

Figure A.9. Phase I induced fault 450 RPM (vertical axis).

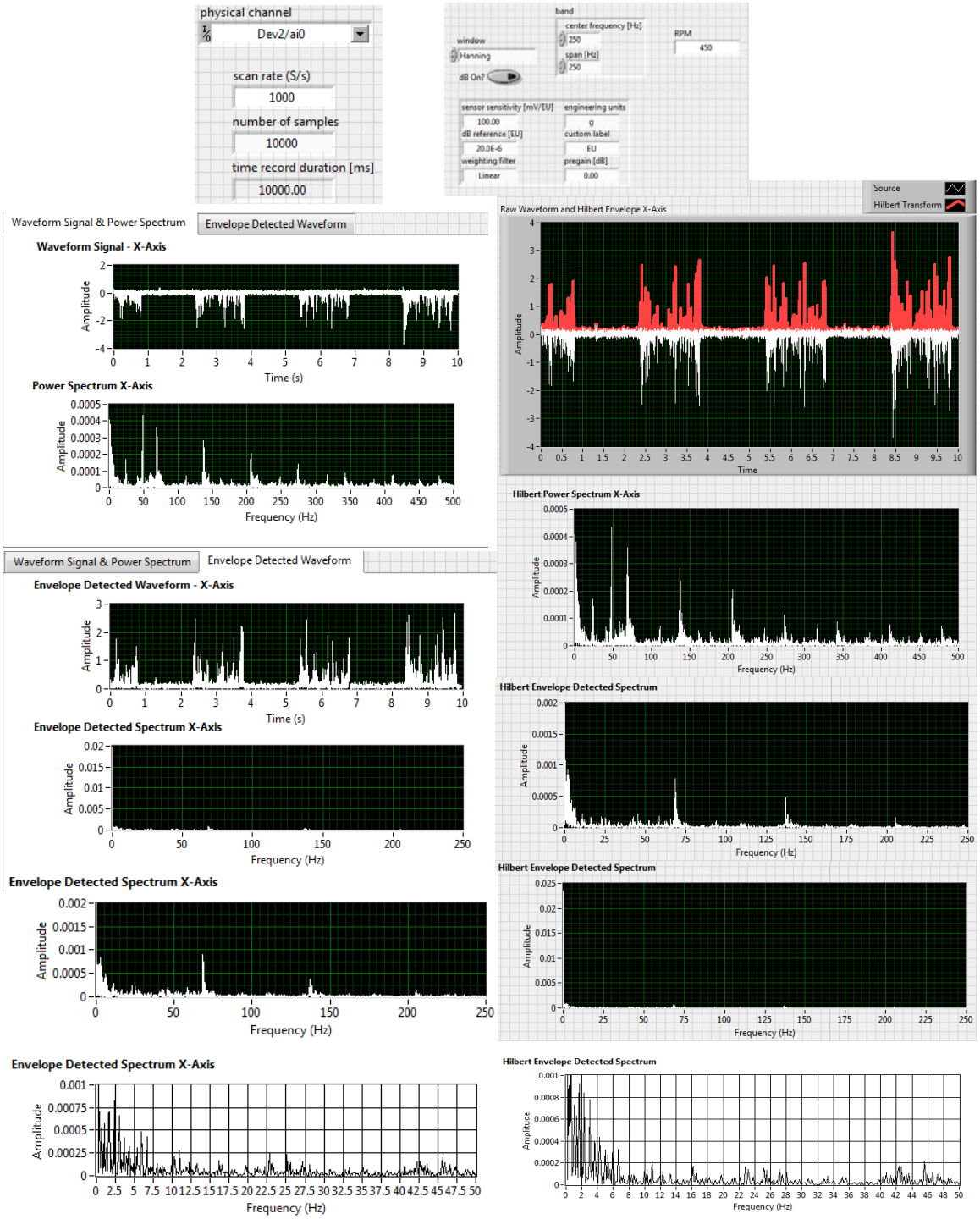

Figure A.10. Phase II induced fault 450 RPM (horizontal axis).

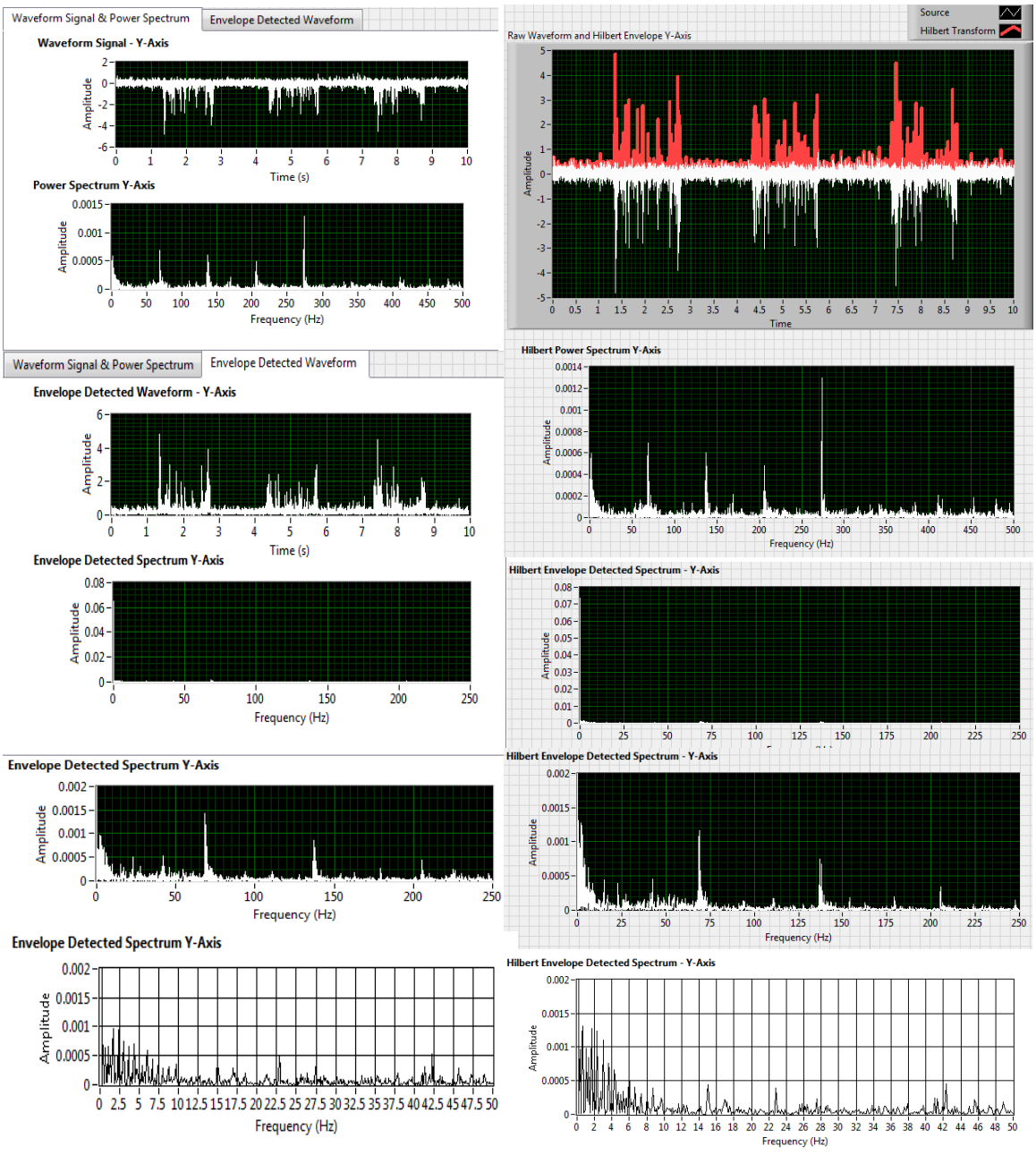

Figure A.11. Phase II induced fault 450 RPM (axial axis).

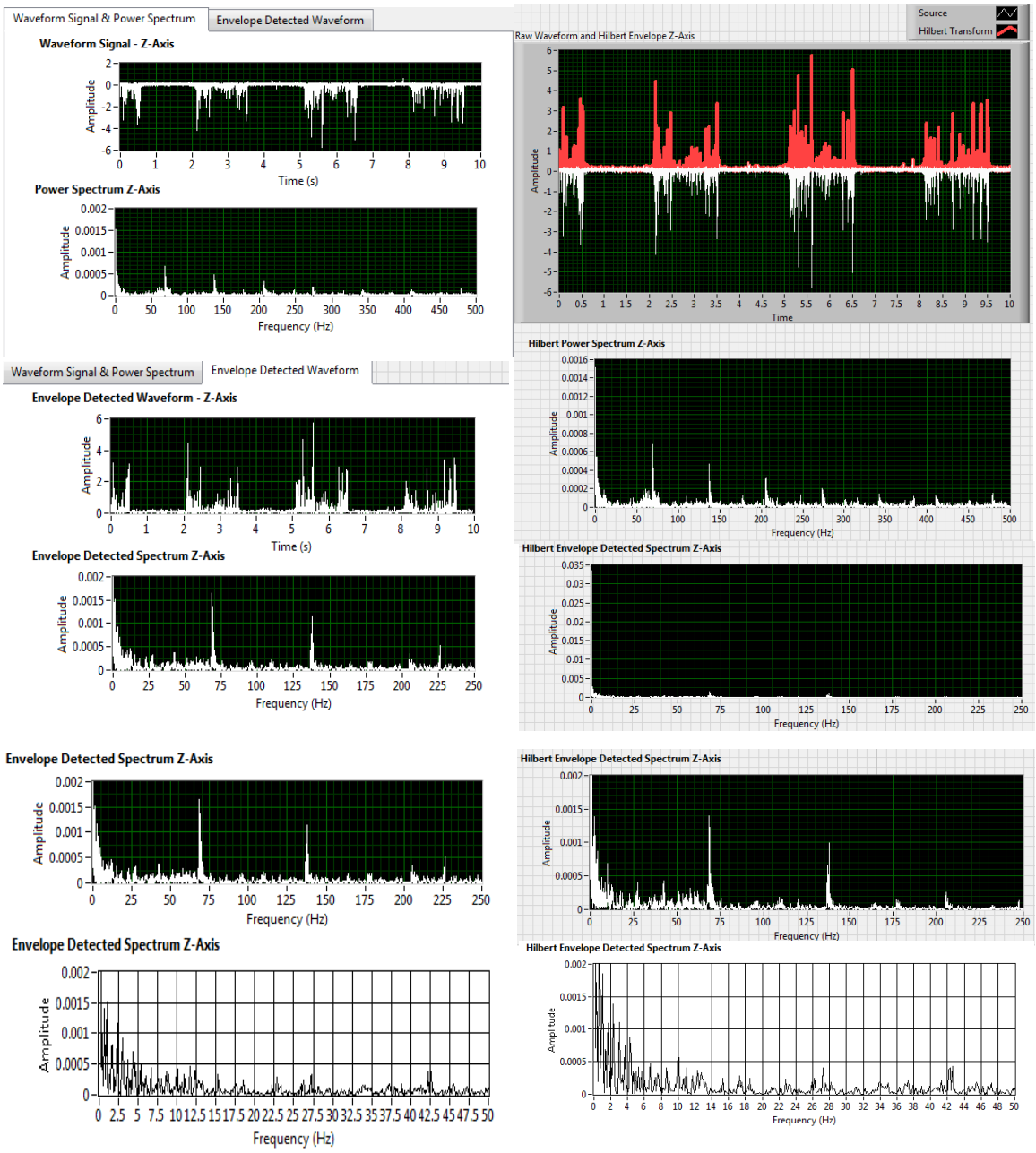

Figure A.12. Phase II induced fault 450 RPM (vertical axis).

Appendix B. Vibration Data at 900 RPM

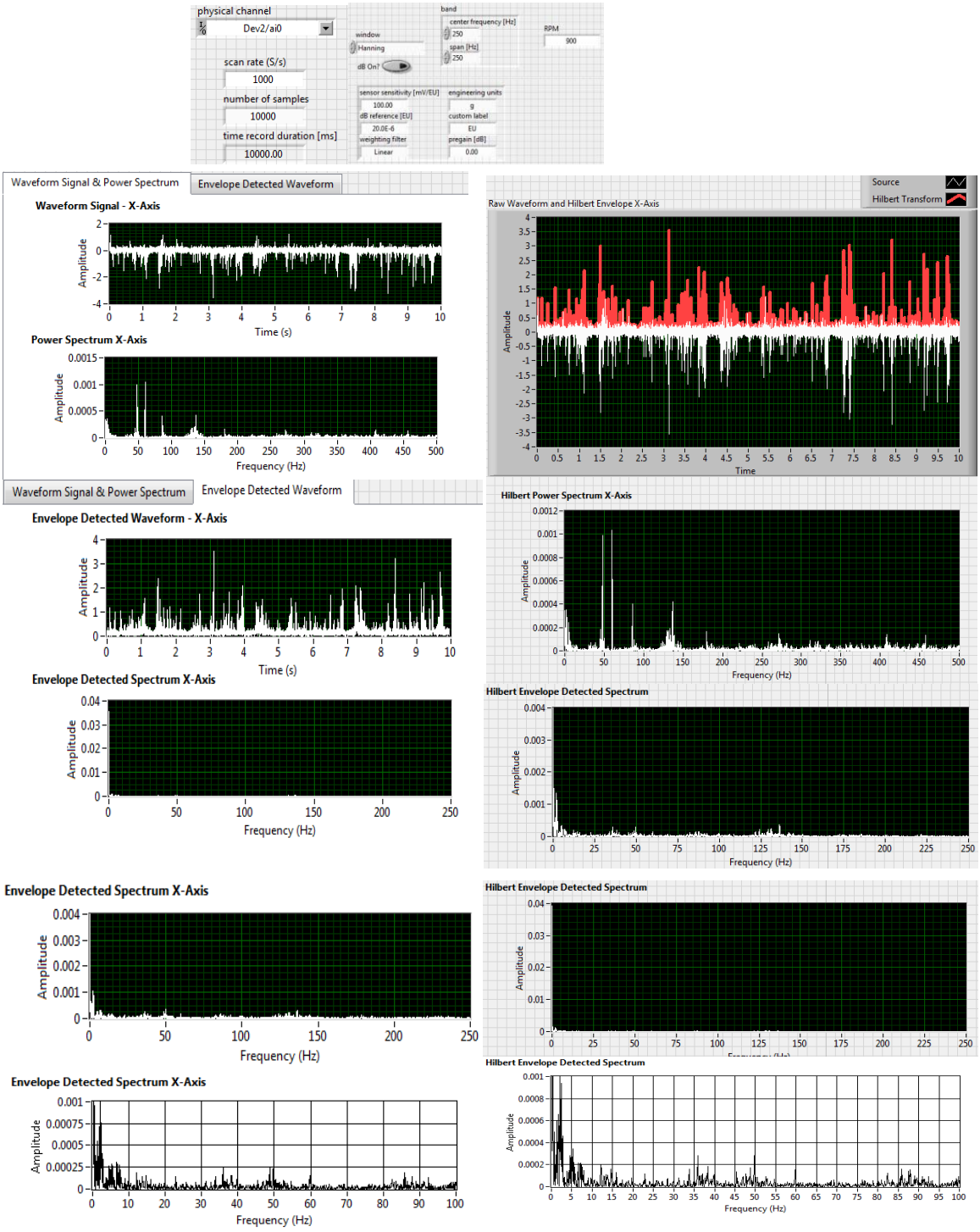

Figure B.1. Lubricated bearing 900 RPM (horizontal axis).

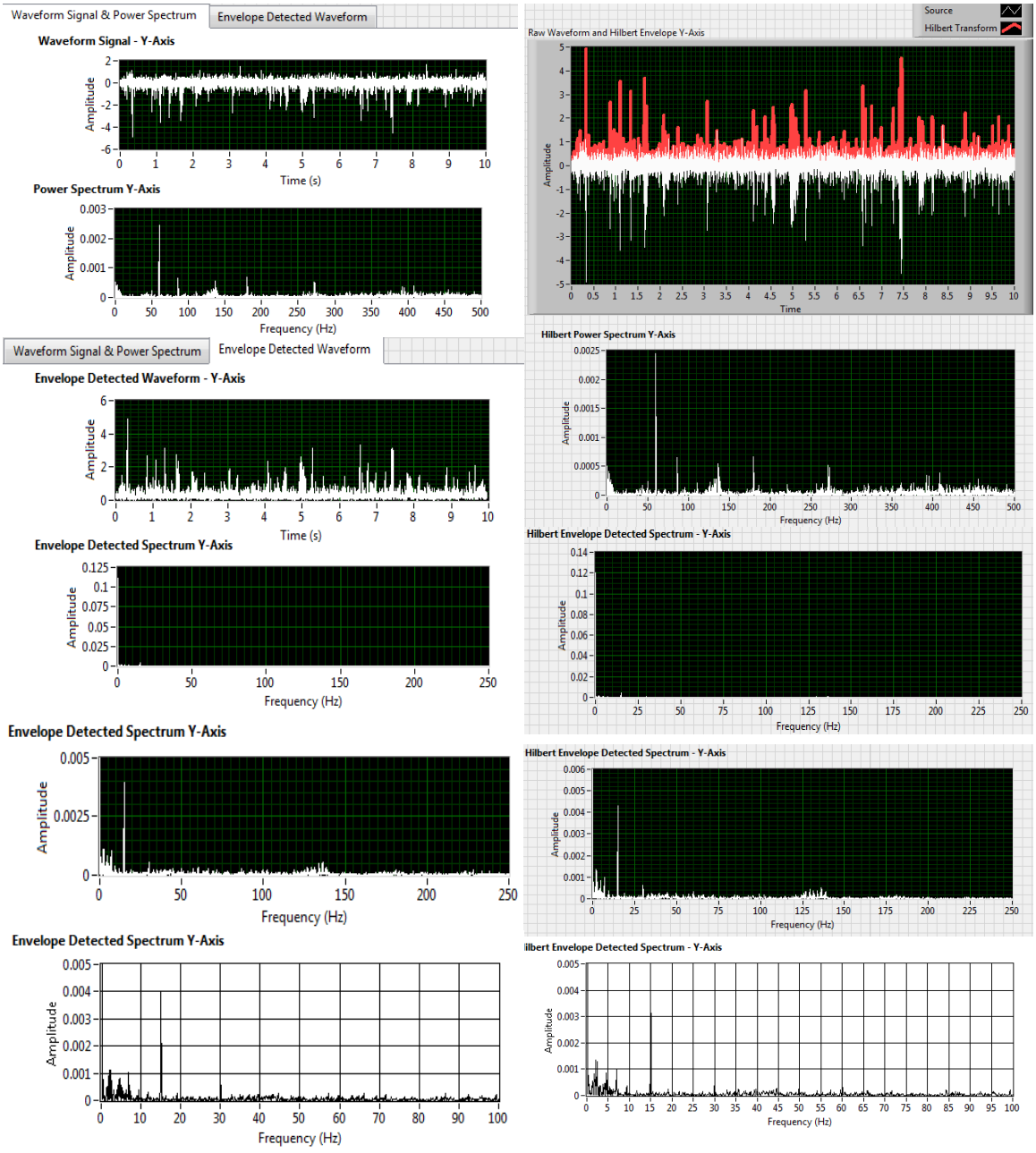

Figure B.2. Lubricated bearing 900 RPM (axial axis).

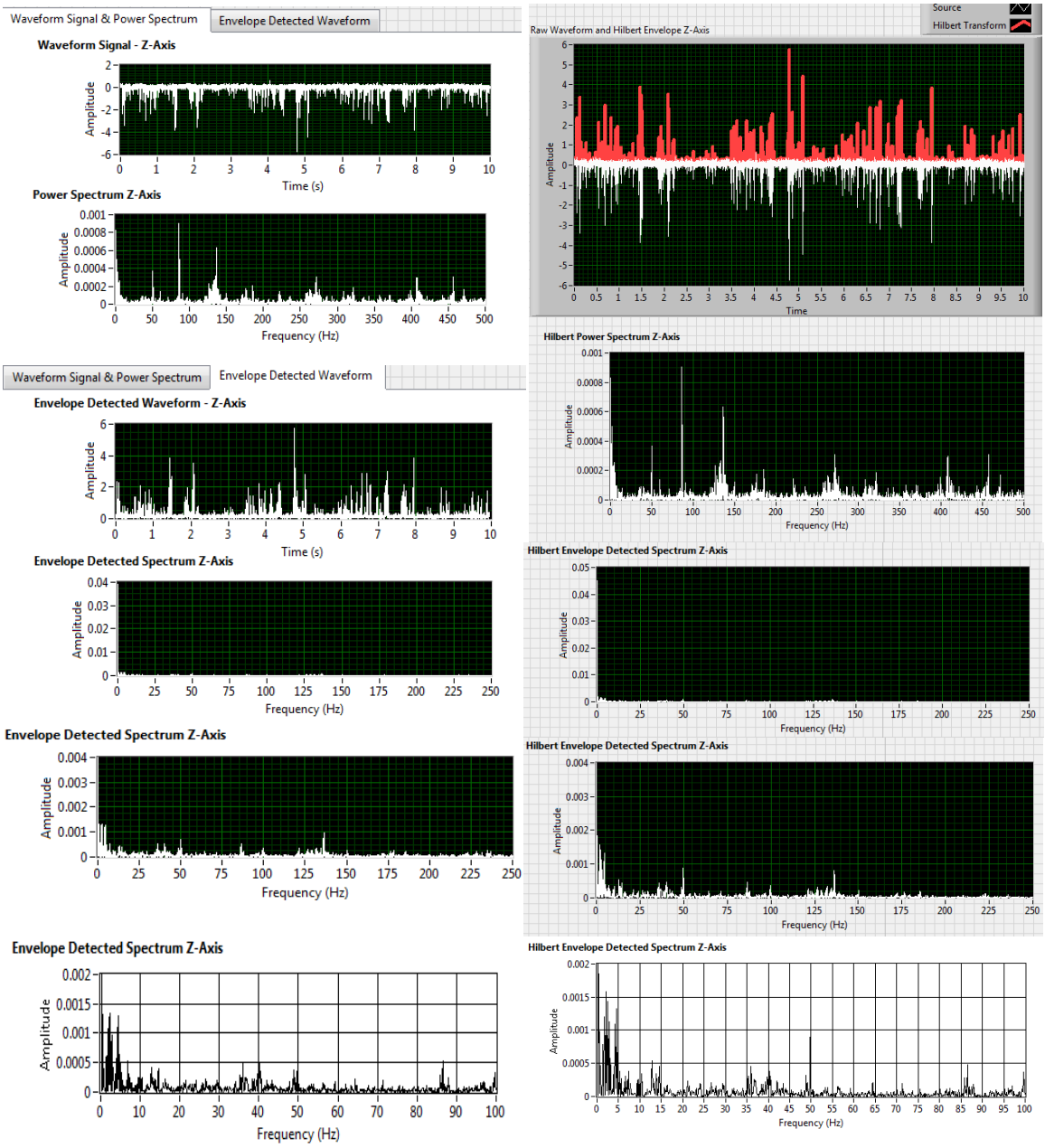

Figure B.3. Lubricated bearing 900 RPM (vertical axis).

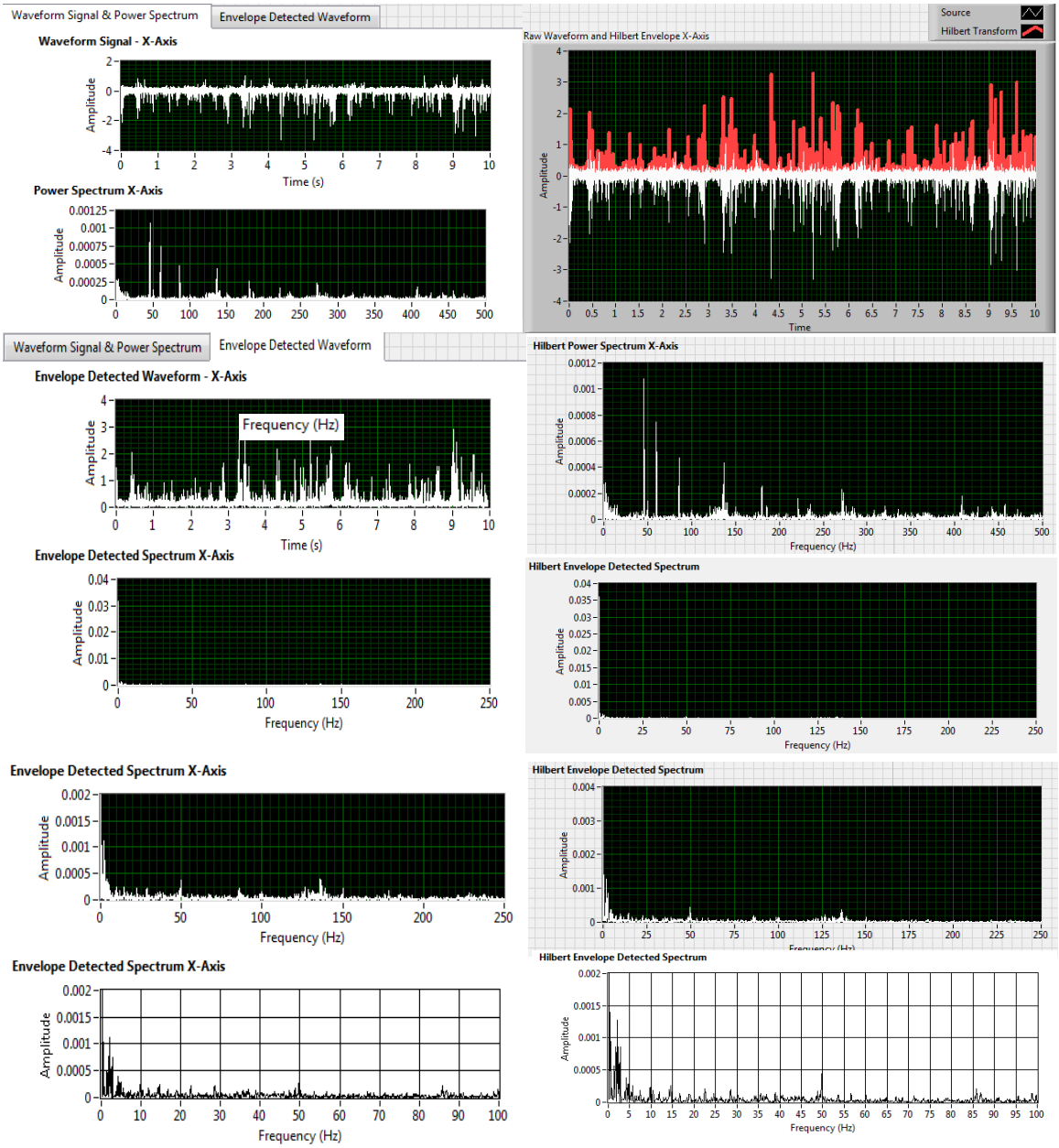

Figure B.4. Phase I induced fault 900 RPM (horizontal axis).

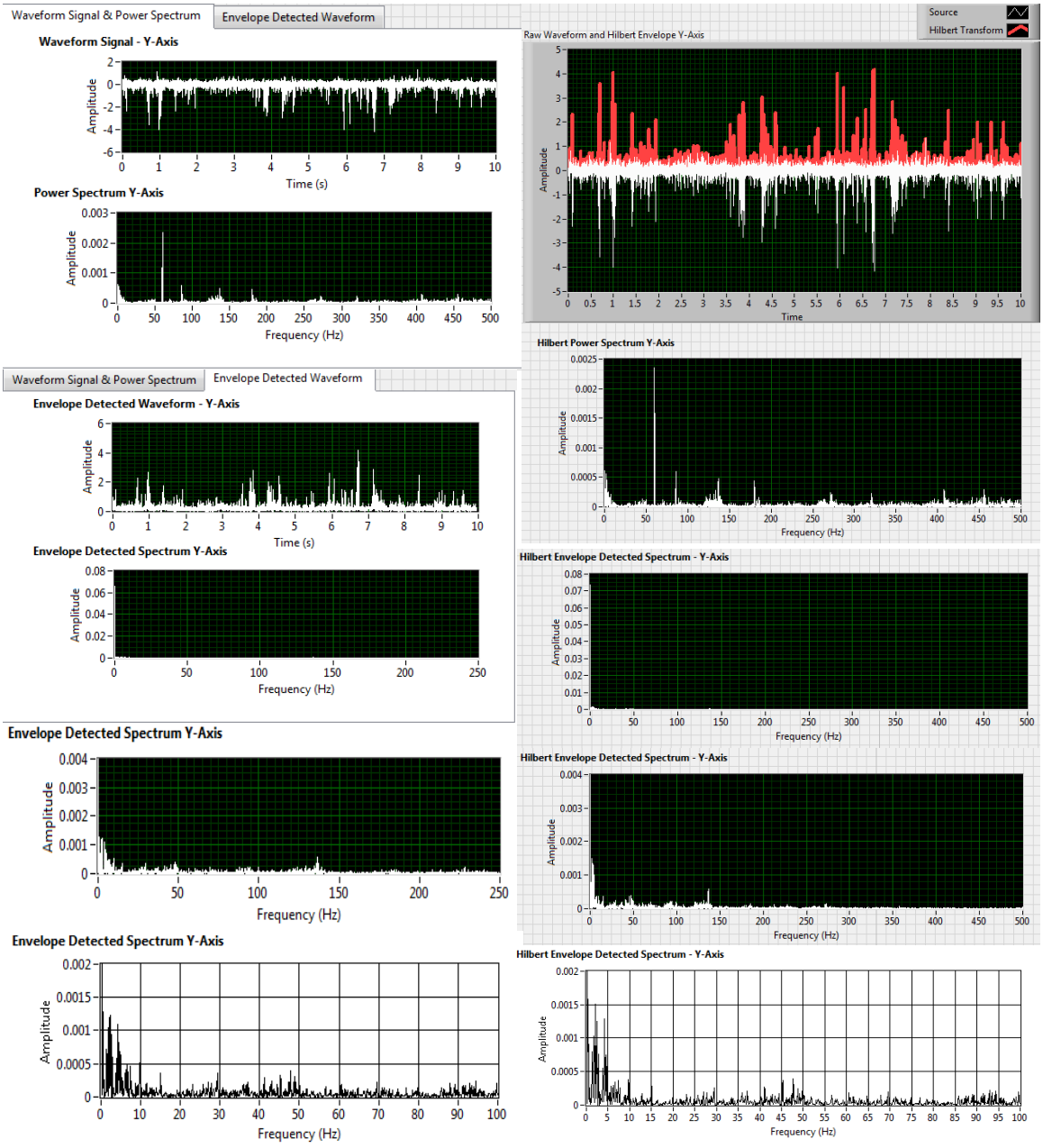

Figure B.5. Phase I induced fault 900 RPM (axial axis).

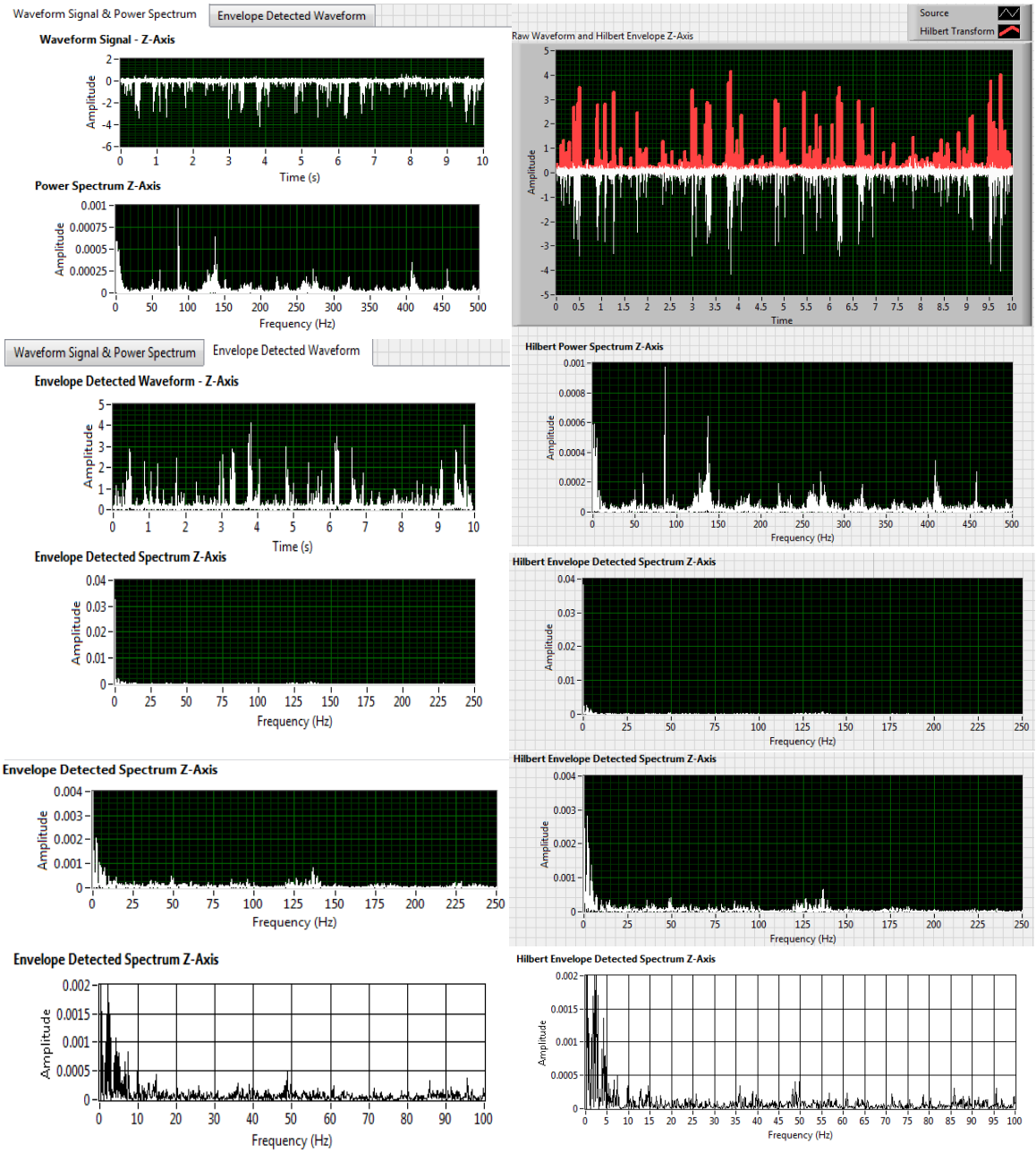

Figure B.6. Phase I induced fault 900 RPM (vertical axis).

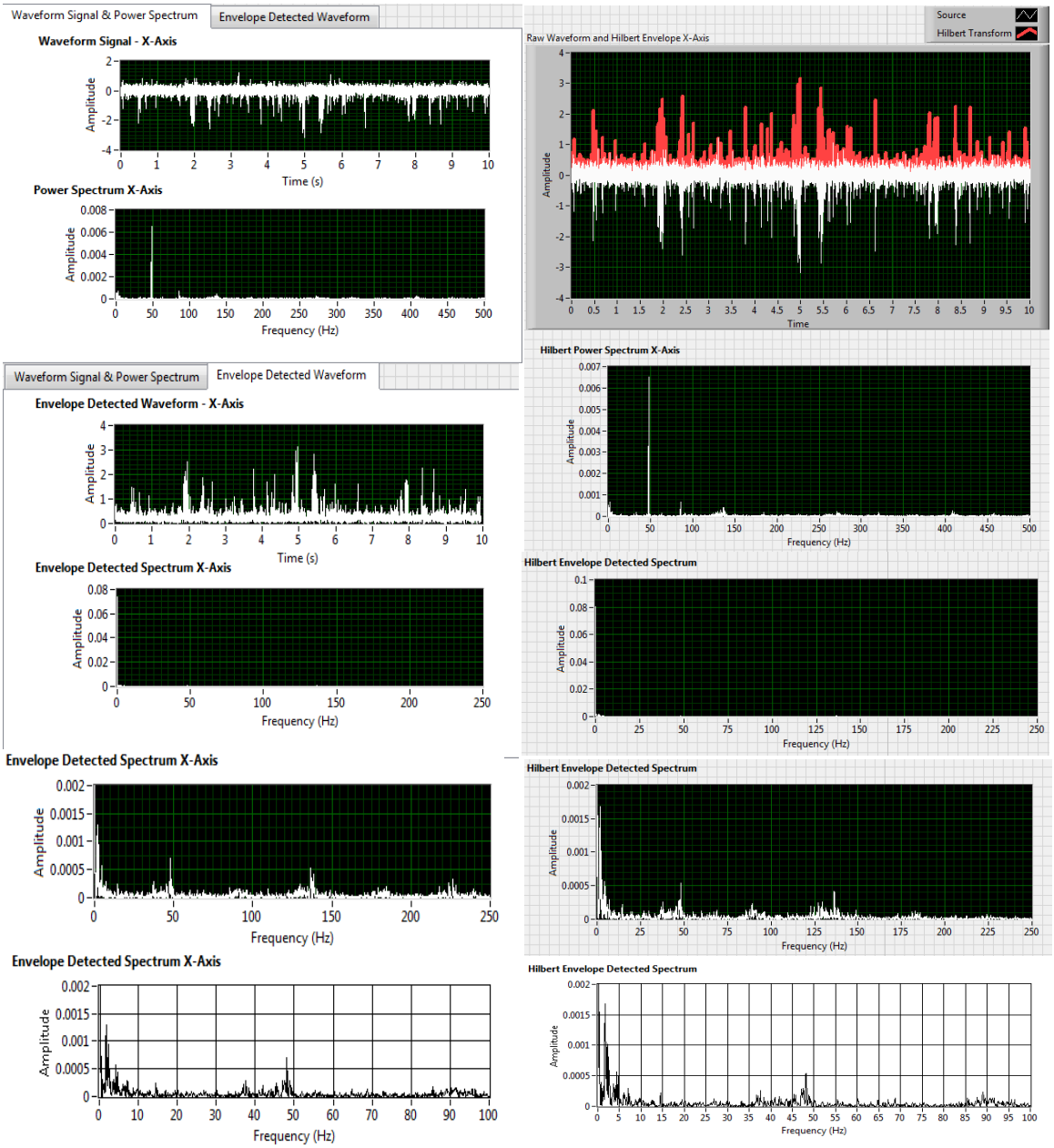

Figure B.7. Phase II induced fault 900 RPM (horizontal axis).

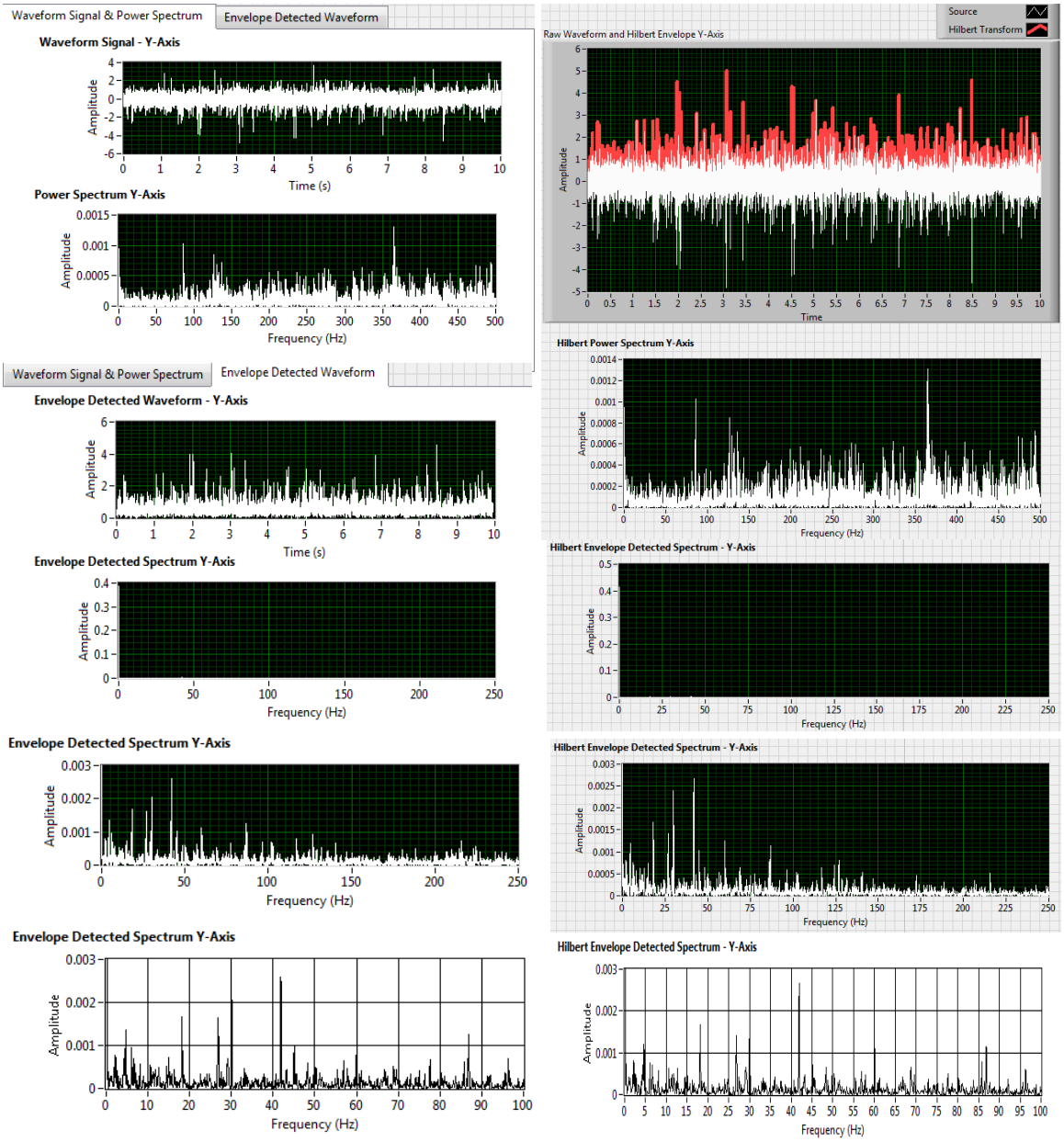

Figure B.8. Phase II induced fault 900 RPM (axial axis).

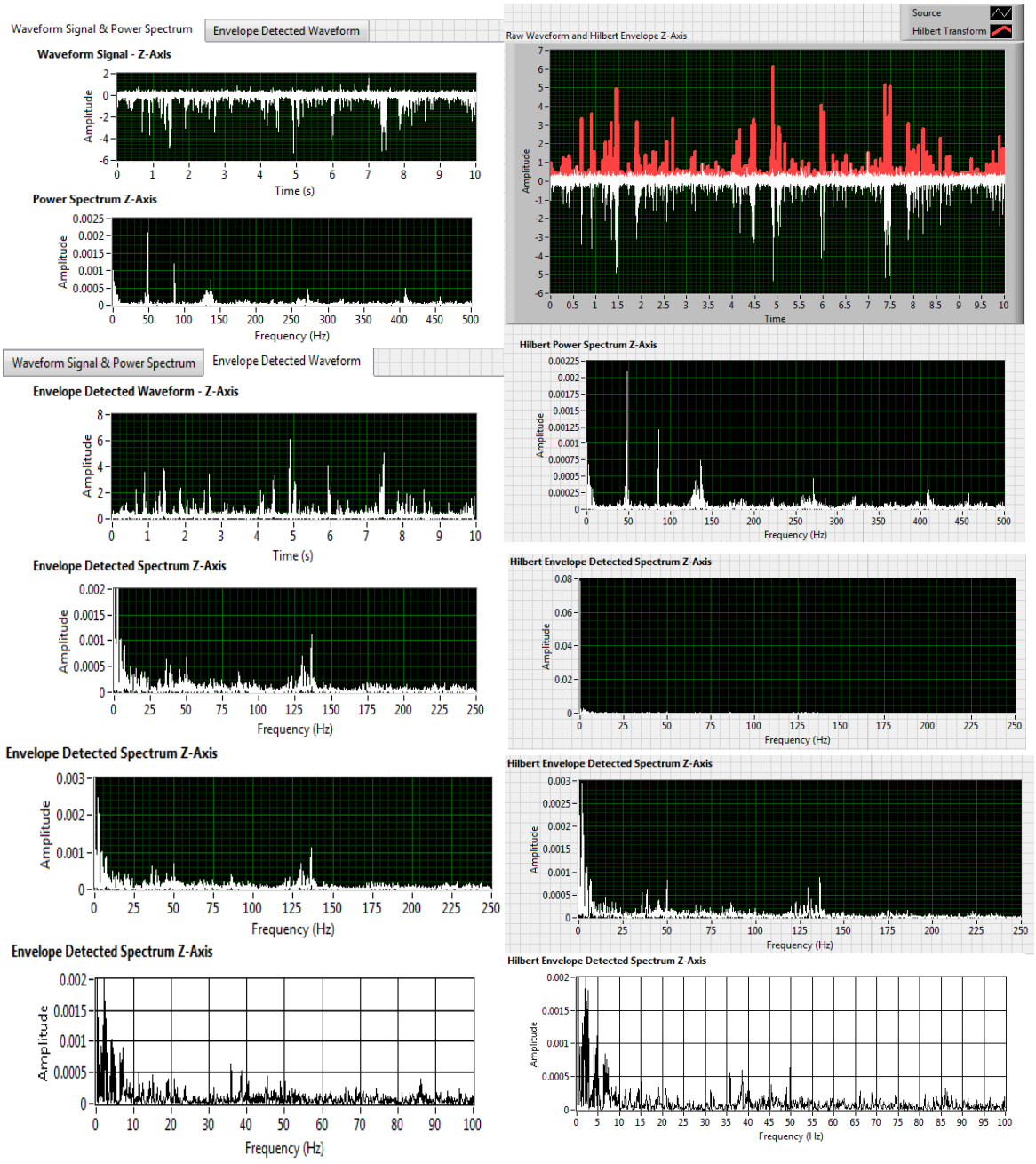

Figure B.9. Phase II induced fault 900 RPM (vertical axis).